



MONASH University

Single-step Conversion of Synthesis Gas into Formaldehyde

Alimohammad Bahmanpour
M.Sc. Chemical Engineering

A thesis submitted for the degree of *Doctor of Philosophy* at
Monash University in 2016
Department of Chemical Engineering
Faculty of Engineering

Copyright notice

Under the Copyright Act 1968, this thesis must be used only under the normal conditions of scholarly fair dealing. In particular no results or conclusions should be extracted from it, nor should it be copied or closely paraphrased in whole or in part without the written consent of the author. Proper written acknowledgement should be made for any assistance obtained from this thesis.

Abstract

Formaldehyde is known as the building block in many industries including resins, polymers, paints and adhesives. It is widely used in furniture and wood processing. The annual production rate of formaldehyde is in the range of 30 million tons globally and the demand of formaldehyde has grown by 2-3 % per year over the past two decades. Industrially, formaldehyde is produced via methanol partial oxidation. Methanol in turn is produced from synthesis gas which is produced via steam reforming of natural gas. Both methanol synthesis and steam reforming process suffer from high exergy loss due to high temperature processes and large purification units. Considering the large quantity of formaldehyde produced in the world, when combined with the high exergy losses, leads to high energy losses and CO₂ emissions globally. Therefore, alternative method for the production process of formaldehyde is needed. This project develops a novel method of formaldehyde production by using equimolar quantities of carbon monoxide and hydrogen in a catalytic slurry phase reaction. Promoted nickel-based catalysts – Ru-Ni/Al₂O₃ and Pd-Ni/Al₂O₃ were used in this project due to their high activity in hydrogenation reactions.

It was observed in this project that formaldehyde yield was significantly higher in the slurry phase (4.6 mmol.L⁻¹.g_{cat}⁻¹) compared to the gas phase (8.2×10⁻³ mmol.L⁻¹.g_{cat}⁻¹). Thermodynamics analysis showed that the reaction is equilibrium limited in the gas phase whereas it is kinetically limited in the liquid phase. It was found that in the slurry reactor increasing the temperature increases the reaction rate but the formaldehyde yield peaks at 353 K, above which the yield reduces. This is in agreement with the fact that the equilibrium constant of the reaction decreases as the temperature increases. Increasing pressure and stirring speed increased the formaldehyde yield.

The reaction mechanism was investigated based on deuterium labelling technique. It was shown that the reactant gases dissolve in the solvent and are adsorbed on the catalyst surface. The adsorbed gases react on the catalyst surface to form formaldehyde which desorbs and immediately hydrates in aqueous conditions to form methylene glycol.

The effect of solvents with high CO and H₂ solubility was investigated in this study since it was found that increasing the solubility of the gases was important to achieve higher production. However, it was observed that in addition to the gases solubility, formaldehyde yield also depends on the

reactivity of the solvents with desorbed formaldehyde. The last step is important to shift the equilibrium of the CO hydrogenation reaction.

In a nutshell, higher pressures were in favour of the reaction but the operating pressure in this study was limited to 100 bar by the maximum available gas cylinder pressure. The most suitable solvent was found to be methanol since it has higher solubility of CO and H₂ compared to water, and similar to water, it also reacts with formaldehyde to shift the equilibrium. Highest yield was achieved by using pure methanol as a solvent at 363 K and 100 bar, which resulted in formaldehyde yield of 15.58 mmol.L⁻¹.g_{cat}⁻¹.

Declaration

This thesis contains no material which has been accepted for the award of any other degree or diploma at any university or equivalent institution and that, to the best of my knowledge and belief, this thesis contains no material previously published or written by another person, except where due reference is made in the text of the thesis.

Monash University

Declaration for thesis based or partially based on conjointly published or unpublished work

General Declaration

In accordance with Monash University Doctorate Regulation 17.2 Doctor of Philosophy and Research Master's regulations the following declarations are made:

I hereby declare that this thesis contains no material which has been accepted for the award of any other degree or diploma at any university or equivalent institution and that, to the best of my knowledge and belief, this thesis contains no material previously published or written by another person, except where due reference is made in the text of the thesis.

This thesis includes two original papers published in peer reviewed journals and one unpublished publications. The core theme of the thesis is single-step conversion of synthesis gas into formaldehyde. The ideas, development and writing up of all the papers in the thesis were the principal responsibility of myself, the candidate, working within the Chemical Engineering Department under the supervision of Dr Akshat Tanksale and A/Prof Andrew Hoadley.

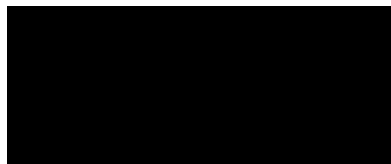
The inclusion of co-authors reflects the fact that the work came from active collaboration between researchers and acknowledges input into team-based research.

In the case of Chapter 2 and Chapter 3, my contribution to the work involved the following:

Thesis chapter	Publication title	Publication status*	Nature and extent of candidate's contribution
2	Critical review and exergy analysis of formaldehyde production processes	Published	Initiation 50% Modelling 100% Writing 70%
3	Formaldehyde production via hydrogenation of carbon monoxide in the aqueous phase	Publihsed	Initiation 50% Experimental works 100% Writing 70%

I have renumbered sections of submitted or published papers in order to generate a consistent presentation within the thesis.

Signed:



Date:

Acknowledgement

I express my sincere appreciation to everyone who helped me to complete my thesis. I sincerely thank my supervisors Dr. Akshat Tanksale and A/Prof Andrew Hoadley for their incredible help and support and their great contribution to this work. It was impossible for me to conduct this research without their supervision and their valuable feedback. It was a great pleasure for me to work with them and learn from them during my candidature. I also would like to thank Monash Institute of Graduate Research (MIGR) for the financial support and giving me this opportunity to conduct my research in one of the best universities in Australia.

I would like to acknowledge the support from the members of CatGreenChem© group, especially from my dear friend, Fan Liang Chan, for his valuable help and support through my candidature. I also would like to thank Sheryl Moh for helping me through this project.

Special thanks to Dr. Peter Nichols and Dr. Ekaterina Pas for their generous help and valuable assistance through my candidature.

I also appreciate the help and support provided by the Chemical Engineering Department staff; Lilyanne Price, Jill Crisfield, and Kim Phu. Specially, I would like to thank Harry Bouwmeester for his generous help throughout my candidature.

Last but not least, I would like to thank my family for supporting me through all these years. I would like to thank my wife, Raha Rajaei, for her invaluable support and encouragement she has given to me. I would like to thank my parents for their never-ending support. There is no way I can thank them enough

Table of Contents

Chapter 1: Introduction	1
1.1 Background	3
1.2 Research Aims	4
1.3 Thesis Structure	5
1.4 References	6
Chapter 2: Literature Review	9
2.1 Introduction	11
2.2 Formaldehyde Production	14
2.2.1 History.....	14
2.2.2 Industrial Methods.....	15
2.2.2.1 Methanol Ballast Process.....	16
2.2.2.2 BASF Process	17
2.2.2.3 FORMOX Process	19
2.2.3 Other Methods.....	21
2.2.3.1 Other Formaldehyde Production Methods from Methanol	21
2.2.3.2 Formaldehyde Production from Methane.....	22
2.3 Kinetics and Mechanism	23
2.3.1 Thermodynamic Investigation of the Reactions	23
2.3.2 Kinetics of Reactions and Mechanism	25
2.3.2.1 Copper and Silver as Catalysts	26
2.3.2.2 Metal Oxides as Catalysts	30
2.4 Latest Advancements in Formaldehyde Production.....	34
2.5 Conclusion.....	36
2.6 References	37
Chapter 3: Formaldehyde Production via CO Hydrogenation in the Aqueous Phase	43
3.1 Introduction	45
3.2 Experiments and Methods.....	47
3.2.1 Catalyst Preparation and Characterization.....	47
3.2.2 Fixed Bed Reactor	48

3.2.3 Slurry Reactor	49
3.3 Investigation of the Thermodynamic Conditions	49
3.4 Catalyst Characterization.....	51
3.5 Comparison of Formaldehyde Production in Fixed Bed and Slurry Reactors	54
3.5.1 Fixed Bed Reactor	54
3.5.2 Slurry Reactor	55
3.5.3 Effect of the Stirring Speed in the Slurry Reactor	60
3.5.4 Effect of the Mass of the Catalyst in the Slurry Reactor	61
3.6 Catalyst Support Stability in the Slurry Reactor	61
3.7 Conclusion	64
3.8 References	64
Chapter 4: Reaction Mechanism of CO Hydrogenation to Formaldehyde in the Aqueous Phase	67
4.1 Introduction.....	69
4.2 Experiments and Methods	73
4.3 Sample Investigation	76
4.4 Determination of the Source of Hydrogen Atoms	77
4.4.1 Labelling H Atoms by Using D ₂	77
4.4.2 Labelling H Atoms by Using D ₂ O and CD ₃ OD	79
4.5 Reaction Mechanism in the Absence of CH ₃ OH	82
4.6 Conclusion	86
4.7 References	87
Chapter 5: Effect of Solvents on the Formaldehyde Production in the Slurry Reactor	89
5.1 Introduction.....	91
5.2 Experiments and Methods	92
5.3 Effect of Solvents on Carbon Monoxide Hydrogenation Process	93
5.4 Effect of temperature on the HCHO yield in methanol solvent	97
5.5 Effect of Solvents on Carbon Dioxide Hydrogenation Process.....	99
5.6 Conclusion	100
5.7 References	100
Chapter 6: Conclusions	103
6.1 Introduction.....	105

6.2 Gas Phase Reaction and Slurry Phase Reaction	105
6.3 Effect of Temperature.....	105
6.4 Effect of Pressure	106
6.5 Effect of Stirring Speed	106
6.6 Reaction Mechanism.....	106
6.7 Effect of Solvents	107
6.8 CO ₂ Hydrogenation	107
Chapter 7: Recommendations and Future Studies	109
7.1 Introduction	111
7.2 Carbon Dioxide Hydrogenation.....	111
7.3 Catalyst Study.....	111
7.4 Process Optimization	112
7.5 <i>In-situ</i> Study of the Reaction Mechanism	112
7.6 Investigation of the Solvent-Formaldehyde Interaction Theory.....	113
Appendix.....	115
A.1 Critical Review and Exergy Analysis of Formaldehyde Production Processes:.....	117
A.2 Formaldehyde Production via Hydrogenation of Carbon Monoxide in the Aqueous Phase	118
A.3 Consistency of the Formaldehyde Detection Methods.....	119
A.4 SEM Images of Fresh Ru-Ni/Al ₂ O ₃ and Pd-Ni/Al ₂ O ₃	120
A.5 Standard solution containing 400 ppm formalin, 100 ppm HCOOH and CH ₃ COOH on HPLC	121

List of Figures

Chapter 2

Figure 2.1: Tree diagram of industrial processes for formaldehyde production	16
Figure 2.2: BASF process schematic diagram	18
Figure 2.3: FORMOX process schematic diagram	20

Chapter 3

Figure 3.1: Schematic diagram of the fixed bed reactor setup	48
Figure 3.2: Schematic diagram of the slurry reactor setup	49
Figure 3.3: Effect of pressure on the Gibbs free energy of the reaction in the aqueous phase, T= 298 K (Oelkers et al., 1995)	51
Figure 3.4: TEM image and size distribution of a) Pd-Ni/Al ₂ O ₃ , Scale bar= 50nm and b) Ru-Ni/Al ₂ O ₃ , Scale bar= 20nm	53
Figure 3.5: XRD patterns of calcined and reduced Pd-Ni/Al ₂ O ₃ and Ru-Ni/Al ₂ O ₃	54
Figure 3.6: Effect of (a) pressure and (b) temperature on the molar yield of HCHO in the fixed bed reactor using Pd-Ni/Al ₂ O ₃	55
Figure 3.7: Reaction constant based on the first 2 hour of the reaction, P=100 bar, Catalyst: Ru-Ni/Al ₂ O ₃	56
Figure 3.8: Effect of temperature on the molar yield of HCHO in the slurry reactor after 48 hours using Ru-Ni/Al ₂ O ₃	57
Figure 3.9: Effect of temperature on molar yield of HCHO in the slurry reactor after 120 hours using Ru-Ni/Al ₂ O ₃	57
Figure 3.10: Shifting the reaction equilibrium in favour of producing HCHO	58
Figure 3.11: Comparison between the results of the fixed bed reactor and the slurry reactor at 293 K and 100 bar for a) Pd-Ni/Al ₂ O ₃ and b) Ru-Ni/Al ₂ O ₃	59
Figure 3.12: Effect of the stirrer rotation speed on the molar yield of HCHO using Ru-Ni/Al ₂ O ₃	60
Figure 3.13: Effect of the mass of the catalyst on the HCHO yield, Catalyst: Ru-Ni/Al ₂ O ₃ , P = 100 bar, T = 353 K	61
Figure 3.14: XRD patterns of fresh and spent Ru-Ni/Al ₂ O ₃ in the slurry phase process	62
Figure 3.15: ²⁷ Al NMR spectra of the fresh and the spent Ru-Ni/Al ₂ O ₃ in the slurry phase process ...	63

Chapter 4

Figure 4.1: Potential reaction mechanisms of CO hydrogenation reaction to HCHO.....	72
Figure 4.2: schematic diagram of the setup equipped with MS.....	74
Figure 4.3: Chromatograms of the standard HCHO solutions (▼ = peak at 17.6 min which was calibrated for HCHO).....	75
Figure 4.4: Calibration Curve of HCHO on HPLC	75
Figure 4.5: HPLC chromatograms of samples taken at various reaction times. Reaction conditions: T = 353 K, P = 100 bar. ▼ = peak associated with standard formalin solution (only peak at 17.6 min was calibrated for HCHO); ▲ = peak associated with methanol	76
Figure 4.6: Mass to charge ratio profiles for HCHO (29), DCDO (30), and CH ₃ OH (31) using 5 vol% CH ₃ OH in H ₂ O as the reaction mixture	78
Figure 4.7: Mass to charge ratio profiles for D ₂ O (20) and CD ₃ OD (34) using 5 vol% CH ₃ OH in H ₂ O as the reaction mixture	79
Figure 4.8: Mass to charge ratio profiles for D ₂ O (20) and CD ₃ OD (34) using 5 vol% CD ₃ OD in D ₂ O as the reaction mixture	80
Figure 4.9: Mass to charge ratio profiles for HCHO (29), DCDO (30), and CH ₃ OH (31) using 5 vol% CD ₃ OD in D ₂ O as the reaction mixture.....	81
Figure 4.10: The effect of the presence of CH ₃ OH in the reaction mixture on the molar yield of HCHO	82
Figure 4.11: The chromatograms of the samples of the run with pure water (no methanol), T=353 K, P=100 bar	84
Figure 4.12: Mass to charge ratio profiles for DCDO (30) and CD ₃ OD (34) using pure H ₂ O as the solvent.....	85

Chapter 5

Figure 5.1: The effect of using different solvents on HCHO production yield, T=353 K, P=100 bar, Catalyst: Ru-Ni/Al ₂ O ₃	94
Figure 5.2: Effect of CH ₃ OH concentration (% v/v) on HCHO yield at T = 353 K, P = 100 bar, Catalyst: Ru-Ni/Al ₂ O ₃	95
Figure 5.3: Effect of the CH ₃ OH mole fraction in the solvent mixture on the HCHO yield at t = 48 h, the lowest value of x tested is 4.5×10 ⁻⁴	95

Figure 5.4: A simplified schematic of HCHO formation, desorption and stabilization in CH₃OH.
Adapted from(Guo et al., 2003) 97

Figure 5.5: Effect of temperature on the molar yield of HCHO, solvent: CH₃OH, P = 100 bar 98

Figure 5.6: Arrhenius plot based on the rate of reaction calculated at t = 5 h, solvent: CH₃OH, P = 100
bar, Catalyst: Ru-Ni/Al₂O₃..... 98

Figure 5.7: CO₂ hydrogenation in the slurry reactor, T=353 K, P=100 bar, Catalyst: Ru-Ni/Al₂O₃ 99

List of Tables

Chapter 2

Table 2.1: Physical properties of monomeric formaldehyde (Reuss et al., 2003)	11
Table 2.2: Heat of formation, heat capacity, and entropy of formaldehyde (J. F. Walker, 1967)	12
Table 2.3: Partial pressure of formaldehyde for the temperature range of 163.75 K to 250.85 K (Spence & Wild, 1935)	13
Table 2.4: Thermodynamic conditions for CH ₃ OH partial oxidation.....	24
Table 2.5: Thermodynamic conditions for CH ₃ OH dehydrogenation	25
Table 2.6: Values for the first and the second rate constants for CH ₃ OH partial oxidation (Bhattacharyya et al., 1967).....	31
Table 2.7: Effects of different supports on the V ₂ O ₅ performance in CH ₃ OH partial oxidation	33

Chapter 3

Table 3.1: Chemical reactions used for the production of HCHO in the gas phase	46
Table 3.2: Thermodynamic conditions of CO hydrogenation reaction to HCHO.....	50
Table 3.3: BET surface area, metal loading, and CO chemisorption data.....	52

Chapter 4

Table 4.1: Possible intermediate and final products based on feedstock and possible mechanisms.	71
---	----

List of Publications

Journal Publications:

A.M. Bahmanpour, A. Hoadley, and A. Tanksale, *Critical review and exergy analysis of formaldehyde production processes. **Reviews in Chemical Engineering***, 2014. **30**(6): p. 583-604.

A.M. Bahmanpour, A. Hoadley, and A. Tanksale, *Formaldehyde production via hydrogenation of carbon monoxide in the aqueous phase. **Green Chemistry***, 2015. **17**(6): p. 3500-3507.

Conference Publications:

A.M. Bahmanpour, A. Hoadley, and A. Tanksale, *Direct formaldehyde production from Synthesis gas, **AIChE annual meeting***, Atlanta, GA, USA, 2014.

Abbreviations

AW	Atomic Weight
BASF	Badische Anilin- und Soda-Fabrik
BET	Brunauer- Emmett- Teller
BFM	Bubble Flow Meter
BPR	Back Pressure Regulator
DFT	Density Functional Theory
FORMOX	Formaldehyde by oxidation
GC	Gas Chromatography
HPLC	High Performance Liquid Chromatography
ICI	Imperial Chemical Industries
MFC	Mass Flow Controller
MS	Mass Spectrometer
NIH	National Institutes of Health
NMR	Nuclear Magnetic Resonance
PF	Particle Filter
PG	Pressure Gauge
TEM	Transmission Electron Microscopy
TOF	Turnover Frequency
TPRS	Temperature Programmed Reaction Spectroscopy
WF	Weight Fraction
XRD	X-ray Diffraction
XRF	X-ray Fluorescence

Symbols

%vol	-	Volume Percent
%wt	-	Weight Percent
g_{cat}	g	Weight of Catalyst in Grams
k_i	s^{-1}	Rate Constant
K	kPa^{-1}	Equilibrium Constant
M_i	$\mu mol.g^{-1}$	Amount of Adsorbed Gas
N_s	$\mu mol.m^{-2}$	Surface Density of Redox Site
P	bar	Pressure
p^*	kPa	Vapor Pressure
T	K	Temperature
X_e	%	Equilibrium Conversion
X	%	Conversion
ΔG	$kJ.mol^{-1}$	Gibbs Free Energy
ΔH	$kJ.mol^{-1}$	Enthalpy Change
ΔS	$J.mol^{-1}.K^{-1}$	Entropy Change

This page is intentionally left blank

Chapter 1:

Introduction

This page is intentionally left blank

1.1 Background

Due to the increasing global energy demand, many researchers have focused on reduction of energy consumption in chemical industry. It is always essential to search for more efficient, energy saving processes for the production of valuable chemicals. In this way, various production methods have been optimized or changed. Many aspects can be considered and evaluated during the production process. Although the yield of the product and the conversion of the reactants are two of the most important factors to consider in a chemical process, other factors such as optimizing the energy consumption rate, lowering the production capital costs and simplifying the downstream process are yet to be considered.

Formaldehyde is considered as one of the main building blocks in petrochemical industry. As one of the main intermediate products, formaldehyde is used to produce phenol-formaldehyde, urea-formaldehyde, and melamine-formaldehyde. The annual production rate of formaldehyde is in the range of 30 million tons globally and the demand of formaldehyde has grown by 2-3 % per year over the past two decades (Ulukardesler et al., 2010). Over 80% of the produced formaldehyde is used as an intermediate product for resin production (National Toxicology, 2010). Recently, it is shown that the industrial process of formaldehyde production suffers from ~57% losses of exergy (i.e. quality energy) (Bahmanpour et al., 2014). Considering the large amount of formaldehyde annually produced, the total energy loss of the formaldehyde production process is considerably high.

It is known that formaldehyde is produced through a relatively long sequence of processes from natural gas. Formaldehyde is produced in three stages: (a) steam reforming of natural gas to produce synthesis gas (b) methanol synthesis and (c) partial oxidation and/or dehydrogenation of methanol to produce formaldehyde. Although many have studied the possibility of production of formaldehyde through a single step process from natural gas to reduce the capital costs and energy losses, relying on natural gas as a depleting fossil fuel is still considered as a disadvantage of this method. Moreover, the low methane conversion and/or formaldehyde selectivity is still considered as the main issue in this method.

Very limited studies on the production of formaldehyde directly from synthesis gas are available (Newton & Dodge, 1933). However, this process was reported not to be successful since only trace

Chapter 1

amount of formaldehyde was reported to be produced. The highest carbon monoxide conversion reported was quite insignificant (0.2%) (Morgan et al., 1932). Since direct formaldehyde production from synthesis gas reduces the number of stages for formaldehyde production (by bypassing methanol production step), successful formaldehyde production in this method can reduce the capital costs of the process. In addition, synthesis gas can be produced through biomass gasification process. Therefore, formaldehyde production through biomass gasification followed by direct synthesis from syngas can lead to a sustainable method of formaldehyde production. The presented thesis is focused on the single step production of formaldehyde from synthesis gas.

1.2 Research Aims

The general aim of this research is to develop and establish a new method of formaldehyde production based on direct synthesis from syngas. The first step is to investigate the possibility of the production of formaldehyde in this way theoretically and experimentally. It is critical to understand the conditions of the process in order to improve the yield. The previous attempts to convert synthesis gas directly into formaldehyde were done by using copper-zinc catalyst. It is very important to find a suitable catalyst for the process based on the conditions at which the experiment is conducted. Optimization of the operating conditions of the process to achieve higher yield of formaldehyde is the next step. A critical step is to investigate the reaction pathway since the bottleneck of the process may be identified through the reaction mechanism. The main aims of this study are summarised here:

- ❖ Feasibility study of the direct conversion of synthesis gas to formaldehyde
- ❖ Direct conversion of synthesis gas to formaldehyde in the gas phase and the slurry phase
- ❖ Investigation of the synthesis gas to formaldehyde reaction pathway
- ❖ The effect of solvents on the yield of formaldehyde in the slurry phase reaction of synthesis gas to formaldehyde

The results then can be used for further improvement of this process which may potentially lead to development of a novel renewable method of formaldehyde production. In the bigger picture, the results of this research can be the elementary steps towards the production of green formaldehyde.

1.3 Thesis Structure

The outline of this thesis is presented here:

Chapter 1: Introduction

This chapter includes the research background and aims as well as the thesis structure as presented here.

Chapter 2: Literature Review

This chapter contains a thorough literature review and discussion about different methods of formaldehyde production and it extensively explains the kinetics of the methanol partial oxidation reaction to formaldehyde. Some of the recent advancements in formaldehyde production are presented and other methods of formaldehyde synthesis are looked into. The contents of this chapter along with the simulation and exergy analysis study done on the methanol ballast process have been published as a journal paper in *Reviews in Chemical Engineering*.

Chapter 3: Formaldehyde Production via CO Hydrogenation in the Aqueous Phase

In chapter 3, the feasibility of direct formaldehyde production from synthesis gas is investigated theoretically using HSC Chemistry software TM. The experimental results of the formaldehyde production processes in the gas phase and in the slurry phase are presented and discussed. The catalyst characterization results are presented and the effects of temperature, pressure, Stirring speed, and the mass of the catalyst are studied. Some of the contents of this chapter are published as a journal paper in *Green Chemistry*.

Chapter 4: Reaction Mechanism of CO Hydrogenation to Formaldehyde in the Aqueous Phase

In this chapter, the reaction mechanism of the carbon monoxide hydrogenation reaction to formaldehyde in the aqueous phase is investigated. The reaction mechanism is studied based on the potential intermediate products in various samples collected from the reaction system during the process as well as determination of the source of atoms participating in the reaction. Based on this study, a paper is currently under preparation for publication.

Chapter 1

Chapter 5: Effect of Solvents on the Formaldehyde Production in the Slurry Reactor

The main aim of chapter 5 is to study the effect of solvents on the formaldehyde yield in the slurry reactor. The idea of catalytic carbon dioxide hydrogenation to formaldehyde is also introduced in this chapter for further studies. Based on this study, a paper is currently under preparation for publication.

Chapter 6: Conclusions

This chapter includes the outcomes of this research. It can be considered as the fulfilment of the aims of this project.

Chapter 7: Recommendations and Future Studies

In this chapter, the main recommendations for the future studies are presented.

Appendix: Published Journal Article Front Pages

1.4 References

- Bahmanpour, A. M., Hoadley, A., & Tanksale, A. (2014). Critical review and exergy analysis of formaldehyde production processes. *Reviews in Chemical Engineering*, 30(6), 583-604.
- Morgan, G. T., Hardy, D. V. N., & Proctor, R. A. (1932). Methanol condensation as modified by alkalized catalysts. *J. Soc. Chem. Ind., London*, 51, 1-7T.
- National Toxicology, P. (2010). Final report on carcinogens background document for formaldehyde. *Report on carcinogens background document (10-5981)*, i-512.
- Newton, R. H., & Dodge, B. F. (1933). The Equilibrium between Carbon Monoxide, Hydrogen, Formaldehyde and Methanol.1 I. The Reactions $\text{CO} + \text{H}_2 = \text{HCOH}$ and $\text{H}_2 + \text{HCOH} = \text{CH}_3\text{OH}$. *Journal of American Chemical Society*, 55(12).
- Ulukardesler, A. H., Atalay, S., & Atalay, F. S. (2010). Determination of optimum conditions and the kinetics of methanol oxidation. *Chemical Engineering and Technology*, 33(1), 167-176.

Monash University

Declaration for Thesis Chapter 2

Declaration by candidate

In the case of Chapter 2, the nature and extent of my contribution to the work was the following:

Nature of contribution	Extent of contribution (%)
Initiation	50
Modelling	100
Writing	70

The following co-authors contributed to the work. If co-authors are students at Monash University, the extent of their contribution in percentage terms must be stated:

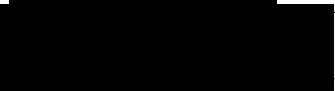
Name	Nature of contribution	Extent of contribution (%) for student co-authors only
Akshat	Initiation	
Tanksale	Reviewing and Editing the Paper	
Andrew	Initiation	
Hoadley	Reviewing and Editing the Paper	

The undersigned hereby certify that the above declaration correctly reflects the nature and extent of the candidate's and co-authors' contributions to this work.

Candidate's
Signature

 Date 24/09/15

Main
Supervisor's
Signature

 Date 24/09/15

This page is intentionally left blank

Chapter 2:

Literature Review

Abstract

Formaldehyde is one of the most important intermediate chemicals and has been produced industrially since 1889. Formaldehyde is a key feedstock in several industries like resins, polymers, adhesives and paints, making it one of the most valuable chemicals in the world. In this chapter, we study the leading commercial processes for formaldehyde production and compare them with recent advancements in catalysis and novel processes. This chapter compares, in extensive detail, the reaction mechanisms and kinetics of water ballast process (or BASF process), methanol ballast process, and Formox process. Thermodynamics of the reactions involved in the formaldehyde production process was investigated using HSC Chemistry™ software.

This Page is intentionally left blank

2.1 Introduction

Formaldehyde (HCHO) is one of the simplest molecules in organic chemistry which has a wide range of applications in chemical processes. It is produced in nature by photochemical processes in atmosphere or by incomplete combustion of organic materials (Reuss et al., 2003). HCHO gas is colorless at ambient temperature with an irritating odour which unfavorably affects eyes and skin. The effects of HCHO on human health have been studied. HCHO is toxic and probably a carcinogen since there is enough evidence that it can cause nasopharyngeal cancer (Cogliano et al., 2005). Some physical properties of monomeric HCHO can be found in Table 2.1 (Reuss et al., 2003):

Table 2.1: Physical properties of monomeric formaldehyde (Reuss et al., 2003)

Properties	Values
Heat of formation at 298.15 K	$-115.9 \pm 6.3 \text{ kJ.mol}^{-1}$
Gibbs energy at 298.15 K	$-109.9 \text{ kJ.mol}^{-1}$
Entropy at 298.15 K	$218.8 \pm 0.4 \text{ kJ.mol}^{-1}.\text{K}^{-1}$
Heat of combustion at 298.15 K	$-561.5 \text{ kJ.mol}^{-1}$
Heat of vaporization at 253.95 K	$23.32 \text{ kJ.mol}^{-1}$
Specific heat capacity at 298.15 K, C_p	$35.425 \text{ J.mol}^{-1}.\text{K}^{-1}$
Heat of solution at 296.15 K	
in water	-62 kJ.mol^{-1}
in methanol	$-62.8 \text{ kJ.mol}^{-1}$
in 1-propanol	$-59.5 \text{ kJ.mol}^{-1}$
in 1-butanol	$-62.4 \text{ kJ.mol}^{-1}$
Cubic expansion coefficient	$2.83 \times 10^{-3} \text{ K}^{-1}$
Specific magnetic susceptibility	-0.62×10^6
Vapour density relative to air	1.04

Chapter 2

HCHO heat of formation, heat capacity, and entropy are given in Table 2.2 for a wide range of temperatures and atmospheric pressure (J. F. Walker, 1967):

Table 2.2: Heat of formation, heat capacity, and entropy of formaldehyde (J. F. Walker, 1967)

Temperature (K)	Heat of formation (kJ.mol ⁻¹)	Heat capacity (J.mol ⁻¹ .K ⁻¹)	Entropy (J.mol ⁻¹ .K ⁻¹)
100	113.5	33.3	182.0
200	114.5	33.5	205.1
298.15	116.0	35.4	218.8
300	116.0	35.5	219.0
400	117.7	39.3	229.7
500	119.3	43.8	239.0
600	120.8	48.2	247.4
800	123.3	56.0	262.3
1000	125.0	62.0	275.5
2000	128.6	754.0	323.8
3000	130.9	79.6	355.4
4000	134.6	81.1	378.5
5000	140.5	81.9	396.7
6000	148.6	82.3	411.7

The gas mixture with air is flammable at 293.15 K or higher. HCHO is considered as a reactive compound. At high temperatures (>423.15 K) it tends to undergo heterogeneous decomposition to produce methanol (CH₃OH) and carbon dioxide (CO₂). But if the temperature goes higher (>623.15 K), it may tend to form synthesis gas (hydrogen (H₂) and carbon monoxide (CO) mixture) (Bone & Smith, 1905; Calvert & Steacie, 1951). It can be easily involved in both oxidation and reduction reactions. For example, in the presence of H₂ it can be reduced to form CH₃OH over a Ni catalyst. Nitric acid (HNO₃), potassium permanganate (KMnO₄), potassium dichromate (K₂Cr₂O₇), or oxygen (O₂) can readily oxidize HCHO to form formic acid (HCOOH), CO₂ and water (J. F. Walker, 1967). At atmospheric pressure, HCHO condenses at 253.95 K and freezes at 155.15 K as a white paste. In the liquid phase, its density is 0.8153 g/cm³ at 253.15K and 0.9172 g/cm³ at 193.15 K. The vapour pressure of the liquefied HCHO has been measured for a wide range of temperatures by Spence and Wild (1935). Measured partial pressures for the temperature range of 163.75 K to 250.85 K are tabulated in Table 2.3:

Table 2.3: Partial pressure of formaldehyde for the temperature range of 163.75 K to 250.85 K (Spence & Wild, 1935)

Temperature (K)	Pressure (kPa)
163.75	0.13
168.75	0.25
174.85	0.48
177.95	0.65
184.05	1.16
187.55	1.63
194.25	2.80
194.85	2.95
201.25	4.72
204.65	6.19
207.85	7.86
208.55	8.22
209.45	8.69
217.35	14.80
219.15	16.62
223.85	21.74
232.55	35.54
234.05	38.74
238.85	49.17
250.85	88.55

According to the measured values, the vapour pressure of liquid HCHO can be determined using the following equation (Spence & Wild, 1935):

$$\log_{10} p^* = -1429/T + 1.75 \log T - 0.0063T + 5.023 \quad (2.1)$$

where p^* is the HCHO vapour pressure in kPa and T is in K.

Many different common uses and industrial applications can be named for HCHO as it is one of the most important compounds in chemical manufacturing industry. HCHO is a building block in the synthesis of industrial resins such as melamine-formaldehyde, urea-formaldehyde and phenol-formaldehyde. Due to the applications of HCHO derivatives in wood processing and furniture, carpeting and textiles, and construction, this chemical is considered as an important material in the global economy (Tang et al., 2009). HCHO can also be used directly to produce other chemicals; glycolonitrile (C_2H_3NO) can be produced by HCHO reaction with hydrocyanic acid (HCN) (Kirk & Othmer, 1991). Acid catalysed reaction between HCHO and olefins may lead to the production of α -

Chapter 2

hydroxymethylated adducts (J. F. Walker, 1967). Methylamine can also be produced by the reaction of HCHO with amines. Due to its high ability to polymerize during long term storage, HCHO is commercially available as an aqueous solution of 37 wt% to 50 wt% concentration known as formalin. CH₃OH is usually added (10-12 wt%) in the solution as the polymerization inhibitor.

The HCHO production and consumption rate have significantly increased during recent years. From 2003 to 2006, the HCHO consumption rate grew at an average of 5.4% worldwide (Bizzari, 2007). In 2007, China as the largest HCHO producer and consumer produced 12 million metric tonnes of HCHO (Tang et al., 2009). Total global HCHO production is approximately 25 to 27 million metric tonnes per year and the growth of the consumption rate of this chemical has been fairly steady over the past twenty years (Ulukardesler et al., 2010). Considering its steady consumption rate and its application as a base chemical in more than 50 industries (Reuss et al., 2003), it is important to review the current production processes and identify novel technologies which may lead to more efficient and sustainable production in the future.

2.2 Formaldehyde Production

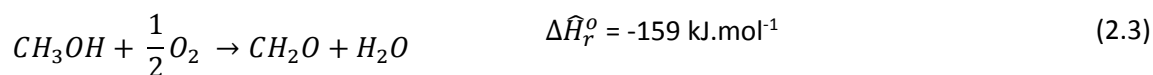
2.2.1 History

HCHO was first accidentally produced by Alexander Mikhailovich Butlerov in 1859 while he was attempting to produce methylene glycol (CH₂(OH)₂) by the hydrolysis of methylene acetate (Butlerov, 1859). In aqueous solutions, CH₂(OH)₂ is stable while isolation of this chemical leads to the decomposition of the unstable glycol to HCHO and water (F. Walker, 1933). Butlerov also produced solid HCHO polymers through the reaction between methylene iodide (CH₂I₂) and silver oxalate (Ag₂C₂O₄), but he did not realize that the monomer can be achieved by vaporization. He also prepared a new compound or polymer through the reaction between CH₂I₂ and silver oxide (Ag₂O). The new compound was reacted with ammonia (NH₃) to form a crystalline compound. Although he did not realise that HCHO was produced through his experiments, he stated that these reactions are expected to produce the unknown "formyl-aldehyde". In 1868, August Wilhelm von Hofmann produced and identified HCHO by passing CH₃OH vapour and air over a heated Pt spiral (Hofmann, 1868). Therefore he was the first person to produce HCHO by CH₃OH oxidation and identify the product. This process is still mainly used for HCHO production, with the changes in catalysts. By reacting hydrogen sulphide

(H₂S) and its acid solution, Hofmann was able to produce trithioformaldehyde ((CH₂S)₃) and later he was able to form HCHO polymer by vaporization of this chemical (Hofmann, 1869). According to Tollens proposal for regulation of the CH₃OH to air ratio and increasing the yield of the process, industrial production of HCHO was achieved in 1882 (Reuss et al., 2003). HCHO was first produced commercially by catalytic partial oxidation of CH₃OH with air over an unsupported Cu catalyst at atmospheric pressure. Later Cu was replaced by Ag to increase the yield from 43 - 47% yield using Cu to 67% using Ag) (Roeda, 2003; Trillat, 1903). There was an attempt to produce HCHO by non-catalytic oxidation of propane (C₃H₈) and butane (C₄H₁₀) in the United States. However, a wide range of co-products were produced and it required a complicated and costly separation system. Therefore, CH₃OH partial oxidation was the preferred choice of process (J. F. Walker, 1967) which is discussed further.

2.2.2 Industrial Methods

The sequence of HCHO production is made of three main stages- steam reforming of natural gas leads to the production of synthesis gas which is converted to CH₃OH via CH₃OH synthesis reaction (hydrogenation of CO) and eventually partial oxidation of CH₃OH leads to HCHO production. HCHO is industrially produced mainly through two major reactions; one is CH₃OH dehydrogenation (equation 2.2) and the other one is partial oxidation of CH₃OH (equation 2.3). These reactions are as follows:



Currently HCHO is industrially produced from CH₃OH using two major processes; the air deficient process or silver contact process through which CH₃OH goes through both dehydrogenation and partial oxidation reaction to produce HCHO (used by BASF, Borden, Bayer, Degussa, ICI, Celanese, DuPont, Mitsubishi and Mitsui) (Brenk, 2010; Qian et al., 2003). The other process involves an excess of air, known as the FORMOX process, in which only partial oxidation of CH₃OH takes place (used by Lummus, Montecatini, Hiag/Lurgi, and Perstorp/Reichold) (Brenk, 2010; Qian et al., 2003; Reuss et al., 2003). These two process routes are shown in a tree diagram in Figure 2.1. The air deficient process

Chapter 2

can be further classified into two types – the methanol ballast process and the water ballast process (or BASF process). In the methanol ballast process only CH_3OH and air are used in the reactant feed stream and low single pass CH_3OH conversion is achieved (used by ICI and Degussa). In the water ballast process, steam is also added to the feed stream and comparatively higher single pass CH_3OH conversion is achieved.

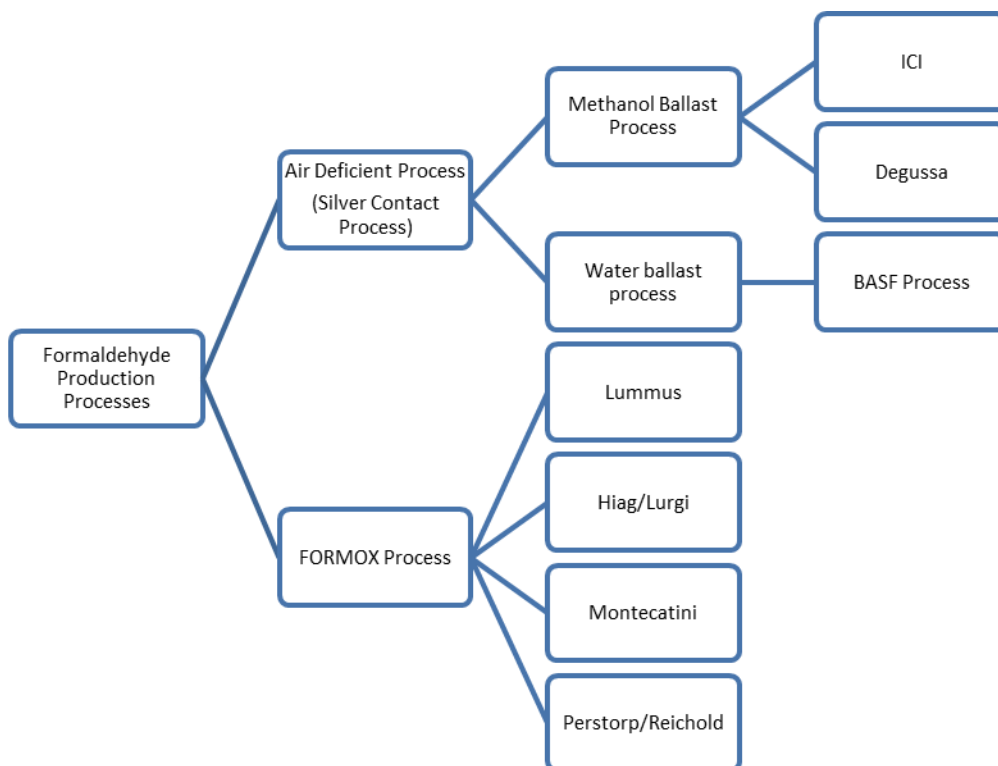


Figure 2.1: Tree diagram of industrial processes for formaldehyde production

2.2.2.1 Methanol Ballast Process

Methanol ballast process has been mentioned as one of the common methods of HCHO production in industry, used by some of the known producers of HCHO (e.g. ICI and Degussa)(Qian et al., 2003). In the ICI process (first patented in 1940 (Arthur & Maurice, 1940)), the silver crystals are formed in a 1 cm thick layer inside the reactor which is directly mounted on the heat recovery system. Silver crystal held by silver metal gauze is used in the Degussa process. The reactor operates at 788.15-823.15 K. In this method, heat is immediately recovered after the product stream leaves the reactor (Chauvel &

Lefebvre, 1989). Single pass conversion is relatively low in methanol ballast process and unconverted CH_3OH is recycled for higher overall conversion achievement.

2.2.2.2 BASF Process

The BASF process is the most widely applied industrial HCHO synthesis process and involves passing CH_3OH over a silver catalyst. A schematic diagram of the BASF process (Fig. 2.2) shows that a fresh mixture of CH_3OH and water enters an evaporator along with process air and is mixed with off-gas recycled from the absorption column. Part of the required heat in the evaporator is supplied by using the first stage of the absorption column. The reactor used in this process contains a thin layer of silver grains placed between silver gauze. A cooler is located immediately after the reactor to prevent further possible reactions.

In order to control the temperature of the reactor, the water content of the fresh feed and CH_3OH to O_2 ratio can be adjusted. The ratio controls the temperature of the process and determines the dominant reaction (either equation (2.2) or (2.3)) through which HCHO is produced. "Scheme A" shown in Fig. 2.2, contains overhead light components of the absorption column and heavier components can be recycled in "Scheme B". The desirable composition of the final formalin solution defines whether or not any of the mentioned streams should be used.

final product are affected by the water content of the fresh feed. Therefore, an optimum ratio should be used. The water to CH₃OH ratio of 2:3 or 0.67 has been suggested in literature (Reuss et al., 2003).

As mentioned before, both partial oxidation and direct dehydrogenation of CH₃OH take place when silver catalysts are used. However, the selectivity of HCHO can be limited considering the following reactions:



Methyl formate (C₂H₄O₂) and HCOOH are the other main by-products of this process and are generally removed as impurities by anion exchange.

2.2.2.3 FORMOX Process

Many researchers have discussed the effects of using other catalysts. The most important catalysts which have been discussed are iron/molybdenum or vanadium oxide in the Formox process. The Mo/Fe atomic ratio in this process is usually between 1.5 and 3. Small amounts of other materials such as V₂O₅, Cr₂O₃, CuO, P₂O₅ and CoO are also present in the catalyst. At atmospheric pressure, CH₃OH is almost completely converted in the temperature range of 543.15-673.15 K. However, if the temperature exceeds 743.15 K, oxidation of HCHO to CO becomes significant:



A schematic diagram of the FORMOX process is shown in Fig. 2.3. As it can be seen, the CH₃OH feed stream passes through a steam evaporator and enters the reactor. Similar to the BASF process, a cooler is located directly after the reactor. Products are cooled down to 383.15 K before entering the absorption column. One of the key controllers of the HCHO concentration in this process is the

Chapter 2

amount of water added at the top of absorption column. The product stream goes through an anion-exchange in order to minimize the formation of HCOOH . The final product stream contains up to 55 wt% HCHO and 0.5 – 1.5 wt% CH_3OH . CH_3OH conversion is around 98 to 99% in case of high selectivity and activity. The overall plant yield can be between 88 and 91%.

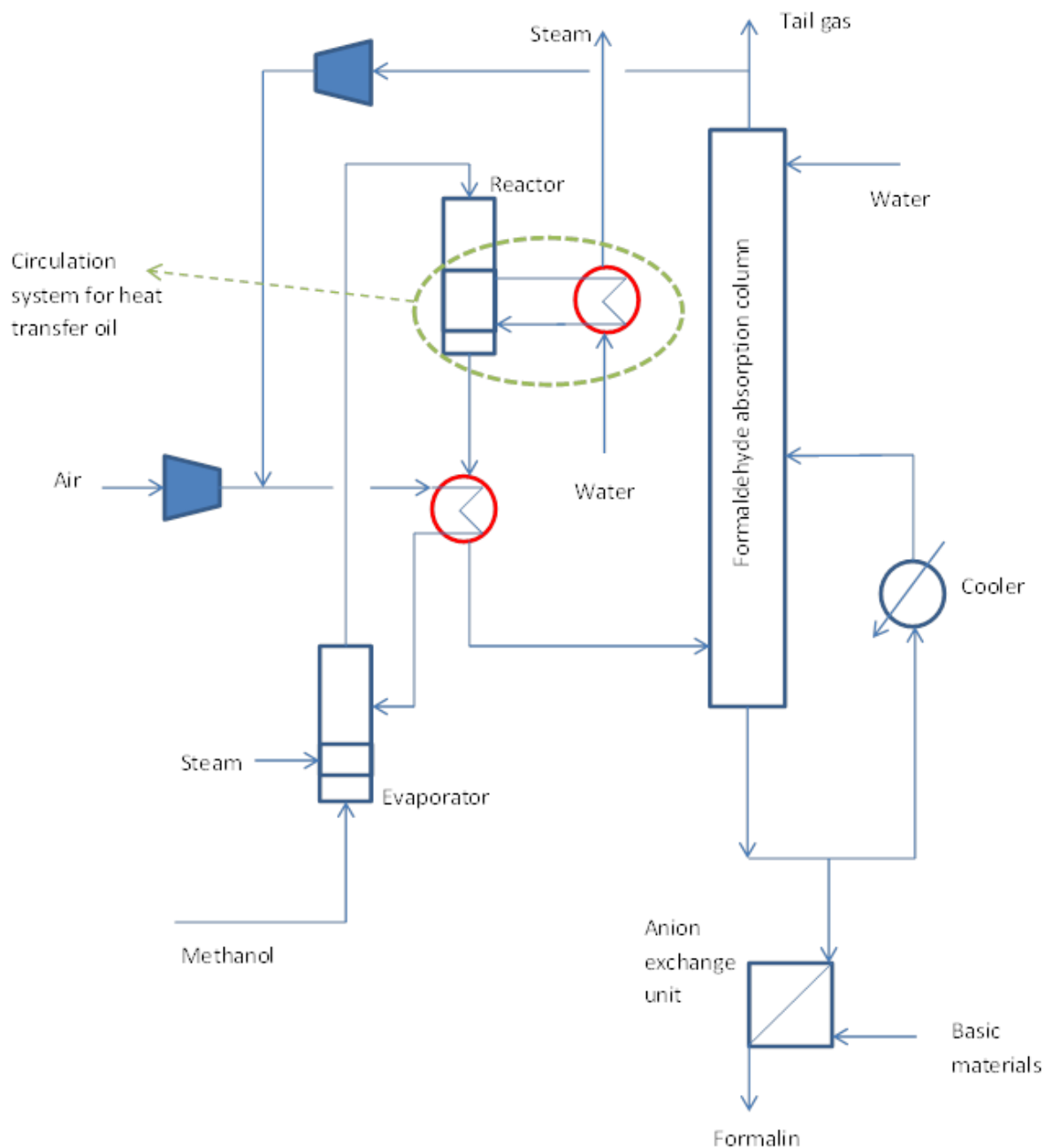


Figure 2.3: FORMOX process schematic diagram

Due to the lower temperature and the higher stability of the catalysts in the direct oxidation of CH₃OH to HCHO, this method is attracting more attention compared with the silver-based catalytic process. Adkins and Peterson (1931) reported Iron molybdenum as a suitable catalyst for CH₃OH oxidation to HCHO. It was commercially used as one of the main catalysts in the HCHO production process in the 1950s. In industrial processes, a combination of Fe₂(MoO₄)₃ and MoO₃ has been used as the catalyst this combination may have a higher life time and higher selectivity compared with pure Fe₂(MoO₄)₃ catalyst. The effects of different Mo to Fe atomic ratios in Fe₂(MoO₄)₃ catalysts on catalyst activity and selectivity towards HCHO have been investigated in literature and will be discussed in kinetics and mechanism section. It is found out that ratios above 1.5:1 provide desirable results (Soares et al., 2001).

2.2.3 Other Methods

There are many other methods through which HCHO can be produced. In many of these methods either CH₃OH or hydrocarbon gases are used as the source of HCHO production. Therefore, these methods are categorized in two groups as indicated below:

2.2.3.1 Other Formaldehyde Production Methods from Methanol

Many researchers have investigated other methods of HCHO production from CH₃OH using different operating conditions. Brackman (1959) reported that by passing O₂ through a stirred mixture of liquid CH₃OH and cupric nitrate tri-hydrate complex at 298.15 K, 80% yield of HCHO based on the amount of O₂ consumed can be achieved. Dehydrogenation of CH₃OH is another subject which has been discussed by some researchers (Newton & Dodge, 1933; Sabatier & Mailhe, 1910; B. A. Sexton, 1981; Su et al., 1992; Zaza et al., 1994); Sabatier and Mailhe (1910) studied this process and declared that this reaction is a reversible one. Later, Newton and Dodge (1933) derived the following equilibrium relation for this reversible reaction:

$$\log_{10} K_p = \left(\frac{4600}{T} - 8.48 \right) \quad (2.8)$$

Where T (K) is the equilibrium temperature and K_p is the equilibrium constant for this reaction. However, there are three undesirable side reactions which might occur during this process. They can

Chapter 2

be controlled by controlling the operating conditions. These reactions are pyrolytic decomposition of HCHO and oxidation to HCOOH, CO, CO₂ and water;



Aries (1960) described that elevated pressures in CH₃OH dehydrogenation process prevents the formation of HCOOH in the products stream. Passing CH₃OH and air over a finely divided silver catalyst at 202.65-1013.25 kPa and 973.15 to 1073.15 K, the product gas mixture contained HCHO, traces of water and unreacted CH₃OH, but no HCOOH.

Punderson (1960) suggested a combination of Ag, Cu and Si as a new CH₃OH dehydrogenation catalyst. According to his patent, by combination of 98.8% Ag, 1% Cu, and 0.2% Si, an active catalyst was made through which 70% CH₃OH conversion and 82% HCHO yield was possible. By using the combination of 97.8% Ag, 2% Cu, and 0.2% Si even better results were achieved, 71.5% CH₃OH conversion at the end of the seventh cycle in the process was achieved using the latter catalyst while it was exposed to pure CH₃OH vapour in the temperature range of 873.15-973.15 K.

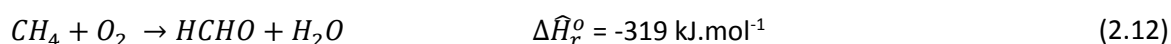
Considering the difficulty of the separation of HCHO from the water produced by partial oxidation of CH₃OH to HCHO, CH₃OH dehydrogenation has been studied as an alternative method using types of reactors such as inorganic membrane reactors (Deng & Wu, 1994) and slurry reactors (Shreiber & Roberts, 2000) using different catalysts.

2.2.3.2 Formaldehyde Production from Methane

Direct oxidation of methane (CH₄) to form HCHO is another method which has been extensively discussed (Blair & Wheeler, 1923; Polnišer et al., 2011; H. Zhang et al., 2006; X. Zhang et al., 2003). This process has the obvious advantage of producing HCHO in a single stage, however low selectivity and yield of HCHO are the main issues faced in this process (Bobrova et al., 2007). Many attempts have been made to increase the selectivity of HCHO and in some studies approximately 80% selectivity was achieved (J. Zhang et al., 2011), but the issue of low CH₄ conversion (<2%) remained unresolved. In a recent study (J. Zhang et al., 2012a), NO₂ has been introduced as a promoter and the process took

place in a very short residence time. Highest CH₄ conversion (24.3%) and yield (9%) was achieved in this study for this process so far. CO is the main by-product of this process.

Among the catalysts which have been used for partial oxidation of CH₄ to HCHO, iron oxide, molybdenum oxide (MoO₃), and vanadium oxide (V₂O₅) are the most common catalysts (He et al., 2009; Launay et al., 2007; X. Zhang et al., 2003). It is difficult to activate the relatively inert CH₄ on the surface of a catalyst in order to make HCHO considering the weak chemisorption of CH₄ on the catalyst surface (Michalkiewicz et al., 2008). CH₄ oxidation (eq. (2.12)) and HCHO oxidation (eq. (2.6)) occur in this process dominantly:



As it can be seen, further oxidation of HCHO may lead to CO₂ production for which oxygen should be the limiting reactant which significantly affects CH₄ conversion. Further considerations are that metal-oxygen bonds on the catalyst surface may lead to higher catalyst activity, but lower HCHO selectivity (Fajardo et al., 2008). High temperature increases the CH₄ activation and the kinetics of the process, but also leads to complete oxidation of CH₄ to CO₂, instead of HCHO synthesis (A. W. Sexton et al., 1998). In order to prevent unfavourable oxidation of HCHO to CO₂, a short residence time is required. One positive effect is that the high surface area of the catalyst support has been shown to improve CH₄ conversion (Bobrova et al., 2007).

2.3 Kinetics and Mechanism

In the following section, the reactions through which HCHO is being produced in industrial processes—namely partial oxidation and dehydrogenation of CH₃OH— are investigated and the kinetics and mechanism of the mentioned reactions are discussed.

2.3.1 Thermodynamic Investigation of the Reactions

The two main reactions which participate in HCHO production in industrial processes are partial oxidation of CH₃OH and CH₃OH dehydrogenation. Therefore, these reactions will be investigated thermodynamically in this section. The specifications of each reaction, including enthalpy, entropy,

Chapter 2

Gibbs free energy change, and equilibrium coefficients at different temperatures have been investigated using HSC Chemistry™ software. The results for the range of temperature of 273.15 to 1273.15 K for these reactions are tabulated in Tables 2.4 and 2.5:

Table 2.4: Thermodynamic conditions for CH₃OH partial oxidation

$$\text{CH}_3\text{OH}(g) + \frac{1}{2}\text{O}_2 \leftrightarrow \text{CH}_2\text{O}(g) + \text{H}_2\text{O}(g)$$

T	ΔH	ΔS	ΔG	Log(K)
K	kJ.mol ⁻¹	J.mol ⁻¹ .K ⁻¹	kJ.mol ⁻¹	
273.15	-149.694	64.454	-167.299	31.995
323.15	-149.182	66.180	-170.568	27.573
373.15	-148.761	67.392	-173.909	24.346
423.15	-148.424	68.243	-177.301	21.888
473.15	-148.162	68.829	-180.729	19.954
523.15	-147.971	69.214	-184.180	18.391
573.15	-147.845	69.446	-187.647	17.103
623.15	-147.777	69.560	-191.123	16.022
673.15	-147.760	69.586	-194.602	15.102
723.15	-147.788	69.546	-198.080	14.309
773.15	-147.854	69.458	-201.556	13.618
823.15	-147.952	69.336	-205.026	13.011
873.15	-148.075	69.191	-208.489	12.474
923.15	-148.219	69.030	-211.944	11.993
973.15	-148.382	68.858	-215.392	11.562
1023.15	-148.561	68.679	-218.830	11.173
1073.15	-148.754	68.495	-222.260	10.819
1123.15	-148.961	68.307	-225.680	10.497
1173.15	-149.172	68.123	-229.090	10.201
1223.15	-149.388	67.943	-232.492	9.929
1273.15	-149.610	67.765	-235.885	9.679

As it can be seen, the reaction is promising from the thermodynamics point of view. Enthalpy change does not change significantly with temperature. High equilibrium coefficients and highly negative Gibbs free energy change show high possibility of reaction. Negative Gibbs free energy change which decreases with temperature shows that increasing temperature makes the reaction “more spontaneous”. However, considering the reaction as an exothermic one, temperature increase lowers the equilibrium coefficient based on Le Chatelier’s principle.

Table 2.5: Thermodynamic conditions for CH₃OH dehydrogenation
$$\text{CH}_3\text{OH}(g) \leftrightarrow \text{CH}_2\text{O}(g) + \text{H}_2(g)$$

T	ΔH	ΔS	ΔG	Log(K)
K	kJ/mol	J/mol.K	kJ/mol	
273.15	91.887	108.018	62.382	-11.930
323.15	92.895	111.409	56.893	-9.197
373.15	93.805	114.030	51.254	-7.175
423.15	94.619	116.079	45.500	-5.617
473.15	95.346	117.706	39.654	-4.378
523.15	95.993	119.008	33.734	-3.369
573.15	96.566	120.054	27.757	-2.530
623.15	97.071	120.899	21.732	-1.822
673.15	97.513	121.583	15.670	-1.216
723.15	97.901	122.139	9.576	-0.692
773.15	98.238	122.589	3.458	-0.234
823.15	98.530	122.956	-2.681	0.170
873.15	98.782	123.254	-8.837	0.529
923.15	98.998	123.494	-15.006	0.849
973.15	99.180	123.686	-21.185	1.137
1023.15	99.329	123.836	-27.374	1.398
1073.15	99.446	123.948	-33.568	1.634
1123.15	99.532	124.026	-39.768	1.850
1173.15	99.595	124.081	-45.971	2.047
1223.15	99.633	124.113	-52.176	2.228
1273.15	99.649	124.125	-58.382	2.395

In this reaction, CH₃OH is dehydrogenated on the surface of the catalyst. The temperature increase is clearly in favour of this reaction. At low temperatures, the low equilibrium coefficient and the high positive Gibbs free energy show that the reaction may not occur at ambient conditions. In the temperature range of 1123.15-1173.15 K, the reaction becomes fairly spontaneous.

2.3.2 Kinetics of Reactions and Mechanism

Regarding the kinetics and mechanism of CH₃OH conversion to HCHO, the reactions will be discussed in different groups classified based on the catalysts used; Cu, Ag, and metal oxides. Since in the

Chapter 2

classical process of HCHO production Ag or Cu catalysts have been used, first the kinetics and mechanism related to the reactions of this group will be discussed and then metal oxide catalytic reactions for HCHO production are extensively studied.

2.3.2.1 Copper and Silver as Catalysts

HCHO was first produced commercially by catalytic partial oxidation of CH₃OH with air over an unsupported Cu catalyst at atmospheric pressure. Later Cu was replaced by Ag due the higher yield when using the latter as the catalyst (43 to 47% yield obtained using Cu and 67% using Ag) (Roeda, 2003; Trillat, 1903). Ag is also more selective towards forming HCHO compared with Cu (Thomas, 1920). A detailed study on kinetics and mechanism of CH₃OH oxidation on the surface of Cu (110) by flash decomposition spectroscopy was done by Wachs and Madix (1978b). In order to distinguish between the H atom on the hydroxyl group and the methyl group for mechanistic study, deuterium-substituted methanol (CH₃OD) was used. According to this study, chemisorption of CH₃OH on the surface of oxygen-free Cu was lower compared to the surface of pre-oxide Cu (110). CH₃OH was oxidized while adsorbed to make methoxide (CH₃O) and deuterium oxide (D₂O). Adsorption occurs at 180 K on the surface and produced CH₃O which was then decomposed to form HCHO and H₂ at 365 K. In a parallel way, but to a lesser extent, some of the chemisorbed CH₃OH was oxidized to form HCOO which in turn decomposed to CO₂ and H₂. Based on this study, both decomposition reactions occurred at a first order rate with the following rate constants:

$$k_{(H_2CO/CH_3OH)} = 5.2 \pm 1.6 \times 10^{12} e^{\left(\frac{-92.5 \pm 0.4(kJ.mol^{-1})}{RT}\right)} (s^{-1}) \quad (2.13)$$

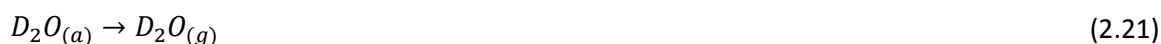
$$k_{(CO_2/CH_3OH)} = 8.0 \pm 2.0 \times 10^{13} e^{\left(\frac{-129.3 \pm 0.8(kJ.mol^{-1})}{RT}\right)} (s^{-1}) \quad (2.14)$$

As the researchers mentioned, the HCHO selectivity of the oxidation of CH₃OD on Cu (110) was 80% and CO₂ selectivity was 20%. Based on this study, the following mechanism was proposed for formation of HCHO from CH₃OH on a Cu surface:





A similar study was done by Wachs and Madix (1978a) on a silver surface, using temperature programmed reaction spectroscopy (TPRS) to distinguish between hydroxyl and methyl H atoms. They showed that the pre-oxide Ag surface showed a higher ability to dissociatively chemisorb CH₃OH on the catalyst surface. The process of CH₃OH oxidation on Ag (110) and Cu (110) was investigated and similarities and differences are verified. Based on this research, the following reactions are observed for Ag (110):



The amount of adsorbed CH₃OH increases as the O₂ exposure increases as a result of the interaction of the hydroxyl group of CH₃OH and surface O atom. CH₃O and D₂O form on the catalyst surface in both cases. However, unlike Cu, the adsorbed D₂O and O₂ on the Ag surface desorb eventually due to weaker binding compared with Cu. Based on the work by Wachs and Madix, the mechanism of CH₃OH oxidation over Cu and Ag do not differ significantly. However, considering different activities of these catalysts, different selectivity for each material is achieved. The Ag surface is more active for decomposition of intermediate products compared with Cu. Reaction 2.24 between CH₃O and HCHO

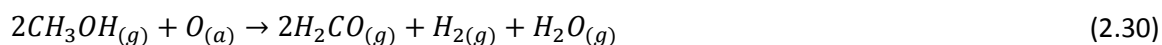
Chapter 2

to form $C_2H_4O_2$ was observed on the Ag surface, but not on Cu. This is due to the higher activity of Ag for the decomposition of adsorbed CH_3O to HCHO and hence HCHO is produced at a lower substrate temperature which increases the residence time of HCHO on the Ag surface.

A study by Francis et al. (1994) on CH_3OH oxidation over oxygenated Cu surface confirmed the results achieved earlier (Leibslle et al., 1994) that the kinetics of this reaction depends on initial oxygen exposure of the Cu surface and the surface temperature. At low temperatures (150-350 K) CH_3OH reacts with adsorbed oxygen in a 2:1 ratio to generate the adsorbed CH_3O species based on the following reaction:



The formed CH_3O is stable at this temperature range, however, as the temperature increases the stability of the formed CH_3O decreases and at medium temperatures (350-400 K), CH_3O decomposes to form HCHO and H_2 . Therefore, the following reaction is achieved:



At high temperatures (above 500 K), the stoichiometry of the reaction changes and CH_3OH reacts with adsorbed oxygen atom in a 1:1 ratio to form HCHO according to the following reaction:



This mechanism is confirmed by Barnes et al. (1990) because of the lack of H_2 production at temperatures below 320 K and above 470 K. The presence of surface oxygen is believed to be critical in this process. It is believed that pre-oxidizing is necessary in order to activate the surface of the catalyst. But over exposure of the catalyst to O_2 can poison the active sites and reduce the catalyst activity. Researchers proposed that as a dual site combination is necessary for high reactivity, overloading the catalyst with surface oxygen may disable the Cu^0 sites and consequently reduce the activity of the catalyst.

The effect of O_2 on the activation of Ag catalyst in the CH_3OH oxidation reaction has been investigated by many researchers. Based on the study done by Schlögl et. al. (Bao, Barth, et al., 1993; Bao, Muhler, et al., 1993; A. Nagy et al., 1998; A. J. Nagy et al., 1999), three types of O-Ag interactions can be found. (1) Dissociative chemisorption of molecular O_2 leads to atomic oxygen species adsorbed on the surface of the Ag (111) and Ag (110). This species is referenced as O_α and it participates in the CH_3OH oxidation

mechanism and oxygen desorption proposed by Wachs and Madix (1978a). (2) Atomic oxygen species, referenced as O_β , dissolves in Ag bulk and does not participate in the oxidation reaction directly. (3) Investigation of Ag (111) at temperatures around 900 K shows that atomic oxygen segregates from the bulk catalyst to the surface by interstitial diffusion to form the atomic oxygen species referenced as O_γ . There is a general agreement among the researchers that O_β does not participate in the oxidation reaction directly. However, there is a discussion about the effects of O_α and O_γ on the mechanism of this reaction. Some researchers have claimed that O_γ is likely to be the active agent in CH_3OH oxidative dehydrogenation since O_α desorbs at 600 K and it cannot be the dominant species on the catalyst surface for CH_3OH oxidation at 900 K (Bao, Muhler, et al., 1993). Based on Wachs and Madix (1978a), Andreasen et al. (2003) asserted that presence of O_α can justify the industrial HCHO synthesis process and O_γ is not necessarily involved, and that Schlögl group's conclusion about the leading role of O_γ is only valid at ultrahigh vacuum in which they have conducted their research. According to the study done by Waterhouse et al. (2004) the population of each atomic oxygen species depends on temperature and structure of the Ag catalyst. They declared that O_α species is dominant at low temperatures, while at industrial operating conditions, O_γ plays the leading role and drives the process towards oxidative dehydrogenation reaction. Van Veen et al. (2002) used a temporal-analysis-of-products method and pulse experiment to investigate the mechanism of oxidative hydrogenation of CH_3OH on Ag catalyst. Based on their findings, at temperatures higher than 550 K O_γ provides a highly selective oxidative hydrogenation reaction to generate HCHO where at lower temperatures O_α plays an important role in non-selective oxidation of CH_3OH at high surface coverage. However, according to their research, low coverage of O_α may improve the selectivity significantly. Some researchers have investigated the effects of different operating conditions on oxidation of CH_3OH and HCHO production using Ag catalyst. Based on a study done by Cao and Gavriilidis (2005), as reactor temperature increases from 500 K to 620 K, CO_2 production rate increases and HCHO selectivity decreases. This is in agreement with the results achieved by Van Veen et al. (2002) as they indicated a strong role of O_α in CO_2 production and low selectivity towards HCHO which is unlike the role of O_γ . As the reactor temperature exceeds 620 K, HCHO selectivity increases and CO_2 concentration decreases which proves the role of O_γ as indicated in the results by Van Veen et al. (2002). The O_2 concentration in the gas phase was another aspect which was investigated by Cao and Gavriilidis (2005). As the O_2 concentration increased from 1.6 to 3.68 Vol%, CO_2 concentration and CH_3OH conversion increased and HCHO selectivity decreased.

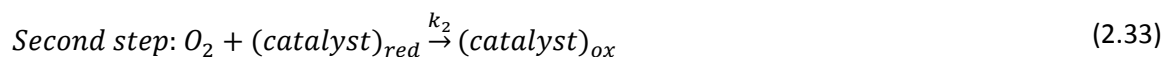
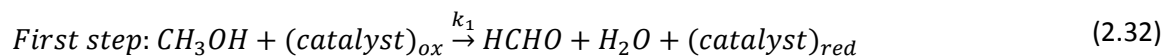
Chapter 2

Qian et al. (2003) investigated the effects of temperature on CH₃OH oxidation process and HCHO yield. HCHO yield gradually increased until it reached its maximum at 923 K. At higher temperatures, HCHO yield decreased which was accompanied by an increase in the yield of CO and H₂ which showed HCHO decomposition. They also investigated the effects of residence time on CH₃OH conversion and HCHO selectivity which showed that in the range of 0.06-0.45 s residence time, CH₃OH conversion increased while HCHO selectivity decreased at higher residence times. The effect of water vapour was also quantified by increasing the H₂O/CH₃OH molar ratio from 0 to 2. While CH₃OH conversion constantly increased with H₂O/CH₃OH ratio, HCHO selectivity reached its maximum at around the molar ratio of 0.75.

While many studies have discussed the kinetics, mechanism, and optimum operating conditions of the oxidation reaction on Cu and Ag catalysts, partial oxidation of CH₃OH on metal oxides has attracted higher attention. In the following section we discuss the application of metal oxides as catalysts.

2.3.2.2 Metal Oxides as Catalysts

Bailey and Craver (1921) patented a method of CH₃OH oxidation into HCHO using metal oxides (V₂O₅ in particular) as catalysts. Since then many researchers have investigated the kinetics and mechanism of the reactions which occur on the surface of these metal oxides in the presence of CH₃OH and other materials. In a kinetic study done by Bhattacharyya et al. (1967), the CH₃OH oxidation reaction was investigated at 519.15 K, 537.15 K and 554.15 K using V₂O₅ as the catalyst. Based on their study, the Mars-van Krevelen redox mechanism (Mars & van Krevelen, 1954) was suggested in which CH₃OH reduced the catalyst and formed HCHO and water (equation 2.32) and in the next step, O₂ exposure re-oxidized the reduced catalyst (equation 2.33):



According to their study, the following rate of reaction was obtained assuming a steady state pattern:

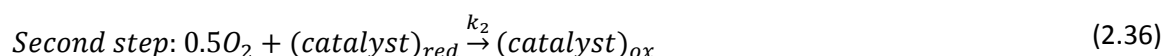
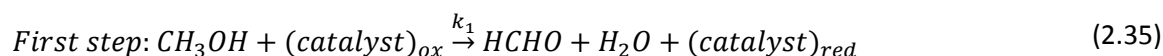
$$r = \frac{2k_1k_2P_mP_{O_2}}{k_1P_m + 2k_2P_{O_2}} \quad (2.34)$$

Where k_1 and k_2 refer to rate constants for the first and second step, respectively, which were evaluated at each temperature at which the reaction was investigated. The results are given in Table 2.6:

Table 2.6: Values for the first and the second rate constants for CH₃OH partial oxidation (Bhattacharyya et al., 1967)

Rate constants moles of HCHO/(moles of CH ₃ OH.s. m ³ .kPa)	Temperature (K)		
	519.15	537.15	554.15
k_1	2.96	5.93	15.3
k_2	0.26	0.49	1.09

In a more detailed study, Mann and Dosi (1973) studied the kinetics of the same reaction on vanadium oxide-molybdenum oxide (V₂O₅-MoO₃) in the range of temperatures (523.15 K to 803.15 K), catalyst metal oxides ratio (0 to 1), and CH₃OH concentration in air (5 to 10%). Based on their study, the best results were obtained at 733.15 K and by V₂O₅/MoO₃ weight ratio of 1/4. Optimum CH₃OH concentration in air is detected to be 8%. The same two-stage redox mechanism which was applied by Bhattacharyya et al. (1967), has been considered in this study, too:



Based on this research, the following rate equation is achieved for this reaction:

$$r = \frac{k_1 P_m}{1 + \left(\frac{k_1 P_m}{2k_2 P_{\text{O}_2}^{0.5}} \right)} \quad (2.37)$$

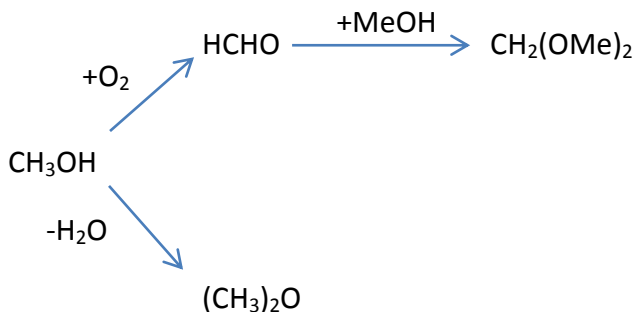
Where k_1 and k_2 are the rate constants for first and second step, respectively. The value of k_1 and k_2 can be found based on the Arrhenius-law-based equations given for these two rate constants:

Chapter 2

$$\log k_1 = 0.773 - \frac{2.358 \times 10^3}{T(K)} \quad (2.38)$$

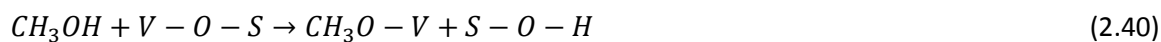
$$\log k_2 = 0.157 - \frac{2.04 \times 10^3}{T(K)} \quad (2.39)$$

Tatibouët and Germain (1981) investigated MoO₃ as catalyst for CH₃OH oxidation reaction. They used dilute CH₃OH–O₂ mixture (CH₃OH /O₂/He molar ratio = 8.2/19.7/72) in the range of 473.15-573.15 K and at atmospheric pressure and concluded that reaction may take two different paths based on the polymorphic crystalline form of MoO₃. On hexagonal surface of MoO₃ surface, CH₃OH goes through dehydration path and dimethyl ether (DME) is produced. Whereas on orthorhombic MoO₃, CH₃OH goes through partial oxidation to form HCHO which may react further with CH₃OH to form its acetal:



In an FTIR study, Busca (1989) observed formation of CH₃O groups upon CH₃OH adsorption over V₂O₅ catalyst. CH₃O groups in turn oxidized to form dioxymethylene (H₂CO₂). HCHO adsorption on the surface of V₂O₅ also formed H₂CO₂ which implies that desorption of H₂CO₂ formed during CH₃OH oxidation may lead to HCHO formation. However, Forzatti et al. (1997) found that at low temperatures (< 435 K) and high CH₃OH availability, H₂CO₂ may react with CH₃OH to form Dimethoxymethane (DMM) while it can preferably desorb as HCHO at high temperatures (> 435 K) and low CH₃OH availability. Therefore, high selectivity towards HCHO is achieved over weak HCHO binding sites of the catalyst. The type of support- such as acidic, basic, or redox- also affects the reaction pathways substantially. Deo and Wachs (1994), showed that different products, such as HCHO, DMM, DME, C₂H₄O₂, and oxides of carbon can be produced over different supports. These products depend upon the pathways taken by surface CH₃O over different supports. Acid sites cause CH₃OH dehydration and DME production. Basic sites oxidize CH₃OH to CH₃ and further convert it into CO and CO₂. On redox

sites, partial oxidation occurs and HCHO, DMM and C₂H₄O₂ can be produced. The desired pathway for HCHO formation is shown below in equations 40 to 42 (Burcham & Wachs, 1999).



SiO₂, ZrO₂, TiO₂, Nb₂O₅, and Al₂O₃ supported V₂O₅ were investigated by Deo and Wachs (1994) and the best results for each catalyst based on HCHO selectivity are tabulated in Table 2.7:

Table 2.7: Effects of different supports on the V₂O₅ performance in CH₃OH partial oxidation

Sample	TOF (s ⁻¹)	Selectivity%				
		FA	MF	DMM	DME	CO ₂ and CO
5% V ₂ O ₅ /SiO ₂	15.1×10 ⁻³	88	0	2	8	2
5% V ₂ O ₅ /ZrO ₂	1.6	94	5	Trace	Trace	Trace
1% V ₂ O ₅ /TiO ₂	2	99+	0	0	Trace	0
2% V ₂ O ₅ /Nb ₂ O ₅	1.2	97	0	1	2	0
20% V ₂ O ₅ /Al ₂ O ₃	6.8×10 ⁻²	46	0	3	50	1

According to these results, the highest HCHO selectivity (more than 99%) and the highest turnover frequency (2 s⁻¹) was achieved by using TiO₂ as the support. Nb₂O₅ also showed high selectivity towards HCHO (97%). Based on the results gained, the reactivity of the supported V₂O₅ as CH₃OH oxidation catalyst depended on the strength of the V-O-Support bond, meaning that the weaker the V-O-Support bond was the higher catalytic reactivity was achieved.

Adkins and Peterson (1931) reported 38% O₂ conversion and 100% O₂ selectivity for HCHO production over MoO₃ catalyst using CH₃OH partial oxidation. Higher O₂ conversion was achieved over FeO₂ but mostly CO₂ was formed which meant complete oxidation of CH₃OH. Mixed oxides of Fe and Mo showed high conversion (>90%) and high selectivity for HCHO and CO. Soares et al. (2001) studied the effects of Mo to Fe atomic ratio by comparing industrial Fe-Mo oxides catalyst (Mo/Fe = 3) with stoichiometric composition (Mo/Fe = 1.5). Higher Mo/Fe atomic ratio resulted in higher surface area and higher selectivity of the catalyst towards HCHO production. However, the activity of the catalyst did not change significantly. Therefore it can be concluded that the Fe₂(MoO₄)₃ stoichiometric phase is the active phase of the catalyst. Wachs' group (Routray et al., 2010) showed that if excess MoO_x is

Chapter 2

added to crystalline $\text{Fe}_2(\text{MoO}_4)_3$ it is deposited as surface monolayer which improves the catalytic performance towards HCHO production. Contrary to Soares et al. (2001), Wach's group (Routray et al., 2010) found that stoichiometric $\text{Fe}_2(\text{MoO}_4)_3$ (Mo/Fe=1.5) has higher surface area compared with catalysts with excess molybdenum oxide. Wach's group (Routray et al., 2010) achieved highest selectivity towards HCHO by using the catalyst Mo/Fe = 2. However, the turnover frequency was higher when using the catalyst Mo/Fe = 1.7. Based on the mechanism suggested for CH_3OH oxidation reaction over FeO_2 and the one for Fe-Mo oxide by Wach's group (Routray et al., 2010), they have concluded that due to the dependence of the HCHO production pathway on the presence of bulk lattice oxygen and considering the incapability of FeO_2 to supply bulk lattice oxygen, the chance of formation of HCHO on FeO_2 is low. On the other hand, considering the high availability of bulk lattice oxygen on the surface of the Fe-Mo catalyst, HCHO and probably DMM may form on the surface of the Fe-Mo catalyst. The following rate of reaction is suggested by the researchers:

$$r = k_{rds}K_{ads}P_{\text{CH}_3\text{OH}}N_s \quad (2.43)$$

Where k_{rds} is the first order rate constant (s^{-1}), K_{ads} is the CH_3OH adsorption equilibrium constant (kPa^{-1}), P represents CH_3OH partial pressure (kPa), and N_s is the surface density of redox sites ($\mu\text{mol.m}^{-2}$).

Based on the studies done by many researchers, many improvements and developments have occurred in this field. However, there are still some issues that can be addressed.

2.4 Latest Advancements in Formaldehyde Production

The recent studies done on HCHO production can mainly be divided into two sections; some of these studies investigated the effects of different modifications done on industrial catalysts for partial oxidation of CH_3OH to produce HCHO. Bell's group (Vining et al., 2011, 2012) investigated the effects of additional zirconium dioxide (ZrO_2) and cerium dioxide (CeO_2) on SiO_2 supported V_2O_5 catalyst for CH_3OH partial oxidation. They found out that by using these bi-layered catalysts, the turnover frequency increased by nearly two orders of magnitude for CH_3OH oxidation compared with mono-layered catalyst. They proposed that the addition of CeO_2 and ZrO_2 can affect the rate-limiting step in the mechanism of CH_3OH partial oxidation which is hydrogen abstraction from V-OCH₃ group. Other researchers have studied other methods for HCHO production. Some recent studies (Beznis et al., 2011; Carlsson et al., 2012; Polnišer et al., 2011; Wang et al., 2012; J. Zhang et al., 2012a, 2012b) have

targeted the CH₄ reactivity and the selectivity towards HCHO production in the process of direct oxidation of CH₄ to HCHO. Exposing the reactants to NO₂ using low residence time (J. Zhang et al., 2012a, 2012b), using periodic operating conditions (Carlsson et al., 2012), and using Cu-Fe pyrophosphate as the catalyst (Polnišer et al., 2011) were suggested. However, simultaneous increase of CH₄ conversion and HCHO selectivity remained unsolved. Lou et al (Lou, Wang, et al., 2007; Lou, Zhang, et al., 2007) suggested using C₂H₆ instead of CH₄. They used a mesoporous SiO₂ supported MoO₃ catalyst to achieve 30% HCHO yield by oxidation of C₂H₄ to HCHO at 836 K. Using a double bed catalyst for simultaneous dehydrogenation of C₂H₆ to C₂H₄ and oxidation of C₂H₄ to HCHO, maximum of 14% HCHO yield was achieved. Since anhydrous dehydrogenation of CH₃OH to HCHO has been an interesting process for researchers because it avoids the formation of water, a recent study was dedicated to the theoretical investigation of this process by using a web-based application called "CatApp" (Lausche et al., 2012). Based on this study, the mechanism of CH₃OH dehydrogenation reaction and different binding energies were investigated over different metal surfaces. They claimed that on the surface of Pt, Pd, and Rh, there is a higher tendency to dehydrogenate HCHO compared with desorption of this chemical. This may lead to CO formation on the surface of these metals as indicated in a study by Tolmactsov et al. (2009).

Although hydrogenation of CO₂ to HCHO was investigated before (Lunev et al., 2001), a high yield of HCHO was never achieved. Recently, Nakata et al. (2014) succeeded to produce HCHO by reduction of CO₂ in an electrochemical procedure. A boron-doped diamond (BDD) electrode was used for electrochemical process under ambient conditions and HCOOH was produced as an intermediate. Relatively high faradaic efficiency (up to 74%) was achieved by using CH₃OH, aqueous salt, or seawater as the electrolyte. Other electrodes such as glassy carbon, tin (Sn), Cu, Ag, and tungsten (W) were used for comparison. The highest faradaic efficiency (74%) for HCHO was achieved by using BDD electrode while HCOOH faradaic efficiency was 15%. Faradaic efficiency for HCHO was about 20% using glassy carbon electrode. No HCHO production was noticed using metal electrodes.

Hydrogenation of CO₂ is not the only method of producing HCHO from CO₂. Recently, in a study by Lambert's group (Gómez-Ramírez et al., 2014), low temperature HCHO production was achieved by partial oxidation of C₂H₆ by using CO₂ as the oxygen source. The catalyst for this process was V₂O₅/Al₂O₃ which was dispersed on barium titanate (BaTiO₃). The catalyst was loaded on a dielectric barrier discharge reactor. Catalyst was activated at near ambient temperature by plasma-excited CO₂ which led to generation of an activated oxide surface. Through the activated catalyst, oxy-

Chapter 2

dehydrogenation of C_2H_6 took place to produce C_2H_4 . Discharge-activated CO_2 molecules reacted with the produced C_2H_4 molecules at this level to generate acetaldehyde (CH_3CHO) which in turn converted to HCHO through oxidative decomposition. 11.4% HCHO yield was achieved through this process upon complete conversion of C_2H_6 .

In a recent study, the industrial process of HCHO production (starting from natural gas steam reforming followed by CH_3OH synthesis and methanol ballast process to form HCHO) was simulated. An exergy analysis was done to measure the exergy efficiency of the process. It is shown that the industrial process suffers from ~57% losses of exergy (Bahmanpour et al., 2014). Therefore, there is a need to improve the HCHO production process.

2.5 Conclusion

Formaldehyde (HCHO) is a highly valuable chemical in the global economy. Methanol synthesis followed by partial oxidation into HCHO is still the leading technology after more than a century; however, new catalysts and process modifications have been made over the years to increase conversion and selectivity of HCHO synthesis. The mechanism of CH_3OH partial oxidation showed that the reaction proceeds via oxidation of gaseous CH_3OH by adsorbed oxygen or hydroxyl species on the catalyst surface to form adsorbed CH_3O species, which decomposes to form HCHO depending upon the reaction temperature. Pre-oxidation of Cu or Ag catalysts to form metal oxides were found to be more active than metals as catalysts for partial oxidation of CH_3OH to HCHO. However, since CH_3O is stable at low temperatures, the reaction is carried out at above 623.15 K. Different types of atomic oxygen species were found to be active in the HCHO production reactions when Ag catalyst was used. Mars-van Krevelen redox mechanism was suggested for the formation of HCHO on the surface of metal oxide catalysts by some researchers and the effects of the addition of the excess MoO_3 in Fe-Mo oxide catalysts were argued. Many recent attempts at improving the HCHO synthesis process have focused on developing new redox catalysts to improve the CH_3OH partial oxidation process. Other proposed methods for HCHO production such as hydrogenation of CO and CO_2 , and C_2H_4 oxidation hold much promise but extensive research is required in catalyst development for these processes.

2.6 References

- Adkins, H., & Peterson, W. R. (1931). The oxidation of methanol with air over iron, molybdenum, and iron-molybdenum oxides. *Journal of the American Chemical Society*, 53(4), 1512-1520.
- Andreasen, A., Lynggaard, H., Stegelmann, C., & Stoltze, P. (2003). A microkinetic model of the methanol oxidation over silver. *Surface Science*, 544(1), 5-23.
- Aries, R. S. (1960). United States Patent No. US2953602.
- Arthur, B. W., & Maurice, N. D. (1940). US2196188 A.
- Bahmanpour, A. M., Hoadley, A., & Tanksale, A. (2014). Critical review and exergy analysis of formaldehyde production processes. *Reviews in Chemical Engineering*, 30(6), 583-604.
- Bailey, G. C., & Craver, A. E. (1921). United States Patent No. US1383059.
- Bao, X., Barth, J. V., Lehmpfuhl, G., Schuster, R., Uchida, Y., Schlögl, R., et al. (1993). Oxygen-induced restructuring of Ag(111). *Surface Science*, 284(1-2), 14-22.
- Bao, X., Muhler, M., Pettinger, B., Schlögl, R., & Ertl, G. (1993). On the nature of the active state of silver during catalytic oxidation of methanol. *Catalysis Letters*, 22(3), 215-225.
- Barnes, C., Pudney, P., Guo, Q., & Bowker, M. (1990). Molecular-beam studies of methanol partial oxidation on Cu(110). *Journal of the Chemical Society, Faraday Transactions*, 86(15), 2693-2699.
- Beznis, N. V., Van Laak, A. N. C., Weckhuysen, B. M., & Bitter, J. H. (2011). Oxidation of methane to methanol and formaldehyde over Co-ZSM-5 molecular sieves: Tuning the reactivity and selectivity by alkaline and acid treatments of the zeolite ZSM-5 agglomerates. *Microporous and Mesoporous Materials*, 138(1-3), 176-183.
- Bhattacharyya, S. K., Janakiram, K., & Ganguly, N. D. (1967). Kinetics of the vapor-phase oxidation of methyl alcohol on vanadium pentoxide catalyst. *Journal of Catalysis*, 8(2), 128-136.
- Bizzari, S. N. (2007). *CEH Marketing Research Report: Formaldehyde*.
- Blair, E. W., & Wheeler, T. S. (1923). The estimation of formaldehyde and acetaldehyde. *The Analyst*, 48(564), 110-112.
- Bobrova, I. I., Bobrov, N. N., Simonova, L. G., & Parmon, V. N. (2007). Direct catalytic oxidation of methane to formaldehyde: New investigation opportunities provided by an improved flow circulation method. *Kinetics and Catalysis*, 48(5), 676-692.
- Bone, W. A., & Smith, H. L. (1905). XCIV. - The thermal decomposition of formaldehyde and acetaldehyde. *Journal of the Chemical Society, Transactions*, 87, 910-916.
- Brackman, W. (1959). United States Patent No. US2883426.
- Brenk, M. (2010). WO2010022923 A1.
- Burcham, L. J., & Wachs, I. E. (1999). The origin of the support effect in supported metal oxide catalysts: In situ infrared and kinetic studies during methanol oxidation. *Catalysis Today*, 49(4), 467-484.
- Busca, G. (1989). On the mechanism of methanol oxidation over vanadia-based catalysts: a FT-IR study of the adsorption of methanol, formaldehyde and formic acid on vanad. *Journal of Molecular Catalysis*, 50(2), 241-249.
- Butlerov, A. M. (1859). Ueber einige Derivate des Iodmethylens. *Ann.*, 111, 242-252.
- Calvert, J. G., & Steacie, E. W. R. (1951). Vapor phase photolysis of formaldehyde at wavelength 3130Å. *The Journal of Chemical Physics*, 19(2), 176-182.
- Cao, E., & Gavriilidis, A. (2005). Oxidative dehydrogenation of methanol in a microstructured reactor. *Catalysis Today*, 110(1-2), 154-163.

Chapter 2

- Carlsson, P. A., Jing, D., & Skoglundh, M. (2012). Controlling selectivity in direct conversion of methane into formaldehyde/methanol over iron molybdate via periodic operation conditions. *Energy and Fuels*, 26(3), 1984-1987.
- Chauvel, A., & Lefebvre, G. (1989). *Petrochemical Processes (Volume 1: Synthesis-Gas Derivatives and Major Hydrocarbons)*: Institut Francais du Petrole Publications.
- Cogliano, V. J., Grosse, Y., Baan, R. A., Straif, K., Secretan, M. B., & El Ghissassi, F. (2005). Meeting report: summary of IARC monographs on formaldehyde, 2-butoxyethanol, and 1-tert-butoxy-2-propanol.
- Deng, J., & Wu, J. (1994). Formaldehyde production by catalytic dehydrogenation of methanol in inorganic membrane reactors. *Applied Catalysis A, General*, 109(1), 63-76.
- Deo, G., & Wachs, I. E. (1994). Reactivity of Supported Vanadium Oxide Catalysts: The Partial Oxidation of Methanol. *Journal of Catalysis*, 146(2), 323-334.
- Fajardo, C. A. G., Niznansky, D., N'Guyen, Y., Courson, C., & Roger, A. C. (2008). Methane selective oxidation to formaldehyde with Fe-catalysts supported on silica or incorporated into the support. *Catalysis Communications*, 9(5), 864-869.
- Forzatti, P., Tronconi, E., Elmi, A. S., & Busca, G. (1997). Methanol oxidation over vanadia-based catalysts. *Applied Catalysis A: General*, 157(1-2), 387-408.
- Francis, S. M., Leibsle, F. M., Haq, S., Xiang, N., & Bowker, M. (1994). Methanol oxidation on Cu(110). *Surface Science*, 315(3), 284-292.
- Gómez-Ramírez, A., Rico, V. J., Cotrino, J., González-Elipe, A. R., & Lambert, R. M. (2014). Low temperature production of formaldehyde from carbon dioxide and ethane by plasma-Assisted catalysis in a ferroelectrically moderated dielectric barrier discharge reactor. *ACS Catalysis*, 4(2), 402-408.
- He, J., Li, Y., An, D., Zhang, Q., & Wang, Y. (2009). Selective oxidation of methane to formaldehyde by oxygen over silica-supported iron catalysts. *Journal of Natural Gas Chemistry*, 18(3), 288-294.
- Hofmann, A. W. v. (1868). Zur Kenntniss des Methylaldehyds. *Ann.*, 145, 357.
- Hofmann, A. W. v. (1869). Zur Kenntniss des Methylaldehyds II. *Ber.*, 2, 152-160.
- Kirk, R. E., & Othmer, D. F. (1991). *Kirk-Othmer Encyclopedia of Chemical Technology*: John Wiley and Sons.
- Launay, H., Loidant, S., Nguyen, D. L., Volodin, A. M., Dubois, J. L., & Millet, J. M. M. (2007). Vanadium species in new catalysts for the selective oxidation of methane to formaldehyde: Activation of the catalytic sites. *Catalysis Today*, 128(3-4 SPEC. ISS.), 176-182.
- Lausche, A. C., Hummelshoj, J. S., Abild-Pedersen, F., Studt, F., & Norskov, J. K. (2012). Application of a new informatics tool in heterogeneous catalysis: Analysis of methanol dehydrogenation on transition metal catalysts for the production of anhydrous formaldehyde. *Journal of Catalysis*, 291, 133-137.
- Leibsle, F. M., Francis, S. M., Haq, S., & Bowker, M. (1994). Aspects of formaldehyde synthesis on Cu(110) as studied by STM. *Surface Science*, 318(1-2), 46-60.
- Lou, Y., Wang, H., Zhang, Q., & Wang, Y. (2007). SBA-15-supported molybdenum oxides as efficient catalysts for selective oxidation of ethane to formaldehyde and acetaldehyde by oxygen. *Journal of Catalysis*, 247(2), 245-255.
- Lou, Y., Zhang, Q., Wang, H., & Wang, Y. (2007). Catalytic oxidation of ethylene and ethane to formaldehyde by oxygen. *Journal of Catalysis*, 250(2), 365-368.
- Lunev, N. K., Shmyrko, Y. I., Pavlenko, N. V., & Norton, B. (2001). Selective formation of formaldehyde from carbon dioxide and hydrogen over PtCu/SiO₂. *Applied Organometallic Chemistry*, 15(2), 148-150.

- Mann, R. S., & Dosi, M. K. (1973). Kinetics of vapor-phase oxidation of methyl alcohol on vanadium pentoxide-molybdenum trioxide catalyst. *Journal of Catalysis*, 28(2), 282-288.
- Mars, P., & van Krevelen, D. W. (1954). Oxidations carried out by means of vanadium oxide catalysts. *Chemical Engineering Science*, 3, Supplement 1(0), 41-59.
- Michalkiewicz, B., Sreńscek-Nazzal, J., Tabero, P., Grzmil, B., & Narkiewicz, U. (2008). Selective methane oxidation to formaldehyde using polymorphic T-, M-, and H-forms of niobium(V) oxide as catalysts. *Chemical Papers*, 62(6), 106-113.
- Nagy, A., Mestl, G., Rühle, T., Weinberg, G., & Schlögl, R. (1998). The dynamic restructuring of electrolytic silver during the formaldehyde synthesis reaction. *Journal of Catalysis*, 179(2), 548-559.
- Nagy, A. J., Mestl, G., Herein, D., Weinberg, G., Kitzelmann, E., & Schlögl, R. (1999). The correlation of subsurface oxygen diffusion with variations of silver morphology in the silver-oxygen system. *Journal of Catalysis*, 182(2), 417-429.
- Nakata, K., Ozaki, T., Terashima, C., Fujishima, A., & Einaga, Y. (2014). High-yield electrochemical production of formaldehyde from CO₂ and seawater. *Angewandte Chemie - International Edition*, 53(3), 871-874.
- Newton, R. H., & Dodge, B. F. (1933). The Equilibrium between Carbon Monoxide, Hydrogen, Formaldehyde and Methanol. I. The Reactions CO + H₂ = HCOH and H₂ + HCOH = CH₃OH. *Journal of American Chemical Society*, 55(12).
- Polnišer, R., Štolcová, M., Hronec, M., & Mikula, M. (2011). Structure and reactivity of copper iron pyrophosphate catalysts for selective oxidation of methane to formaldehyde and methanol. *Applied Catalysis A: General*, 400(1-2), 122-130.
- Punderson, J. O. (1960). United States Patent No.
- Qian, M., Liauw, M. A., & Emig, G. (2003). Formaldehyde synthesis from methanol over silver catalysts. *Applied Catalysis A: General*, 238(2), 211-222.
- Reuss, G., Disteldorf, W., Gamer, A. O., & Hilt, A. (2003). *Ullmann's Encyclopedia of Industrial Chemistry* (6 ed. Vol. 15). Weinheim: Wiley.
- Roeda, D. D., F. (2003). Preparation of formaldehyde using a silver-containing ceramic catalyst. *Journal of Labelled Compounds and Radiopharmaceuticals*, 46, 449.
- Routray, K., Zhou, W., Kiely, C. J., Grünert, W., & Wachs, I. E. (2010). Origin of the synergistic interaction between MoO₃ and iron molybdate for the selective oxidation of methanol to formaldehyde. *Journal of Catalysis*, 275(1), 84-98.
- Sabatier, P., & Mailhe, A. (1910). Actions des oxydes métalliques sur les alcools primaires. *Ann. Chim. Phys.*, 20, 289-352.
- Sexton, A. W., Kartheuser, B., Batiot, C., Zanthoff, H. W., & Hodnett, B. K. (1998). The limiting selectivity of active sites on vanadium oxide catalysts supported on silica for methane oxidation to formaldehyde. *Catalysis Today*, 40(2-3), 245-250.
- Sexton, B. A. (1981). Methanol decomposition on platinum (111). *Surface Science*, 102(1), 271-281.
- Shreiber, E. H., & Roberts, G. W. (2000). Methanol dehydrogenation in a slurry reactor: Evaluation of copper chromite and iron/titanium catalysts. *Applied Catalysis B: Environmental*, 26(2), 119-129.
- Soares, A. P. V., Farinha Portela, M., Kiennemann, A., Hilaire, L., & Millet, J. M. M. (2001). Iron molybdate catalysts for methanol to formaldehyde oxidation: Effects of Mo excess on catalytic behaviour. *Applied Catalysis A: General*, 206(2), 221-229.
- Spence, R., & Wild, W. (1935). The thermal reaction between chlorine and formaldehyde. *Journal of the American Chemical Society*, 57(6), 1145-1146.
- Su, S., Prairie, M. R., & Renken, A. (1992). Reaction mechanism of methanol dehydrogenation on a sodium carbonate catalyst. *Applied Catalysis A, General*, 91(2), 131-142.

Chapter 2

- Tang, X., Bai, Y., Duong, A., Smith, M. T., Li, L., & Zhang, L. (2009). Formaldehyde in China: Production, consumption, exposure levels, and health effects. *Environment International*, 35(8), 1210-1224.
- Tatibouët, J. M., & Germain, J. E. (1981). A structure-sensitive oxidation reaction: Methanol on molybdenum trioxide catalysts. *Journal of Catalysis*, 72(2), 375-378.
- Thomas, M. D. (1920). PREPARATION OF FORMALDEHYDE.1. *Journal of the American Chemical Society*, 42(5), [867]-882.
- Tolmacsov, P., Gazsi, A., & Solymosi, F. (2009). Decomposition and reforming of methanol on Pt metals supported by carbon Norit. *Applied Catalysis A: General*, 362(1-2), 58-61.
- Trillat, A. (1903). Investigation on the Catalytic Oxidation of the Alcohols. *Bulletin de la Societe Chimique de France*, 29(3), 35.
- Ulukardesler, A. H., Atalay, S., & Atalay, F. S. (2010). Determination of optimum conditions and the kinetics of methanol oxidation. *Chemical Engineering and Technology*, 33(1), 167-176.
- Van Veen, A. C., Hinrichsen, O., & Muhler, M. (2002). Mechanistic studies on the oxidative dehydrogenation of methanol over polycrystalline silver using the temporal-analysis-of-products approach. *Journal of Catalysis*, 210(1), 53-66.
- Vining, W. C., Strunk, J., & Bell, A. T. (2011). Investigation of the structure and activity of VO_x/ZrO₂/SiO₂ catalysts for methanol oxidation to formaldehyde. *Journal of Catalysis*, 281(2), 222-230.
- Vining, W. C., Strunk, J., & Bell, A. T. (2012). Investigation of the structure and activity of VO_x/CeO₂/SiO₂ catalysts for methanol oxidation to formaldehyde. *Journal of Catalysis*, 285(1), 160-167.
- Wachs, I. E., & Madix, R. J. (1978a). The oxidation of methanol on a silver (110) catalyst. *Surface Science*, 76(2), 531-558.
- Wachs, I. E., & Madix, R. J. (1978b). The selective oxidation of CH₃OH to H₂CO on a copper(110) catalyst. *Journal of Catalysis*, 53(2), 208-227.
- Walker, F. (1933). Early history of acetaldehyde and formaldehyde: A chapter in the history of organic chemistry. *Journal of Chemical Education*, 546-551.
- Walker, J. F. (1967). *Formaldehyde* (3 ed. Vol. 12). New York: Reinhold Publishing Corporation.
- Wang, Z. C., Dietl, N., Kretschmer, R., Ma, J. B., Weiske, T., Schlangen, M., et al. (2012). Direct conversion of methane into formaldehyde mediated by [Al₂O₃]₊ at room temperature. *Angewandte Chemie - International Edition*, 51(15), 3703-3707.
- Waterhouse, G. I. N., Bowmaker, G. A., & Metson, J. B. (2004). Influence of catalyst morphology on the performance of electrolytic silver catalysts for the partial oxidation of methanol to formaldehyde. *Applied Catalysis A: General*, 266(2), 257-273.
- Zaza, P., Randall, H., Doepper, R., & Renken, A. (1994). Dynamic kinetics of catalytic dehydrogenation of methanol to formaldehyde. *Catalysis Today*, 20(3), 325-334.
- Zhang, H., Sun, K., Feng, Z., Ying, P., & Li, C. (2006). Studies on the SbO_x species of SbO_x/SiO₂ catalysts for methane-selective oxidation to formaldehyde. *Applied Catalysis A: General*, 305(1), 110-119.
- Zhang, J., Burklé-Vitzthum, V., & Marquaire, P. M. (2012a). NO₂-promoted oxidation of methane to formaldehyde at very short residence time - Part II: Kinetic modeling. *Chemical Engineering Journal*, 197, 123-134.
- Zhang, J., Burklé-Vitzthum, V., & Marquaire, P. M. (2012b). NO₂-promoted oxidation of methane to formaldehyde at very short residence time. Part I: Experimental results. *Chemical Engineering Journal*, 189-190, 393-403.

- Zhang, J., Burklé-Vitzthum, V., Marquaire, P. M., Wild, G., & Commenge, J. M. (2011). Direct conversion of methane in formaldehyde at very short residence time. *Chemical Engineering Science*, 66(24), 6331-6340.
- Zhang, X., He, D. H., Zhang, Q. J., Ye, Q., Xu, B. Q., & Zhu, Q. M. (2003). Selective oxidation of methane to formaldehyde over Mo/ZrO₂ catalysts. *Applied Catalysis A: General*, 249(1), 107-117.

Monash University

Declaration for Thesis Chapter 3

Declaration by candidate

In the case of Chapter 3, the nature and extent of my contribution to the work was the following:

Nature of contribution	Extent of contribution (%)
Initiation	50
Experiments	100
Analysis	80
Writing	70*

The following co-authors contributed to the work. If co-authors are students at Monash University, the extent of their contribution in percentage terms must be stated:

Name	Nature of contribution	Extent of contribution (%) for student co-authors only
Akshat Tanksale	Initiation Analysis Reviewing and Editing the Paper	
Andrew Hoadley	Initiation Analysis Reviewing and Editing the Paper	

The undersigned hereby certify that the above declaration correctly reflects the nature and extent of the candidate's and co-authors' contributions to this work.

Candidate's Signature  Date 24/09/15

Main Supervisor's Signature  Date 24/09/15

Chapter 3:

Formaldehyde Production via CO Hydrogenation in the Aqueous Phase

Abstract

In order to study a new chemical process, one may need to study the possibility of the process theoretically and experimentally first before any further studies. Once the possibility has been approved, there might be a chance to improve the production yield by optimizing the operating conditions. In this chapter, the thermodynamic conditions of the carbon monoxide hydrogenation reaction to formaldehyde are discussed using the HSC Chemistry™ software and experimental data for both gas phase and aqueous phase reactions. The feasibility of producing formaldehyde directly from synthesis gas is proved. However, gas phase hydrogenation of carbon monoxide into formaldehyde is thermodynamically limited and therefore, results in low carbon monoxide conversion of only 1.02×10^{-4} %. On the other hand, the aqueous phase hydrogenation of carbon monoxide into formaldehyde is found to be thermodynamically favourable and kinetically limited. Highest carbon monoxide conversion of 19.14% and selectivity of 100% is achieved by using Ru-Ni/Al₂O₃ catalyst at 353 K and 100 bar in the aqueous phase. The rapid hydration of formaldehyde in the aqueous phase to form methylene glycol shifts the carbon monoxide hydrogenation reaction equilibrium towards formaldehyde formation. Increasing the pressure and stirring speed increase the production yield of formaldehyde.

This page is intentionally left blank

3.1 Introduction

As discussed in chapter 2, formaldehyde (HCHO) is produced in three stages – (a) Steam reforming of natural gas to produce syngas (Table 3.1, Eq.3.1), (b) Methanol (CH₃OH) Synthesis (Eq. 3.2) and (c) partial oxidation of CH₃OH to produce HCHO (Eq. 3.3). Alternatively, HCHO is produced via dehydrogenation of CH₃OH (Eq. 3.4) (Reuss et al., 2003; Walker, 1967). However, these are all high temperature and high pressure reactions which require combustion, compression and large process units for purification, which are the root cause of energy losses (Li et al., 2014; Rosen & Scott, 1988). We have recently shown that this series of processes from natural gas to HCHO production suffers from ~57% losses in exergy (i.e. energy quality) (Bahmanpour et al., 2014). Given the large amount of HCHO produced in the world, when combined with the high losses in exergy, leads to high energy losses and also high CO₂ emissions, globally. As mentioned in chapter 2, the effort of the researchers to overcome this issue by finding ways to produce HCHO directly from natural gas by partial oxidation of CH₄ (Eq. 3.5) was not successful due to low CH₄ conversion and/or poor selectivity towards formation of HCHO (Blair & Wheeler, 1923; Dake & Chaudhari, 1985; Purwanto et al., 1996) since the rate of HCHO decomposition into CO and H₂ is much greater than the rate of partial oxidation of CH₄, especially at temperatures in excess of 373 K, which means that in order to produce HCHO selectively, one must limit the conversion of CH₄ in Eq. 3.5 to a very small value. Moreover, if we consider that natural gas is a valuable energy resource, it becomes evident that an alternative feedstock for HCHO production is much needed. An alternative is direct conversion of synthesis gas into HCHO. Syngas can be produced from a range of sources including biomass and allows the mole fractions of CO to H₂ to be controlled more easily through the use of H₂O and CO₂ which is helpful in climate change abatement (Chan & Tanksale, 2014).

Chapter 3

Table 3.1: Chemical reactions used for the production of HCHO in the gas phase

Reaction Name	Reaction Stoichiometry		Equation No.
Steam Reforming	$CH_4 + H_2O \rightleftharpoons CO + 3H_2$	$\Delta\hat{H}_r^o = +206 \text{ kJ. mol}^{-1}$	(3.1)
Methanol Synthesis	$CO + 2H_2 \rightleftharpoons CH_3OH$	$\Delta\hat{H}_r^o = -91 \text{ kJ. mol}^{-1}$	(3.2)
Methanol Partial Oxidation	$CH_3OH + \frac{1}{2}O_2 \rightarrow HCHO + H_2O$	$\Delta\hat{H}_r^o = -159 \text{ kJ. mol}^{-1}$	(3.3)
Methanol Dehydrogenation	$CH_3OH \rightleftharpoons HCHO + H_2$	$\Delta\hat{H}_r^o = +84 \text{ kJ. mol}^{-1}$	(3.4)
Methane Partial Oxidation	$CH_4 + O_2 \rightarrow HCHO + H_2O$	$\Delta\hat{H}_r^o = -319 \text{ kJ. mol}^{-1}$	(3.5)
Syngas to Formaldehyde in Gas Phase	$CO + H_2 \rightleftharpoons HCHO$	$\Delta\hat{H}_r^o = -5.4 \text{ kJ. mol}^{-1}$, $\Delta G^o = +34.6 \text{ kJ. mol}^{-1}$	(3.6)

Gas phase hydrogenation of CO to produce HCHO (Equation 3.6) suffers from positive Gibbs free energy change of the reaction (Newton & Dodge, 1933). Only trace amount of HCHO in the product has been reported with the highest CO conversion of 0.2% (Morgan et al., 1932). Therefore, direct conversion of synthesis gas into HCHO has not been studied extensively. In this chapter, hydrogenation of CO into HCHO in a slurry reactor is presented as a viable alternative. By comparing with gas phase conversion in a fixed bed reactor, it is demonstrated that the thermodynamic limitation can be overcome in the slurry reactor. A low temperature active catalyst is desirable for the slurry phase reaction as the reaction was found to be favourable below 373 K. Generally, Ni Pd and Ru are considered as active hydrogenation catalysts in the literature for many reactions (Abdur-Rashid et al., 2002; Araki & Ponc, 1976; Fatsikostas & Verykios, 2004; Goodman et al., 1980; Hashiguchi et al., 1995; Jessop et al., 1994; Kidambi et al., 2004; Kroll et al., 1996; Niu et al., 2001; Noyori & Hashiguchi, 1997). Based on the density functional theory (DFT) studies done in the literature, Pd and Ni have been shown to produce HCHO as an intermediate of CO hydrogenation to produce CH₃OH (Neurock, 1999; Remediakis et al., 2004). Previous studies have also shown that bi-metallic Pd-Ni catalyst has better reducibility and higher metal surface area (Tanksale et al., 2008). Therefore, Pd-Ni and Ru-Ni supported on γ -Al₂O₃ were used as the catalysts in this study.

3.2 Experiments and Methods

3.2.1 Catalyst Preparation and Characterization

The catalysts used in this process were produced by the wet impregnation method followed by calcination. Nickel nitrate ($(\text{NO}_3)_2 \cdot 6\text{H}_2\text{O}$, Sigma-Aldrich), ruthenium chloride ($\text{RuCl}_3 \cdot x\text{H}_2\text{O}$, Sigma-Aldrich) and palladium nitrate (10 wt% $\text{Pd}(\text{NO}_3)_2$ in 10wt% nitric acid, Sigma-Aldrich) were used as Ni, Ru and Pd precursors, respectively. The desirable amounts of Ni and noble metal precursors were added simultaneously to commercial $\gamma\text{-Al}_2\text{O}_3$ suspended in 20 ml water. The mixture was stirred at 333 K for 6 h. The suspension was then dried at 373 K overnight. The dried catalyst was calcined at 873 K for 6 h.

Fixed bed reactor tests were started by reducing the catalyst *in-situ* prior to the experiment by flowing $50 \text{ ml} \cdot \text{min}^{-1}$ of H_2 through the catalyst bed at 673 K for 5 h followed by purging with Ar at 673 K for 1 h. The catalyst bed was cooled to room temperature under Ar flow overnight. For the slurry reactor tests, the same procedure of catalyst reduction was carried out *ex-situ*.

BET surface area of the support was measured by the N_2 physisorption method in Micrometric ASAP2020 at 77 K. CO chemisorption was used to measure the amount of active sites of each catalyst and the metal dispersion percentage using ASAP2020 (Micrometrics). X-ray Florescence (XRF) spectroscopy was used to determine the actual mass percentage of the metals using an Ametek Spectro iQ II XRF. X-ray Diffraction (XRD) patterns of fresh calcined and reduced catalysts were recorded using a REGAKU MiniFlex 600 X-ray diffraction instrument equipped with a Ni-filtered $\text{Cu K}\alpha$ radiation in order to study the situation of the catalyst before and after reduction as well as the catalyst support stability. XRD patterns were gained for 2θ using step size of 0.01. Transmission Electron Microscopy (TEM) was used to evaluate the particle size of each promoter (Pd and Ru) in the fresh calcined catalysts and ImageJ 1.48 (National Institutes of Health) was used to generate the particle size distribution. The catalyst characterization results are discussed in the results and discussion section.

Chapter 3

3.2.2 Fixed Bed Reactor

A schematic diagram of the custom made fixed bed reactor setup is illustrated in Figure 3.1. CO and H₂ gases were mixed in 1:1 mole ratio (30 ml.min⁻¹ each) using mass flow controllers in a gas manifold prior to feeding it in the fixed bed reactor. The reactor was Swagelok ¼" OD seamless tube in which 1 g of catalyst was fixed using quartz wool. The reactor was heated by a tube furnace which was used for *in-situ* reduction of the catalyst prior to the test. A back pressure regulator controlled the desired pressure upstream in the system. The gas stream leaving the back pressure regulator was passed through a scrubber containing 40 ml of 5 vol% CH₃OH in water to recover HCHO. CH₃OH was used in order to prevent hydrated HCHO molecules from polymerization. At the end of the run, the HCHO concentration was measured using the photometric cell test kit (Merck Millipore) in a DR 5000™ UV/VIS spectrophotometer (HACH Company, USA) at 575nm wavelength using a chromotropic acid method (Kennedy, 1994). The tests were conducted at different operating conditions. A range of pressures (20bar, 40bar, 85bar, and 117bar) and temperatures (293 K and 313 K) were tested.

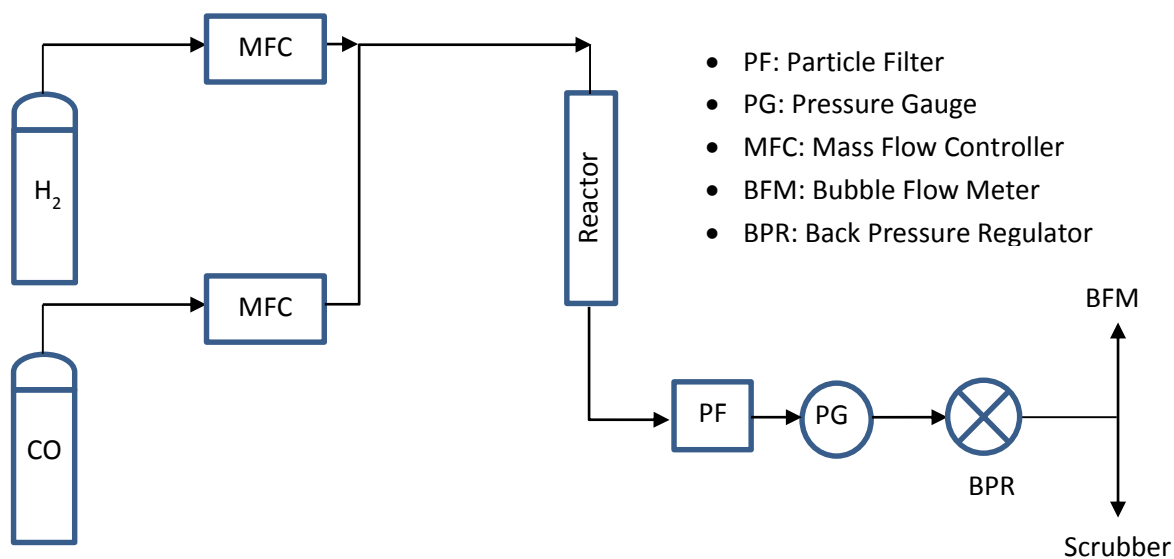


Figure 3.1: Schematic diagram of the fixed bed reactor setup

3.2.3 Slurry Reactor

The slurry reactor (batch reactor), illustrated in Figure 3.2, was charged with 40 ml of 5 vol% CH₃OH in water. 1 g of the desired catalyst was reduced *ex-situ* before adding it to the batch reactor. The reactor was subsequently pressurized to 100 bar with equimolar mixture of CO and H₂. Subsequently the reactor was heated to the desired temperature (293 K, 333 K, 353 K, 373 K, or 403 K). During the run, liquid samples were collected at regular intervals through the dip tube. the HCHO concentration was measured using the photometric cell test kit (Merck Millipore) with a DR 5000™ UV/VIS spectrophotometer (HACH Company, USA) at 575 nm wavelength using a chromotropic acid method. In this method, 4.5 ml of 75% sulphuric acid (H₂SO₄) was measured in a plastic tube. 0.1 g of chromotropic acid disodium salt dehydrate (C₁₀H₁₀Na₂O₁₀S₂) was added to the tube and was shaken vigorously. 3 ml of the sample (diluted if required) was added to the mixture. The intensity of the violet colour resulting from the reaction was checked using the spectrophotometer and quantified based on the pre-prepared calibration curve.

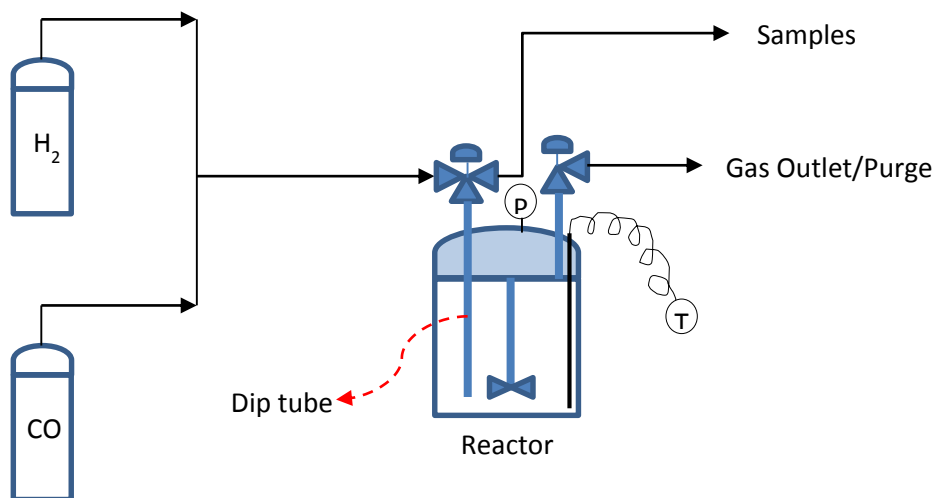


Figure 3.2: Schematic diagram of the slurry reactor setup

3.3 Investigation of the Thermodynamic Conditions

Hydrogenation of CO into HCHO in the gas phase and aqueous phase was thermodynamically investigated using the HSC Chemistry® version 7.11 (Outotec, Finland) software and published data

Chapter 3

(Oelkers et al., 1995) for a wide range of temperatures (298-623 K) and pressures (50-500 bar). The results (Table 3.2) show that the Gibbs free energy (ΔG) of the reaction is positive in the gas phase and it increases with increasing temperature. Therefore the reaction is non-spontaneous at all temperatures above 298 K. The equilibrium constant of the gas phase reaction is significantly low ($8.76 \times 10^{-7} \text{ mol}^{-1}$ at 298 K) which, along with positive ΔG , suggests that the forward reaction is not favourable. In the aqueous phase however, ΔG of the reaction is negative at low temperatures and the equilibrium constant is high (17.33 mol^{-1} at 298 K), which suggests that HCHO formation is favourable in the aqueous phase. This is because the heat of solution of HCHO is $-62 \text{ kJ} \cdot \text{mol}^{-1}$ (Reuss et al., 2003) which is relatively high while the heat of solution of H_2 and CO is insignificant in comparison. This results in the improvement of the equilibrium conversion. The effect of pressure on the Gibbs free energy of the reaction in the aqueous phase is shown in Figure 3.3. The data presented in this Figure are calculated based on the interpolation of experimental data presented by Oelkers et al (Oelkers et al., 1995). It can be seen that as the operating pressure increases, the Gibbs free energy of the reaction decreases. Although it is concluded that higher pressures are favourable for this reaction, the operating pressure in this study was limited to 100 bar by the maximum available gas cylinder pressure.

Table 3.2: Thermodynamic conditions of CO hydrogenation reaction to HCHO

$\text{CO} + \text{H}_2 \leftrightarrow \text{CH}_2\text{O}$						
Gas Phase				Aqueous Phase		
T	X_e	ΔG	K	X_e	ΔG	K
K	%	$\text{kJ} \cdot \text{mol}^{-1}$	mol^{-1}	%	$\text{kJ} \cdot \text{mol}^{-1}$	mol^{-1}
298	4.38×10^{-3}	34.565	8.760×10^{-7}	31.40	-7.071	17.332
323	4.67×10^{-3}	37.297	9.348×10^{-7}	18.42	-5.648	8.186
373	4.88×10^{-3}	42.933	9.764×10^{-7}	3.86	-1.297	1.519
423	4.86×10^{-3}	48.705	9.711×10^{-7}	5.84×10^{-1}	4.853	2.52×10^{-1}
473	4.70×10^{-3}	54.586	9.405×10^{-7}	8.88×10^{-2}	12.343	4.30×10^{-2}
523	4.49×10^{-3}	60.554	8.983×10^{-7}	1.50×10^{-2}	21.129	8.00×10^{-3}
573	4.26×10^{-3}	66.592	8.523×10^{-7}	1.72×10^{-3}	31.171	1.00×10^{-3}
623	4.03×10^{-3}	72.685	8.068×10^{-7}	3.95×10^{-4}	43.053	2.46×10^{-4}

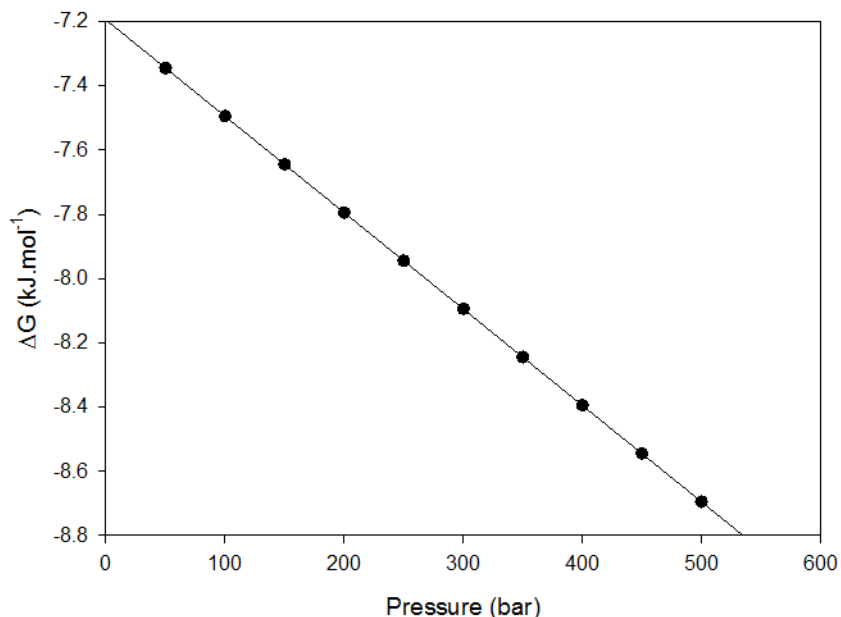


Figure 3.3: Effect of pressure on the Gibbs free energy of the reaction in the aqueous phase, T= 298 K (Oelkers et al., 1995)

Direct hydrogenation of CO to produce HCHO is not practical in the gas phase because of the low equilibrium conversion of the reaction. However, as it can be seen in Table 3.2, the equilibrium conversion of the reaction is significantly higher in the aqueous phase, which is due to low ΔG of the components in the aqueous media. Therefore, the reaction is thermodynamically feasible in the liquid phase and can achieve sufficiently high equilibrium conversion to make this process viable. The reaction is therefore expected to be kinetically limited, which can be improved by the use of an appropriate catalyst.

3.4 Catalyst Characterization

BET surface area of the support and CO-chemisorption results for Pd-Ni and Ru-Ni are shown in Table 3.3. BET surface area is given for the commercial γ -Al₂O₃ before metal impregnation. It is expected that the surface area reduced to some extent after impregnation (Tanksale et al., 2008).

The nominal and actual metal content of the catalysts are presented in Table 3.3, which shows good agreement. The promoter content was calculated based on the mass balance as the actual content of

Chapter 3

the NiO and Al₂O₃ was measured by XRF. Based on the amount of CO adsorption on the catalyst surface, metal dispersion was calculated according to the following formula:

$$Dispersion(\%) = \frac{M_{CO} \times AW}{WF} \times 100 \quad (3.7)$$

where M_{CO} is the amount of adsorbed CO ($\mu\text{mol.g}^{-1}$), AW is the atomic weight of the metals ($\text{g.}\mu\text{mol}^{-1}$), and WF is the weight fraction of the metals in the catalysts. Table 3.3 shows that CO uptake and metal dispersion of Ru-Ni/Al₂O₃ was significantly higher than Pd-Ni/Al₂O₃, even though similar metal loading was used. This suggests that the supported Ru-Ni nanoparticles are much smaller than the Pd-Ni nanoparticles. This is confirmed from the TEM results shown in Figure 3.4. The nanoparticles sizes were estimated using ImageJ software (NIH) and shown in the Figure. The mean particle size of Pd-Ni nanoparticles was 3.69 nm compared to the mean particle size of Ru-Ni nanoparticles of 2.14 nm. Lower particle size and hence higher dispersion of the catalyst nanoparticles is favourable for HCHO formation because it would provide higher surface area for CO and H₂ adsorption which is expected to be a necessary step for hydrogenation reaction. The particles size of the powder catalyst is calculated to be in the range of 10-60 μm based on the SEM images of the catalysts. The SEM images are presented in appendix A.4.

Table 3.3: BET surface area, metal loading, and CO chemisorption data

Catalyst	Nominal Metal Loading (%w/w)	Actual Metal Loading* (%w/w)	Total CO uptake ($\mu\text{mol.g}^{-1}$)	Metal Dispersion (%)	BET Surface area of the Support ($\text{m}^2.\text{g}^{-1}$)
Ru-Ni/Al ₂ O ₃	Ni-10	Ni-9.3	41.96	2.33	108.51
	Ru-1	Ru-1.4			
Pd-Ni/Al ₂ O ₃	Ni-10	Ni-9.5	26.50	1.47	
	Pd-1	Pd-1.3			

* Al₂O₃ and NiO content are measured by XRF. Promoter content is calculated based on mass balance

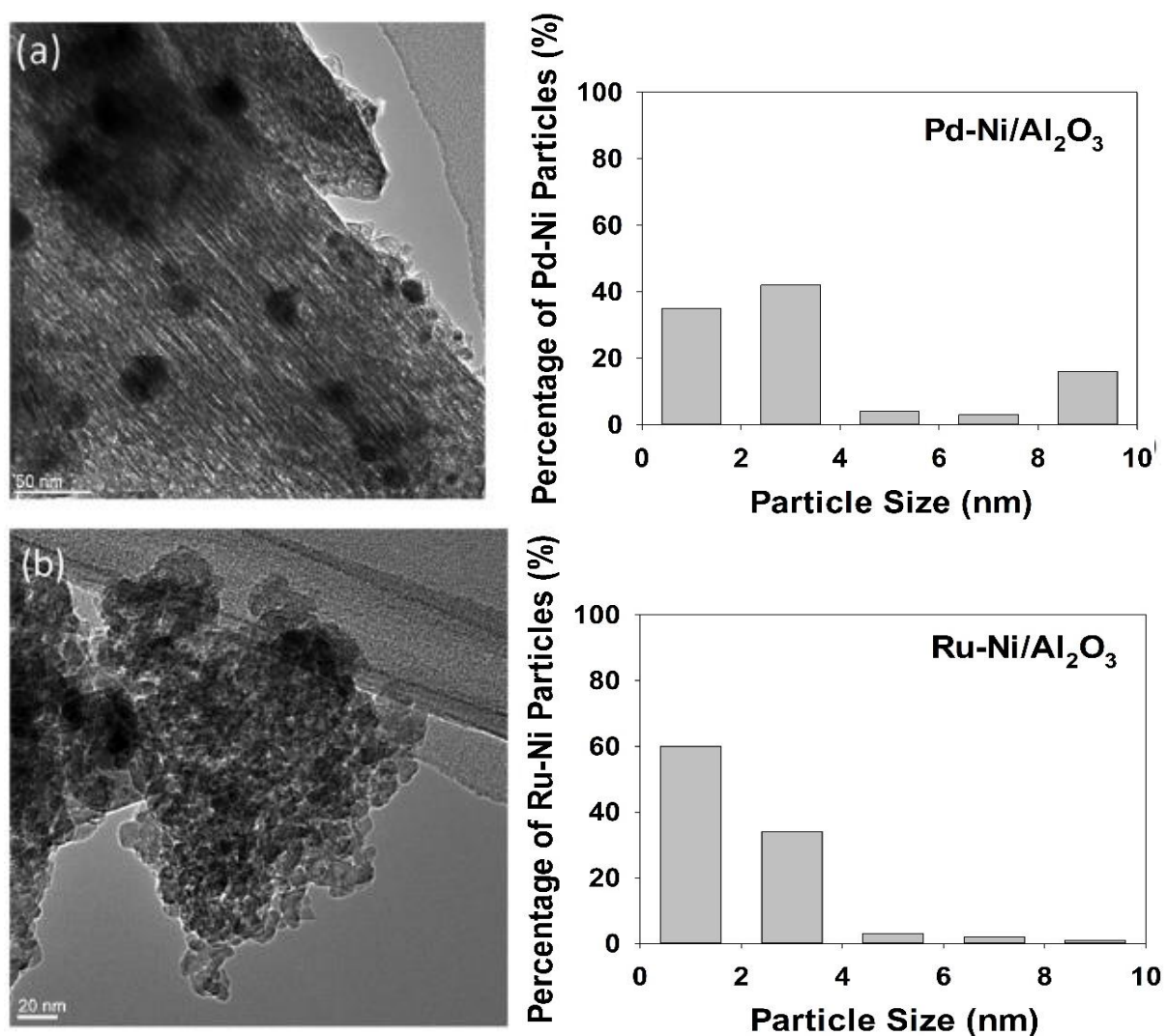


Figure 3.4: TEM image and size distribution of a) Pd-Ni/Al₂O₃, Scale bar= 50nm and b) Ru-Ni/Al₂O₃, Scale bar= 20nm

The XRD patterns of the calcined and reduced Ru-Ni/Al₂O₃ and Pd-Ni/Al₂O₃ catalysts are presented in Figure 3.5. The peaks representing PdO (34.06°) and RuO₂ (28.19° and 34.06°) disappeared after reduction and peaks representing Pd⁰ (40.15°) and Ru⁰ (43.98°) were observed, which confirmed complete reduction of the catalysts (Abu Bakar et al., 2012; Wojcieszak et al., 2010). Broad NiO and Ni⁰ peaks were also observed at 62.88° and 51.83° 2θ angles, which also confirm that the Ni nanoparticles are finely dispersed (Hanson & Norby, 2013).

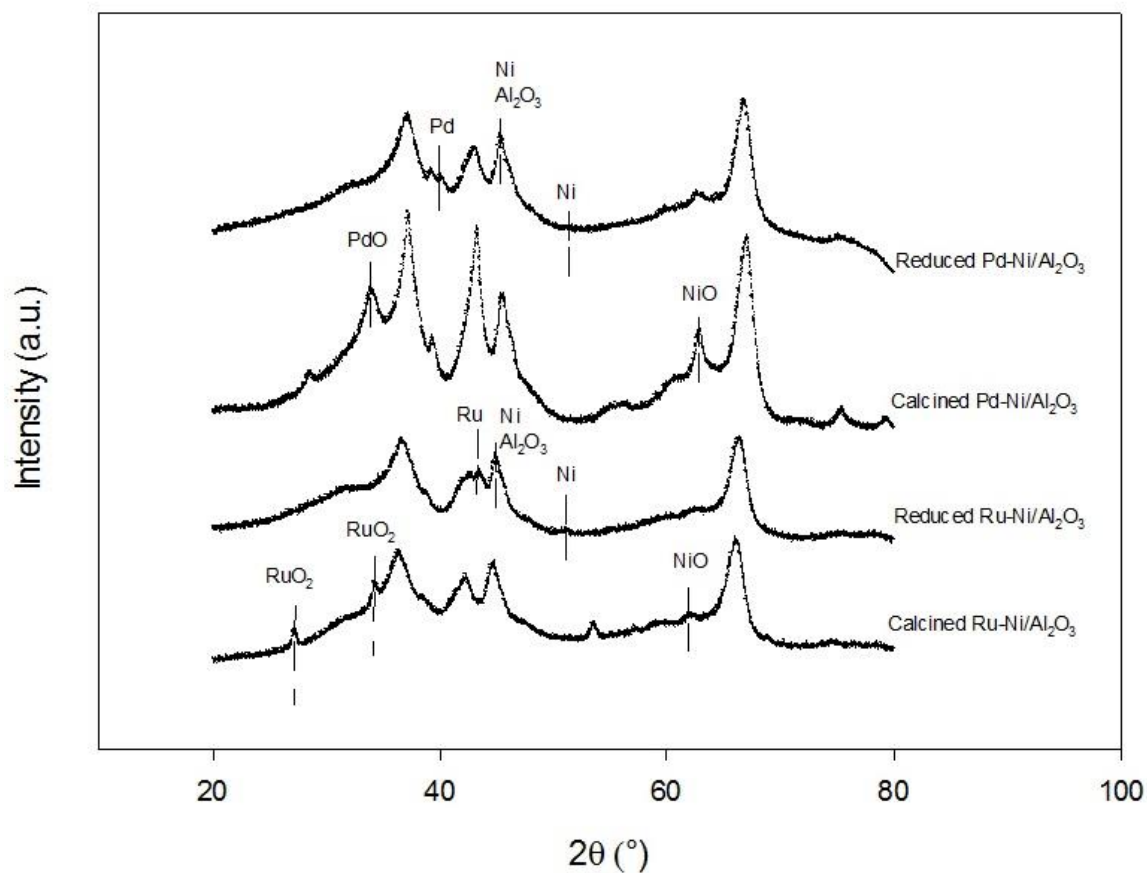


Figure 3.5: XRD patterns of calcined and reduced Pd-Ni/Al₂O₃ and Ru-Ni/Al₂O₃

3.5 Comparison of Formaldehyde Production in Fixed Bed and Slurry Reactors

3.5.1 Fixed Bed Reactor

Figure 3.6 shows the effect of pressure (Figure 3.6a) and temperature (Figure 3.6b) on the molar yield of HCHO using Pd-Ni/Al₂O₃ as the catalyst in the gas phase reaction. It is evident that higher pressures are favourable for CO hydrogenation to HCHO, which is theoretically expected based on the Le

Chatelier's Principle and the previous studies (Newton & Dodge, 1933; Walker, 1967). Since two moles of reactants are combining to form one mole of the product, higher pressure would favour the forward reaction. The highest yield of HCHO ($8.2 \times 10^{-3} \text{ mmol.L}^{-1} \cdot \text{g}_{\text{cat}}^{-1}$) in fixed bed reactor was obtained at 117 bar pressure at 293 K, which equates to conversion of only $1.02 \times 10^{-4} \%$, which is well below the equilibrium conversion. It was also confirmed from the experiments, as shown in Figure 3.6b, higher temperatures are unfavourable for the reaction in the gas phase because the overall yield of HCHO reduced from $4.84 \times 10^{-3} \text{ mmol.L}^{-1} \cdot \text{g}_{\text{cat}}^{-1}$ to less than $2.12 \times 10^{-3} \text{ mmol.L}^{-1} \cdot \text{g}_{\text{cat}}^{-1}$ after 180 min reaction time. $t = 0$ is the control sample which is the sample taken before the start of the experiment.

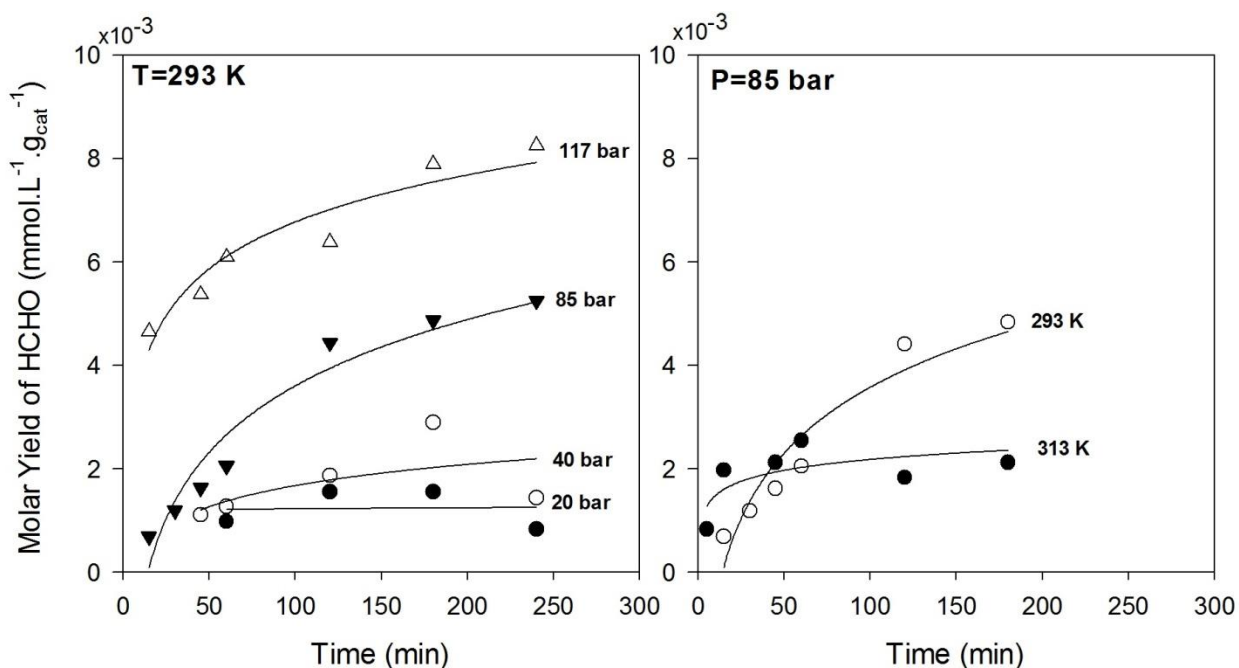


Figure 3.6: Effect of (a) pressure and (b) temperature on the molar yield of HCHO in the fixed bed reactor using Pd-Ni/Al₂O₃

3.5.2 Slurry Reactor

Figure 3.7 shows the Arrhenius plot based on the rate of reaction calculated after $t = 2$ h, assuming first order batch reactor kinetics. The rate of formation is calculated based on the yield of HCHO per unit time. The initial concentration of the reactant gases is calculated based on Henry's law. The highest rate of reaction in the first two hours was $0.0378 \mu\text{mol.L}^{-1} \cdot \text{s}^{-1}$ at 403 K. The activation energy was calculated to be $27.58 \text{ kJ.mol}^{-1}$ for the Ru-Ni/Al₂O₃ as the catalyst. Figure 3.8 and Figure 3.9 show

Chapter 3

the effect of temperature on the yield of HCHO as a function of time. Although the equilibrium constant decreased with increasing temperature in the aqueous phase, HCHO production rate increased which proves that the process was kinetically limited, unlike the gas phase which was thermodynamically limited. After 48 hours, it was observed that HCHO yield was higher at 353 K and 373 K compared to 403 K.

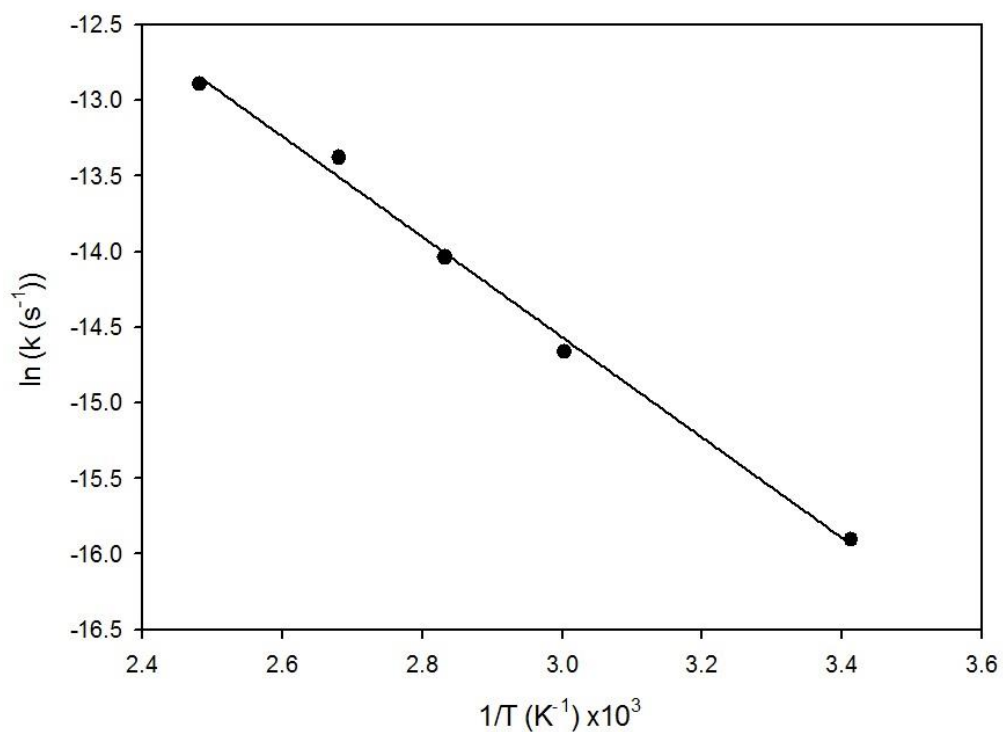


Figure 3.7: Reaction constant based on the first 2 hour of the reaction, P=100 bar, Catalyst: Ru-Ni/Al₂O₃

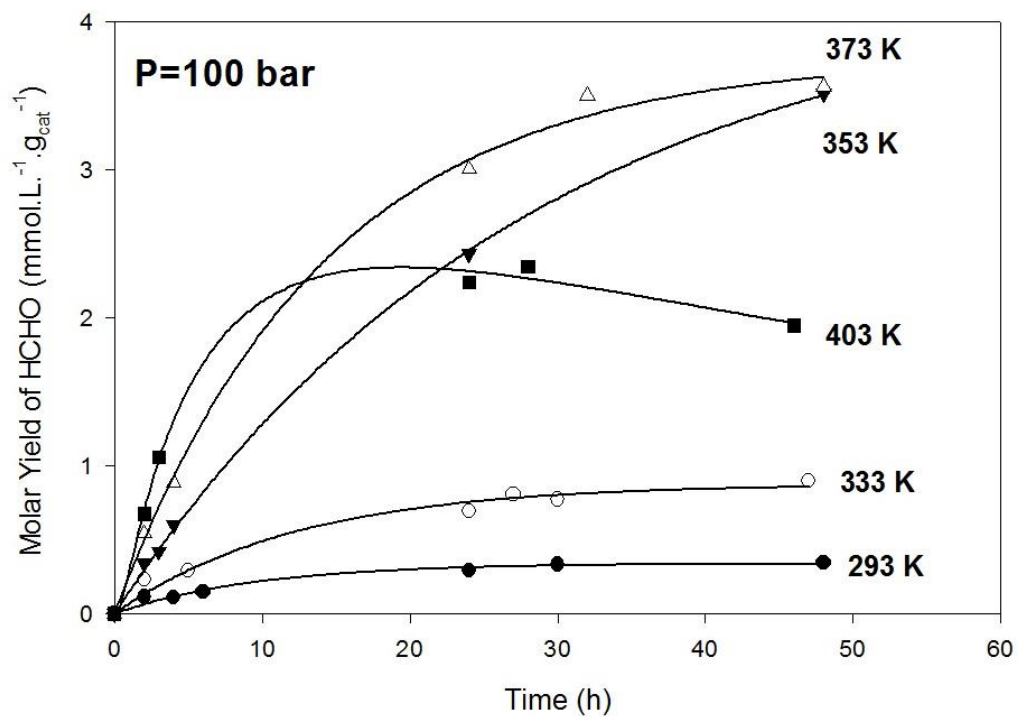


Figure 3.8: Effect of temperature on the molar yield of HCHO in the slurry reactor after 48 hours using Ru-Ni/Al₂O₃

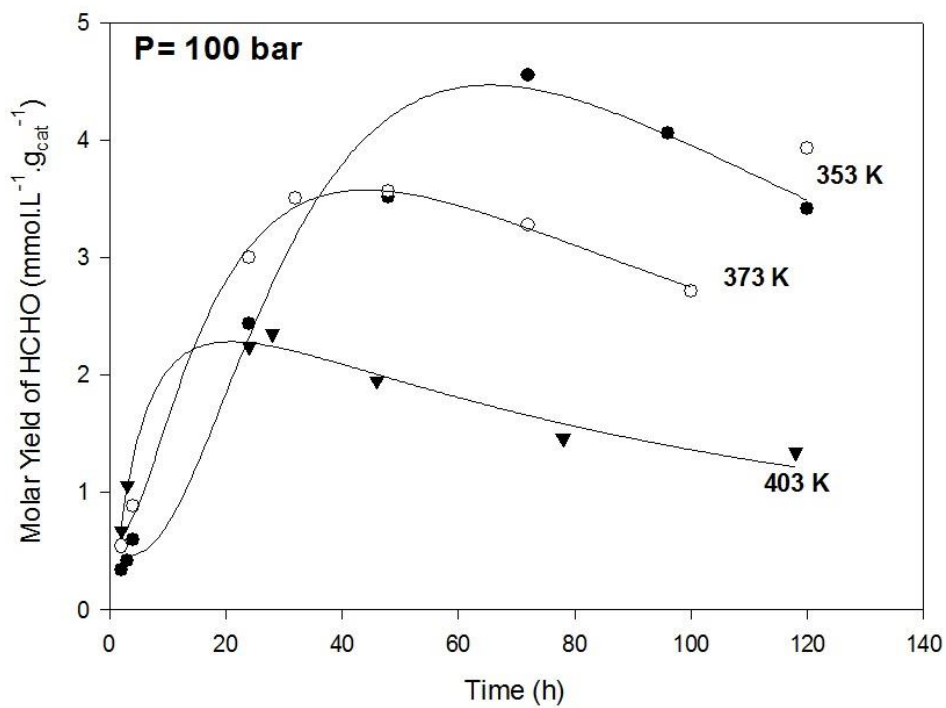


Figure 3.9: Effect of temperature on molar yield of HCHO in the slurry reactor after 120 hours using Ru-Ni/Al₂O₃

Chapter 3

As shown in Figure 3.9, the highest level of the HCHO yield was $4.55 \text{ mmol.L}^{-1}.\text{g}_{\text{cat}}^{-1}$ at 72 hours of operation at 353 K, which is equal to turn over frequency (TOF) of 0.0602 h^{-1} . The highest conversion of soluble CO was 19.14% which is significantly higher compared to published works on gas phase CO hydrogenation (Morgan et al., 1932; Newton & Dodge, 1933). This conversion is also higher than the theoretical equilibrium conversion because the equilibrium is shifted when HCHO is dissolved in water. HCHO reacts with water within 70 ms to form methylene glycol ($\text{CH}_2(\text{OH})_2$) (Boyer et al., 2013). In the solution, HCHO and $\text{CH}_2(\text{OH})_2$ co-exists in dynamic equilibrium with a HCHO/ $\text{CH}_2(\text{OH})_2$ ratio of 1:2499 at STP and pH = 7 (Moret et al., 2014), which means 99.96% of HCHO is converted to $\text{CH}_2(\text{OH})_2$. Therefore, HCHO produced in this method is instantly absorbed in water, shifting the reaction equilibrium in the forward direction, as shown in Figure 3.10. Conversion of HCHO into $\text{CH}_2(\text{OH})_2$ has been well studied in the literature (Boyer et al., 2013; Hasse et al., 1990; Hasse & Maurer, 1991; Maurer, 1986; Winkelman et al., 2000; Winkelman et al., 2002). $\text{CH}_2(\text{OH})_2$ also polymerizes to form polyoxymethylene ($(\text{CH}_2\text{O})_n$) (Maurer, 1986). However, the polymerization reaction rate is much lower compared with the rate of hydration and dehydration reactions and it can be inhibited by CH_3OH (Boyer et al., 2013). Based on the studies done by Winkelman et al, the HCHO hydration rate (k_h) and the equilibrium constant for hydration (K_h) are calculated to be as follows (Winkelman et al., 2000; Winkelman et al., 2002):

$$k_h = 2.04 \times 10^5 \times e^{\frac{-2936}{T}} \quad (3.8)$$

$$K_h = e^{\frac{3769}{T} - 5.494} \quad (3.9)$$



Figure 3.10: Shifting the reaction equilibrium in favour of producing HCHO

It is demonstrated in Figure 3.9 that the HCHO yield peaked in all cases, and that peak shifted towards lower time as the temperature was increased. The final product was checked for the presence of other possible compounds such as ethylene glycol. No other compound was detected in the liquid phase

which indicates loss of HCHO into the gas phase. At high temperatures and low pH values, the HCHO/CH₂(OH)₂ equilibrium shifts towards HCHO which may vaporise into the gas phase (Boyer et al., 2013). CH₂(OH)₂ is known to be very unstable in the gas phase because it tends to dehydrate rapidly to HCHO and water (Kent Iv et al., 2003). Therefore, heating a solution of HCHO and CH₂(OH)₂ may lead to HCHO emission (Boyer et al., 2013).

Comparison of the HCHO yield in the fixed bed reactor and the slurry reactor at identical operating conditions are presented in Figure 3.11. The yield of HCHO in the slurry reactor at room temperature was more than an order of magnitude higher compared to the fixed bed reactor. The TOF of HCHO production was higher for the Ru-Ni/Al₂O₃ than Pd-Ni/Al₂O₃ catalyst in the slurry reactor, which suggests that the former catalyst is more active in the aqueous conditions (Boudart, 1995). At room temperature in the aqueous phase, TOF for Ru-Ni/Al₂O₃ was 0.0475 h⁻¹ compared to 0.0319 h⁻¹ for Pd-Ni/Al₂O₃.

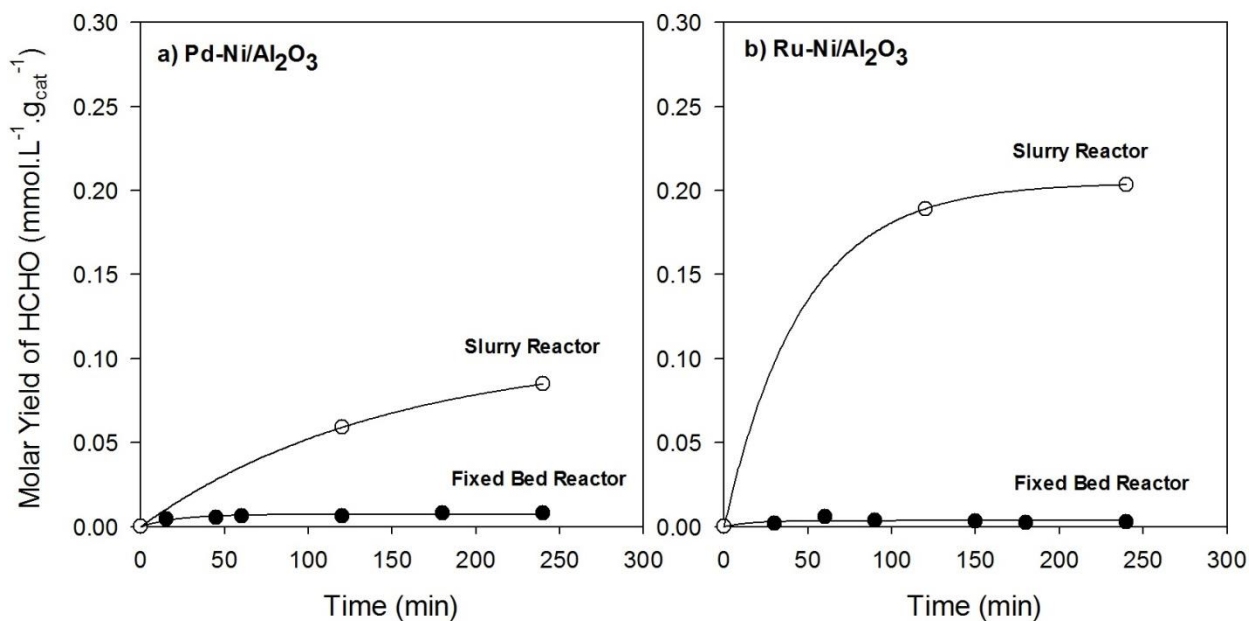


Figure 3.11: Comparison between the results of the fixed bed reactor and the slurry reactor at 293 K and 100 bar for a) Pd-Ni/Al₂O₃ and b) Ru-Ni/Al₂O₃

3.5.3 Effect of the Stirring Speed in the Slurry Reactor

Effect of stirring speed was tested by varying RPM= 0, 400, 800, 1200 at 298 K and 100 bar using Ru-Ni/Al₂O₃. Figure 3.12 shows that the yield of HCHO increased from 0.26 mmol.L⁻¹.g_{cat}⁻¹ to 0.4 mmol.L⁻¹.g_{cat}⁻¹ as the stirring rate increased from 0 RPM to 800 RPM. But further increasing the RPM did not increase the yield of HCHO. There are many factors which affects catalytic conversion in a slurry reaction. In a non-stirred reactor the catalyst particles may settle at the bottom of the reactor which makes the process diffusion limited. Stirring can decrease the mass transfer limitation by increasing the convective mass transfer coefficient and exposing the catalyst surface to the dissolved gases. Increasing the mass transfer coefficient increases the apparent global rate of reaction and this was observed in Figure 3.12. However, once the rate of mass transfer is sufficiently high, further increasing the stirring rate has no impact on the global rate of reaction because the reaction is kinetically controlled (Lou et al., 2010; S Kislik, 2010). Therefore, it can be concluded that at 800 RPM the test was conducted in a kinetically controlled regime.

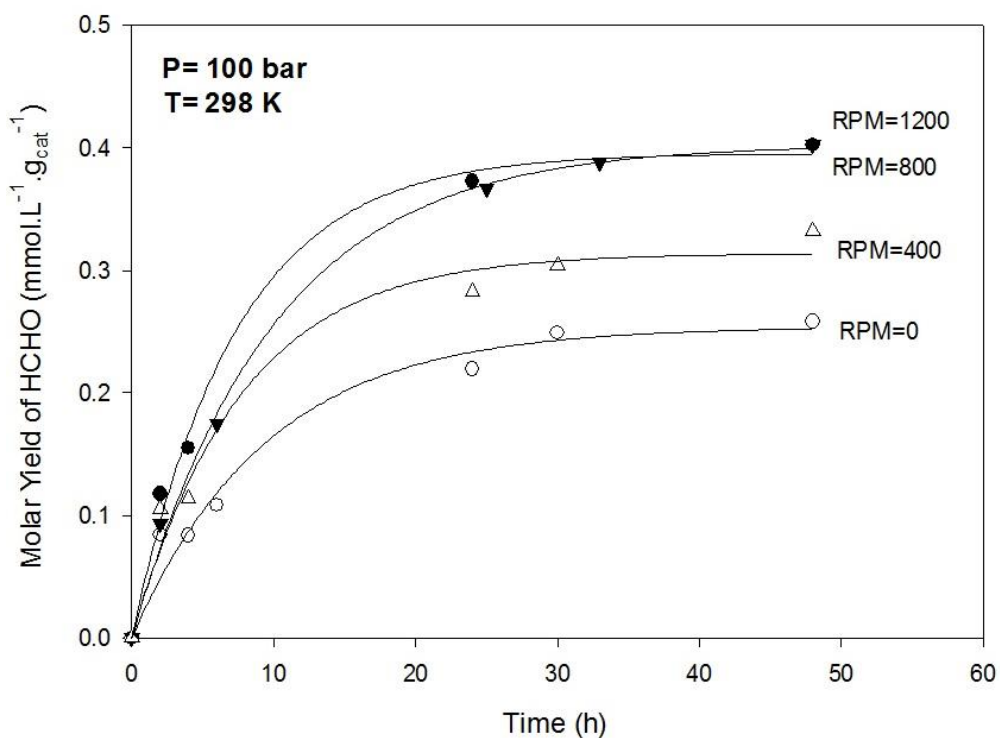


Figure 3.12: Effect of the stirrer rotation speed on the molar yield of HCHO using Ru-Ni/Al₂O₃

3.5.4 Effect of the Mass of the Catalyst in the Slurry Reactor

In order to check the effect of total accessible active sites, the effect of the mass of the catalyst was studied. Three separate tests were conducted at 353 K and 100 bar. 0.5 g, 1 g, and 2g of Ru-Ni/Al₂O₃ were used in each test. The results are presented in Figure 3.13. Based on the following results, it is clear that the HCHO yield increased as the mass of the catalyst increased from 0.5 g to 1g. However, the yield remained constant as the mass of the catalyst increased further to 2 g. This shows that by using 1 g of the catalyst, sufficient active sites are accessed by the reactants.

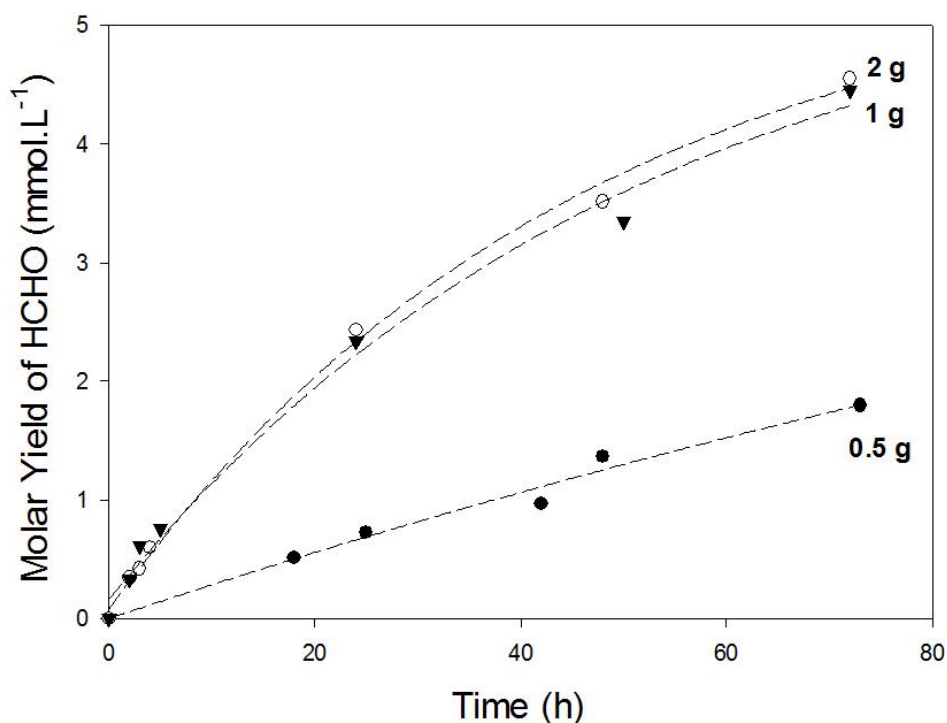


Figure 3.13: Effect of the mass of the catalyst on the HCHO yield, Catalyst: Ru-Ni/Al₂O₃, P = 100 bar, T = 353 K

3.6 Catalyst Support Stability in the Slurry Reactor

The stability of the catalyst support was investigated by studying the XRD patterns of the fresh and spent Ru-Ni/Al₂O₃ catalyst. The XRD patterns are shown in Figure 3.14. It is noticed that the XRD pattern of the spent catalyst at 403 K shows sharp peaks at $2\theta = 14.5^\circ$, 28.2° , 38.3° , 49° , and 49.3° while these peaks are not observed neither in the fresh catalyst nor in the spent catalyst at 353 K. This

Chapter 3

phenomenon was studied and based on previous studies in the literature, it was discovered that the Al_2O_3 support changes phase to form boehmite (AlOOH). Based on previous studies (Ravenelle et al., 2011), the phase change of Al_2O_3 to AlOOH in hot water results in a decrease in surface area. Also it is shown that the coordination of the Al atoms changes through this structural change. Both tetrahedral and octahedral coordination can be observed in Al_2O_3 structure. However, only octahedral coordination of the Al atoms can be seen in boehmite.

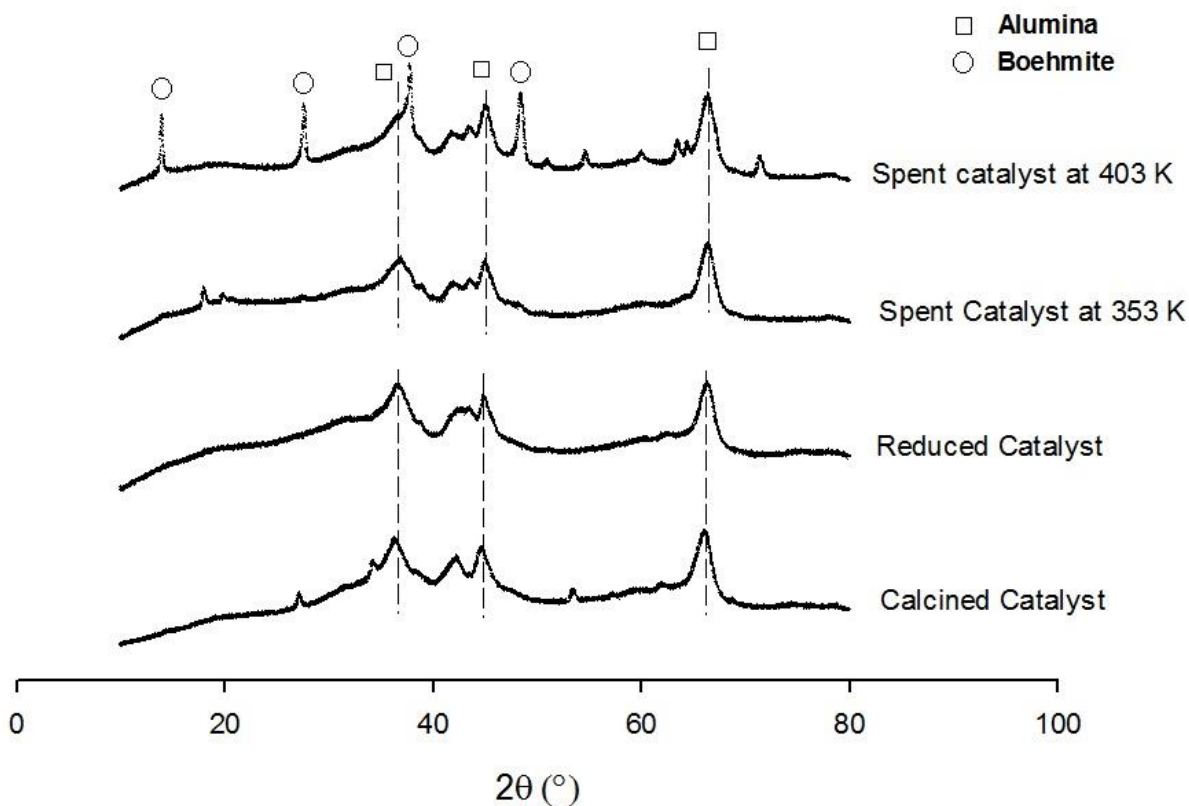


Figure 3.14: XRD patterns of fresh and spent Ru-Ni/ Al_2O_3 in the slurry phase process

The BET surface area of the fresh calcined Ru-Ni and the spent catalyst at 403 K was measured. It was observed that the surface area of the fresh calcined catalyst is $95 \text{ m}^2 \cdot \text{g}^{-1}$ where this value is $83 \text{ m}^2 \cdot \text{g}^{-1}$ for the spent catalyst at 403 K. This measurement shows that the surface area of the catalyst decreases by almost 13% at 403 K. The ^{27}Al NMR spectra of the fresh and the spent catalyst are shown in Figure 3.15. As it can be seen, both tetrahedral and octahedral coordination can be observed for Al

atoms of the fresh and calcined catalyst. However, the Al atoms of the spent catalyst at 403 K only coordinate octahedrally which shows the formation of boehmite.

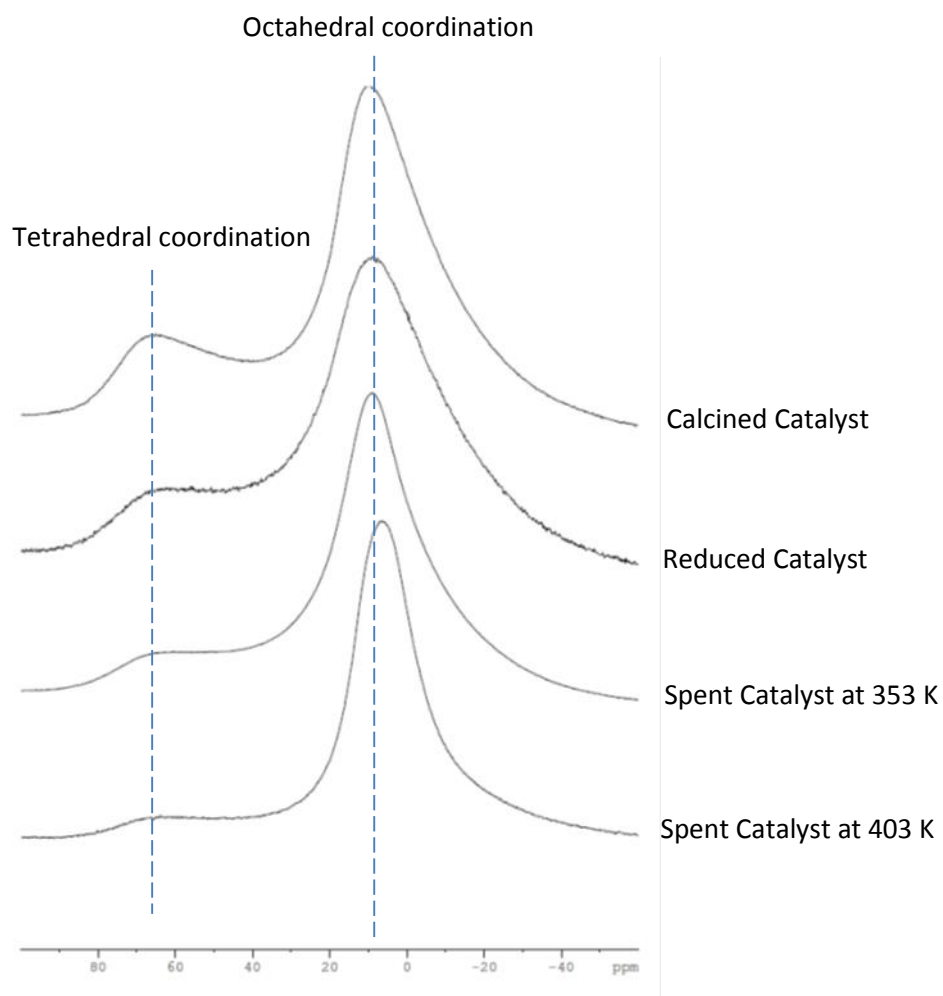


Figure 3.15: ^{27}Al NMR spectra of the fresh and the spent Ru-Ni/ Al_2O_3 in the slurry phase process

Hydration of Al_2O_3 to AlOOH was shown before in the literature at the reforming conditions (Jongorius et al., 2013). However, in this study it is shown that the hydration of Al_2O_3 can occur at lower temperatures in longer test runs.

Chapter 3

3.7 Conclusion

In this chapter, the direct formaldehyde (HCHO) production from synthesis gas in a slurry reactor was investigated. Thermodynamic investigation showed that CO hydrogenation in the gas phase is limited by positive Gibbs free energy (ΔG) at all temperatures above 298 K, whereas in the aqueous phase the reaction is thermodynamically favourable because the ΔG is negative below 383 K. This resulted in low yield of HCHO in the fixed bed reactor, and significantly higher yield in the slurry reactor (8.25×10^{-3} and 8.48×10^{-2} mmol.L⁻¹.g_{cat}⁻¹, respectively, at 298 K in 4 h using Pd-Ni/Al₂O₃). The HCHO yield reduced with temperature in the fixed bed reactor, where it significantly increased with temperature in the slurry reactor. The highest yield of the HCHO was 4.55 mmol.L⁻¹.g_{cat}⁻¹ at 353 K after 72 h, which equates to conversion of 19.14% of soluble CO. This conversion is higher than the equilibrium conversion at this temperature because HCHO produced in the aqueous phase is rapidly absorbed by water and hydrated to produce methylene glycol which shifts the equilibrium of CO hydrogenation reaction towards formaldehyde production. It is concluded that Al₂O₃ is stable at the recommended reaction conditions (T = 353 K, P = 100 bar) in the slurry phase reaction. However, higher temperatures may unfavorably affect the catalyst stability and should be the subject of further investigation. The slurry phase method presented here may be a viable alternative for HCHO production which bypasses the methanol synthesis route. In order to have a better vision of the process and finding the obstacles preventing us from achieving higher production yield, further investigation in the reaction pathway of this process is necessary. Therefore, the reaction mechanism is studied in the next chapter.

3.8 References

- Abdur-Rashid, K., Clapham, S. E., Hadzovic, A., Harvey, J. N., Lough, A. J., & Morris, R. H. (2002). Mechanism of the hydrogenation of ketones catalyzed by trans-dihydrido(diamine)ruthenium(II) complexes. *Journal of the American Chemical Society*, 124(50), 15104-15118.
- Abu Bakar, W. A. W., Ali, R., & Toemen, S. (2012). Catalytic methanation reaction over supported nickel-ruthenium oxide base for purification of simulated natural gas. *Scientia Iranica*, 19(3), 525-534.
- Araki, M., & Ponec, V. (1976). Methanation of carbon monoxide on nickel and nickel-copper alloys. *Journal of Catalysis*, 44(3), 439-448.
- Bahmanpour, A. M., Hoadley, A., & Tanksale, A. (2014). Critical review and exergy analysis of formaldehyde production processes. *Reviews in Chemical Engineering*, 30(6), 583-604.

- Blair, E. W., & Wheeler, T. S. (1923). The estimation of formaldehyde and acetaldehyde. *The Analyst*, 48(564), 110-112.
- Boudart, M. (1995). Turnover Rates in Heterogeneous Catalysis. *Chemical Reviews*, 95(3), 661-666.
- Boyer, I. J., Heldreth, B., Bergfeld, W. F., Belsito, D. V., Hill, R. A., Klaassen, C. D., et al. (2013). Amended safety assessment of formaldehyde and methylene glycol as used in cosmetics. *International journal of toxicology*, 32(6 Suppl), 5S-32S.
- Chan, F. L., & Tanksale, A. (2014). Catalytic steam gasification of cellulose using reactive flash volatilization. *ChemCatChem*.
- Dake, S. B., & Chaudhari, R. V. (1985). Solubility of CO in Aqueous Mixtures of Methanol, Acetic-Acid, Ethanol, and Propionic-Acid. *Journal of Chemical and Engineering Data*, 30(4), 400-403.
- Fatsikostas, A. N., & Verykios, X. E. (2004). Reaction network of steam reforming of ethanol over Ni-based catalysts. *Journal of Catalysis*, 225(2), 439-452.
- Goodman, D. W., Kelley, R. D., Madey, T. E., & Yates Jr, J. T. (1980). Kinetics of the hydrogenation of CO over a single crystal nickel catalyst. *Journal of Catalysis*, 63(1), 226-234.
- Hanson, J., & Norby, P. (2013). In-situ Powder X-ray Diffraction in Heterogeneous Catalysis *In-situ Characterization of Heterogeneous Catalysts* (pp. 121-146): John Wiley & Sons, Inc.
- Hashiguchi, S., Fujii, A., Takehara, J., Ikariya, T., & Noyori, R. (1995). Asymmetric transfer hydrogenation of aromatic ketones catalyzed by chiral ruthenium(II) complexes. *Journal of the American Chemical Society*, 117(28), 7562-7563.
- Hasse, H., Hahnenstein, I., & Maurer, G. (1990). Revised vapor-liquid equilibrium model for multicomponent formaldehyde mixtures. *AIChE Journal*, 36(12), 1807-1814.
- Hasse, H., & Maurer, G. (1991). Vapor-liquid equilibrium of formaldehyde-containing mixtures at temperatures below 320 K. *Fluid Phase Equilibria*, 64(C), 185-199.
- Jessop, P. G., Ikariya, T., & Noyori, R. (1994). Homogeneous catalytic hydrogenation of supercritical carbon dioxide. *Nature*, 368(6468), 231-233.
- Jongierius, A. L., Copeland, J. R., Foo, G. S., Hofmann, J. P., Bruijninx, P. C. A., Sievers, C., et al. (2013). Stability of Pt/ γ -Al₂O₃ catalysts in lignin and lignin model compound solutions under liquid phase reforming reaction conditions. *ACS Catalysis*, 3(3), 464-473.
- Kennedy, E. R. (1994). *NIOSH Manual of Analytical Methods*.
- Kent Iv, D. R., Widicus, S. L., Blake, G. A., & Goddard Iii, W. A. (2003). A theoretical study of the conversion of gas phase methanediol to formaldehyde. *Journal of Chemical Physics*, 119(10), 5117-5120.
- Kidambi, S., Dai, J., Li, J., & Bruening, M. L. (2004). Selective Hydrogenation by Pd Nanoparticles Embedded in Polyelectrolyte Multilayers. *Journal of the American Chemical Society*, 126(9), 2658-2659.
- Kroll, V. C. H., Swaan, H. M., & Mirodatos, C. (1996). Methane reforming reaction with carbon dioxide over Ni/SiO₂ catalyst: I. Deactivation studies. *Journal of Catalysis*, 161(1), 409-422.
- Li, Q., Wu, X., Ma, L., & Hu, S. (2014). Energy analysis of a natural gas purification process based on the process driving model: A case history of the Puguang Gas Field, Sichuan Basin. *Natural Gas Industry*, 34(5), 144-151.
- Lou, Z. N., Xiong, Y., Song, J. J., Shan, W. J., Han, G. X., Xing, Z. Q., et al. (2010). Kinetics and mechanism of Re(VII) extraction and separation from Mo(VI) with trialkyl amine. *Transactions of Nonferrous Metals Society of China (English Edition)*, 20(SUPPL.1), s10-s14.
- Maurer, G. (1986). VAPOR-LIQUID EQUILIBRIUM OF FORMALDEHYDE- AND WATER-CONTAINING MULTICOMPONENT MIXTURES. *AIChE Journal*, 32(6), 932-948.
- Moret, S., Dyson, P. J., & Laurency, G. (2014). Direct synthesis of formic acid from carbon dioxide by hydrogenation in acidic media. [Article]. *Nat Commun*, 5.

Chapter 3

- Morgan, G. T., Hardy, D. V. N., & Proctor, R. A. (1932). Methanol condensation as modified by alkali-catalysts. *J. Soc. Chem. Ind., London*, 51, 1-7T.
- Neurock, M. (1999). First-principles analysis of the hydrogenation of carbon monoxide over palladium. *Topics in Catalysis*, 9(3-4), 135-152.
- Newton, R. H., & Dodge, B. F. (1933). The Equilibrium between Carbon Monoxide, Hydrogen, Formaldehyde and Methanol. I. The Reactions $\text{CO} + \text{H}_2 = \text{HCOH}$ and $\text{H}_2 + \text{HCOH} = \text{CH}_3\text{OH}$. *Journal of American Chemical Society*, 55(12).
- Niu, Y., Yeung, L. K., & Crooks, R. M. (2001). Size-selective hydrogenation of olefins by Dendrimer-encapsulated palladium nanoparticles. *Journal of the American Chemical Society*, 123(28), 6840-6846.
- Noyori, R., & Hashiguchi, S. (1997). Asymmetric Transfer Hydrogenation Catalyzed by Chiral Ruthenium Complexes. *Accounts of Chemical Research*, 30(2), 97-102.
- Oelkers, E. H., Helgeson, H. C., Shock, E. L., Sverjensky, D. A., Johnson, J. W., & Pokrovskii, V. A. (1995). Summary of the Apparent Standard Partial Molal Gibbs Free Energies of Formation of Aqueous Species, Minerals, and Gases at Pressures 1 to 5000 Bars and Temperatures 25 to 1000 °C. *Journal of Physical and Chemical Reference Data*, 24(4), 160.
- Purwanto, Deshpande, R. M., Chaudhari, R. V., & Delmas, H. (1996). Solubility of hydrogen, carbon monoxide, and 1-octene in various solvents and solvent mixtures. *Journal of Chemical and Engineering Data*, 41(6), 1414-1417.
- Ravenelle, R. M., Copeland, J. R., Kim, W. G., Crittenden, J. C., & Sievers, C. (2011). Structural Changes of $\gamma\text{-Al}_2\text{O}_3$ -Supported Catalysts in Hot Liquid Water. *ACS Catalysis*, 1(5), 552-561.
- Remediakis, I. N., Abild-Pedersen, F., & Nørskov, J. K. (2004). DFT study of formaldehyde and methanol synthesis from CO and H₂ on Ni(111). *Journal of Physical Chemistry B*, 108(38), 14535-14540.
- Reuss, G., Disteldorf, W., Gamer, A. O., & Hilt, A. (2003). *Ullmann's Encyclopedia of Industrial Chemistry* (6 ed. Vol. 15). Weinheim: Wiley.
- Rosen, M. A., & Scott, D. S. (1988). Energy and exergy analyses of a production process for methanol from natural gas. *International Journal of Hydrogen Energy*, 13(10), 617-623.
- S Kislik, V. (2010). Chapter 2 - Carrier-Facilitated Coupled Transport Through Liquid Membranes: General Theoretical Considerations and Influencing Parameters. In V. S. Kislik (Ed.), *Liquid Membranes* (pp. 17-71). Amsterdam: Elsevier.
- Tanksale, A., Beltramini, J. N., Dumesic, J. A., & Lu, G. Q. (2008). Effect of Pt and Pd promoter on Ni supported catalysts-A TPR/TPO/TPD and microcalorimetry study. *Journal of Catalysis*, 258(2), 366-377.
- Walker, J. F. (1967). *Formaldehyde* (3 ed. Vol. 12). New York: Reinhold Publishing Corporation.
- Winkelman, J. G. M., Ottens, M., & Beenackers, A. A. C. M. (2000). The kinetics of the dehydration of methylene glycol. *Chemical Engineering Science*, 55(11), 2065-2071.
- Winkelman, J. G. M., Voorwinde, O. K., Ottens, M., Beenackers, A. A. C. M., & Janssen, L. P. B. M. (2002). Kinetics and chemical equilibrium of the hydration of formaldehyde. *Chemical Engineering Science*, 57(19), 4067-4076.
- Wojcieszak, R., Genet, M. J., Eloy, P., Ruiz, P., & Gaigneaux, E. M. (2010). Determination of the size of supported Pd nanoparticles by X-ray photoelectron spectroscopy. Comparison with X-ray diffraction, Transmission electron microscopy, and H₂ chemisorption methods. *Journal of Physical Chemistry C*, 114(39), 16677-16684.

Chapter 4:

Reaction Mechanism of CO Hydrogenation to Formaldehyde in the Aqueous Phase

Abstract

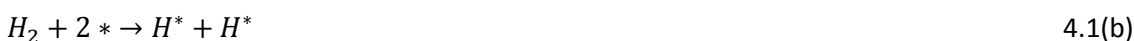
In this chapter, a reaction mechanism is proposed for hydrogenation of carbon monoxide into formaldehyde. Ideally, direct detection of intermediate species of the reaction in-situ is required for deducing reaction mechanism in heterogeneous catalysis. However, considering the harsh operating conditions of the process (i.e. high pressure and aqueous environment), an in-situ surface study was not feasible. Therefore, the reaction mechanism is investigated in this study based on ex-situ investigation of the potential intermediate products in the samples collected during the reaction in addition to isotope labelling. In separate studies deuterated water and methanol were used with hydrogen gas and normal water and methanol were used with deuterium gas to identify the hydrogen transfer steps in formaldehyde formation using a mass spectrometer. The results suggest that both carbon monoxide and hydrogen gases are dissolved into the reaction mixture and adsorbed on the surface of the catalyst. It is proposed that while carbon monoxide is adsorbed as a molecule, hydrogen adsorbs dissociatively. The adsorbed atoms of hydrogen then attach to the adsorbed carbon monoxide to form formaldehyde molecule. It is shown that in the absence of methanol in the reaction mixture, the adsorbed formaldehyde molecules are further hydrogenated to form methanol. However, the selectivity towards formaldehyde is 100% when the solvent contains at least 5 vol% methanol.

This page is intentionally left blank

4.1 Introduction

The conventional process for the production of formaldehyde was presented in detail in chapter 2. The long sequence of production and the high rate of energy loss due to combustion, compression and large purification units in the conventional process leads to relatively low exergy efficiency (~43%) (Bahmanpour et al., 2014; Rosen & Scott, 1988). A novel method of HCHO production was proposed in chapter 3 which could potentially increase the exergy efficiency. Since this is a new method of HCHO production, understanding its reaction mechanism is important so that suitable catalysts and solvents can be identified. Therefore, in this chapter the reaction mechanism of HCHO production through CO hydrogenation is investigated. *In-situ* study of the catalyst surface would be normally necessary to identify the intermediate adsorbed species of reactions. *In-situ* ATR-FTIR has been used in similar processes to investigate the reactions on the catalyst surface (Copeland et al., 2013; Ebbesen et al., 2007). However, considering the harsh conditions in the current work (high pressure and the situation of the catalyst in the aqueous phase), an *in-situ* study of the catalyst surface was not feasible. Therefore, *ex-situ* methods are applied to investigate the reaction mechanism.

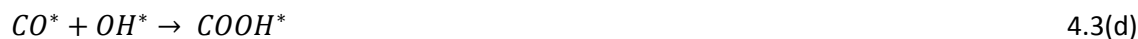
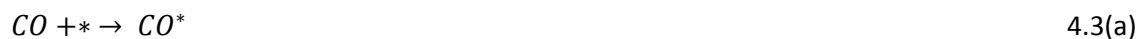
The first step is to consider all possible reaction mechanisms in the process. Based on the source of hydrogen atoms forming HCHO molecule, different reaction mechanisms are applicable. If the source of H atoms is the gaseous H₂ in the reactor, the reaction pathway 4.1 may be proposed:



Another source of H atoms can be dissociative adsorption of water molecules on the catalyst surface as H and OH groups. In which case, the HCHO molecule forms on the surface of the catalyst based on the pathway 4.2 with the formation of formic acid (HCOOH) as the intermediate or hydrated form of

Chapter 4

HCHO known as methylene glycol ($\text{CH}_2(\text{OH})_2$) may be formed directly on the surface of the catalyst based on the reaction pathway 4.3



The last possible mechanism is through carboxylation of CH_3OH through which methyl formate (CH_3OCOH) is formed as an intermediate:





All mentioned reaction mechanisms are summarized in Figure 4.1. Formation of HCHO through dehydrogenation or partial oxidation of CH₃OH in this process is highly unlikely considering the reducing environment in which the reaction occurs. The four mentioned possible mechanisms can be distinguished based on the source of H atoms forming the HCHO molecules and the potential intermediates which may form during the reaction. These mechanisms can be distinguished by using deuterium labelling technique. Table 4.1 presents the possible products of each experiment based on each possible mechanism.

Table 4.1: Possible intermediate and final products based on feedstock and possible mechanisms

Feedstock	Solvent	Products			
		Mechanism 4.1	Mechanism 4.2	Mechanism 4.3	Mechanism 4.4
H₂ and CO	5% CH₃OH in H₂O	HCHO	HCHO	CH ₂ (OH) ₂	HCHO
		Detectable Intermediate: -	Detectable Intermediate: (HCOOH)	Detectable Intermediate: -	Detectable Intermediate: (CH ₃ OCOH)
D₂ and CO	5% CH₃OH in H₂O	DCDO	HCHO	CHDO ₂ HD	HCDO
		Detectable Intermediate: -	Detectable Intermediate: (HCOOH)	Detectable Intermediate: -	Detectable Intermediate: (CH ₃ OCOH/ CH ₃ OCOD)
H₂ and CO	5% CD₃OD in D₂O	HCHO	DCDO	CHDO ₂ HD	HCDO
		Detectable Intermediate: -	Detectable Intermediate: (DCOOD)	Detectable Intermediate: -	Detectable Intermediate: (CD ₃ OCOH/ CD ₃ OCOD)

Chapter 4

Mechanism 4.1 is shown to be feasible based on DFT studies on CO hydrogenation to CH₃OH in the literature (Neurock, 1999; Remediakis et al., 2004). In these studies, it is shown that HCHO can possibly form as an intermediate before conversion to CH₃OH. Hydrogenation of HCOOH to HCHO (mechanism 4.2) is also shown to be feasible in previous studies (Behrens et al., 2012). It is shown that carbon can receive a proton before separation of the hydroxyl group from the carbonyl side. Mechanisms 4.3 and 4.4 are also considered to cover all possible ways of production of HCHO (or CH₂(OH)₂).

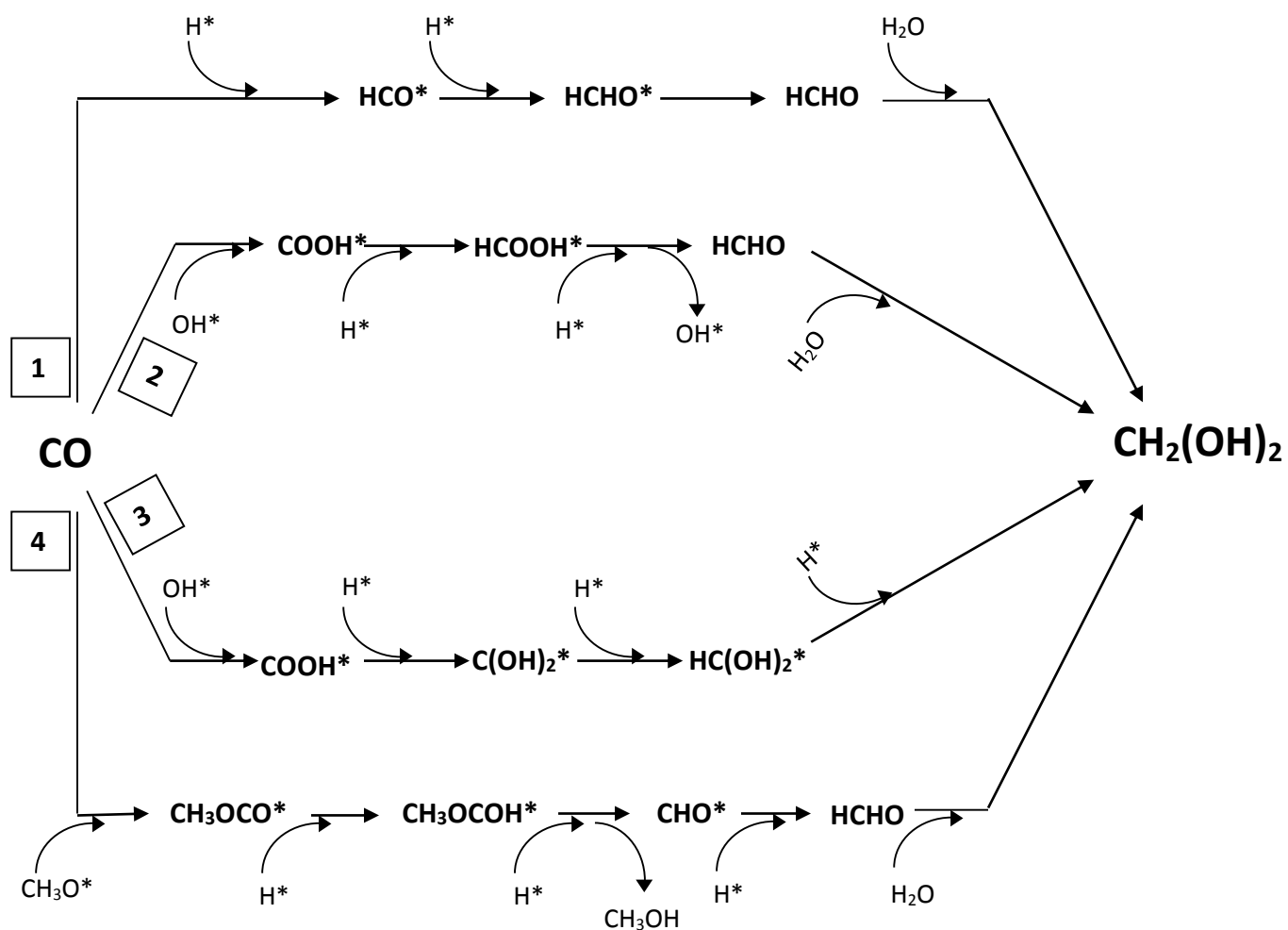


Figure 4.1: Potential reaction mechanisms of CO hydrogenation reaction to HCHO

4.2 Experiments and Methods

The process of catalyst generation, reduction, and examination has been described in chapter 3. Detection of HCHO derivatives and other potential products was done by using RHM-Monosaccharide column (Phenomenex) on HPLC (Agilent) using a refractive Index Detector (RID). HCHO solution (Sigma-Aldrich) was used and diluted to 0.8 mmol.L^{-1} , 1.6 mmol.L^{-1} , 2.5 mmol.L^{-1} , and 3.3 mmol.L^{-1} to generate a calibration curve for detection of methylene glycol ($\text{CH}_2(\text{OH})_2$) which is the hydrated form of HCHO. $10 \mu\text{l}$ of each solution was injected into the column using milli-Q water as the carrier phase. 0.5 ml/min of carrier phase was used and the column was kept at 338 K . RID temperature was kept constant at 318 K . D_2 (Sigma-Aldrich), D_2O and CD_3OD (Merck Millipore) were used in the batch reactor for detection of the source of hydrogen transfer in the HCHO production.

The blank solutions (containing H_2O and CH_3OH in the H_2 replacement experiment and D_2O and CD_3OD in the solvent replacement experiment) as well as the samples taken from the process were heated to 338 K for 10 min . the headspace of each vial was injected into an injection port situated in the carrier gas line. Carrier gas was connected to vacuum chamber through a mass flow controller. The gas stream was sampled using a capillary tube connected to the vacuum chamber which was supplied with an RGA-300 quadrupole mass spectrometer. The carrier gas flow was set to 70 ml/min . The gas samples were checked constantly as the partial pressure of the gas passing through the vacuum chamber was plotted against time. Figure 4.2 shows the schematic diagram of the setup equipped with MS.

Chapter 4

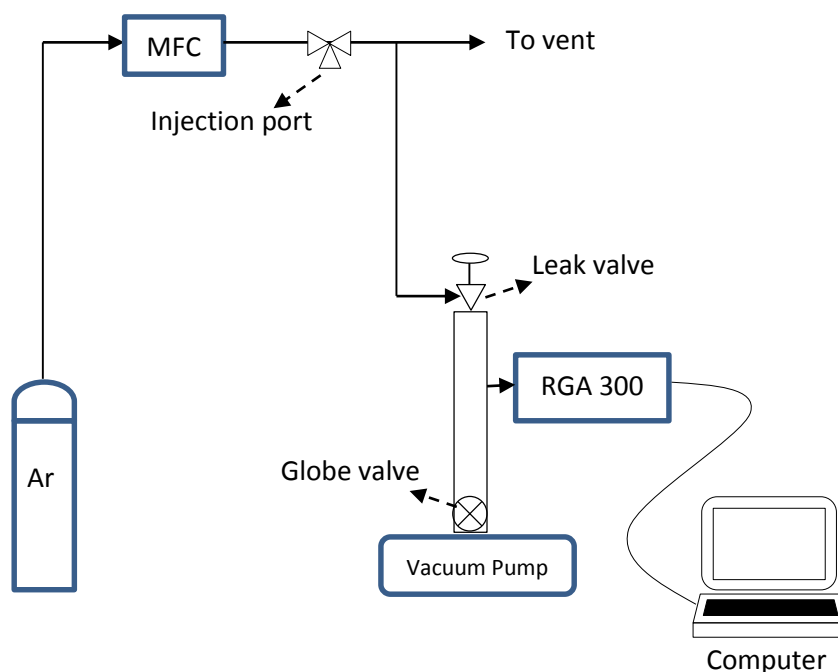


Figure 4.2: schematic diagram of the setup equipped with MS

To detect HCHO or its derivatives on HPLC, different standard formalin solutions were prepared at 0.8 mmol.L^{-1} , 1.6 mmol.L^{-1} , 2.5 mmol.L^{-1} , and 3.3 mmol.L^{-1} . The chromatograms are presented in Figure 4.3. Samples were checked on HPLC and the area underneath the peak representing $\text{CH}_2(\text{OH})_2$ was calibrated based on the concentration. The retention time of the peak was 17.6 min and the calibration curve (Figure 4.4) was linear. This result by itself is interesting since many researchers have tried to detect HCHO or its hydrated form ($\text{CH}_2(\text{OH})_2$) by complicated derivatization methods (Arias-Pérez et al., 1992; Dojahn et al., 2001; Soman et al., 2008). To the author's knowledge, detection of underivatized HCHO on HPLC is reported for the first time in this study.

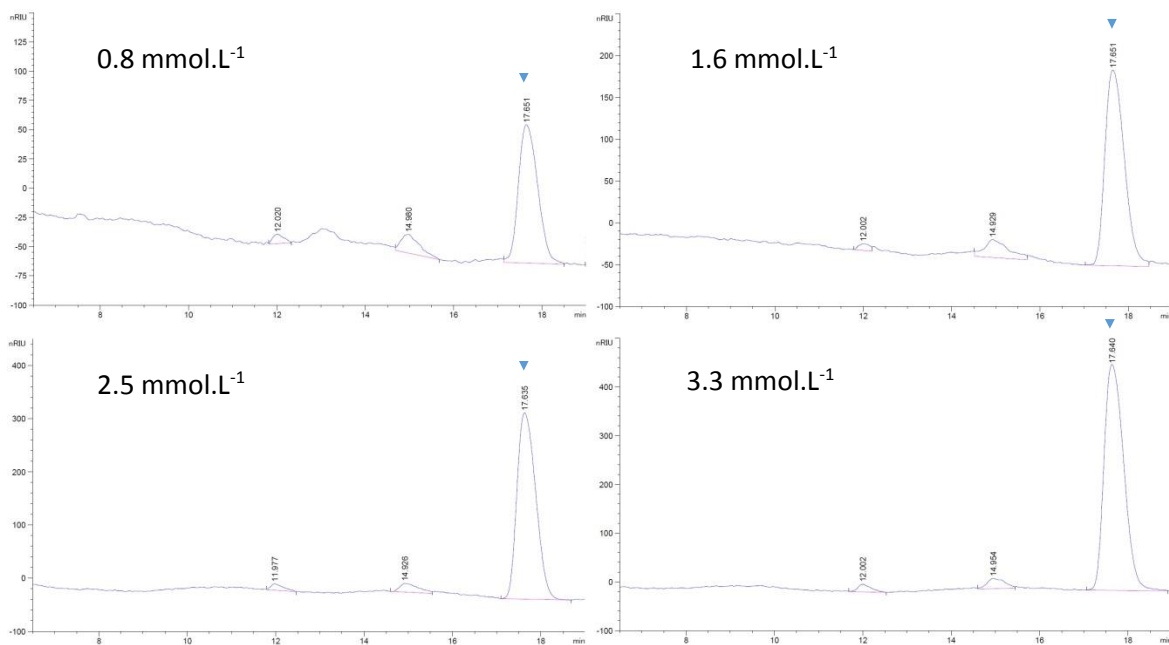


Figure 4.3: Chromatograms of the standard HCHO solutions (▼ = peak at 17.6 min which was calibrated for HCHO)

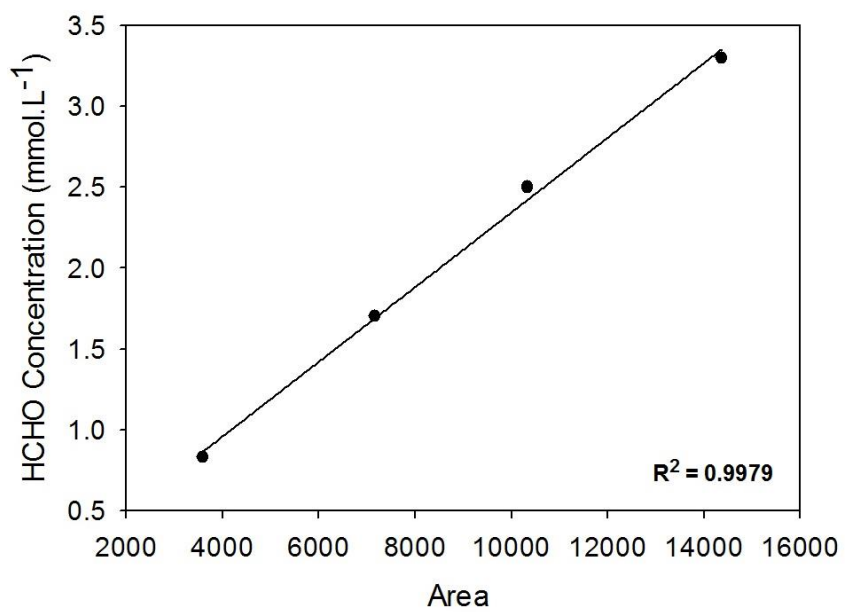


Figure 4.4: Calibration Curve of HCHO on HPLC

Chapter 4

4.3 Sample Investigation

The samples taken from the process were checked on HPLC for detection of $\text{CH}_2(\text{OH})_2$ and any potential intermediate products. The chromatograms are shown in Figure 4.5. Based on the achieved chromatograms, it can be seen that no peak is detected before $\text{CH}_2(\text{OH})_2$ appears at 1.5 h of operation. This indicates that no intermediate products are formed before the formation of HCHO (and consequently $\text{CH}_2(\text{OH})_2$).

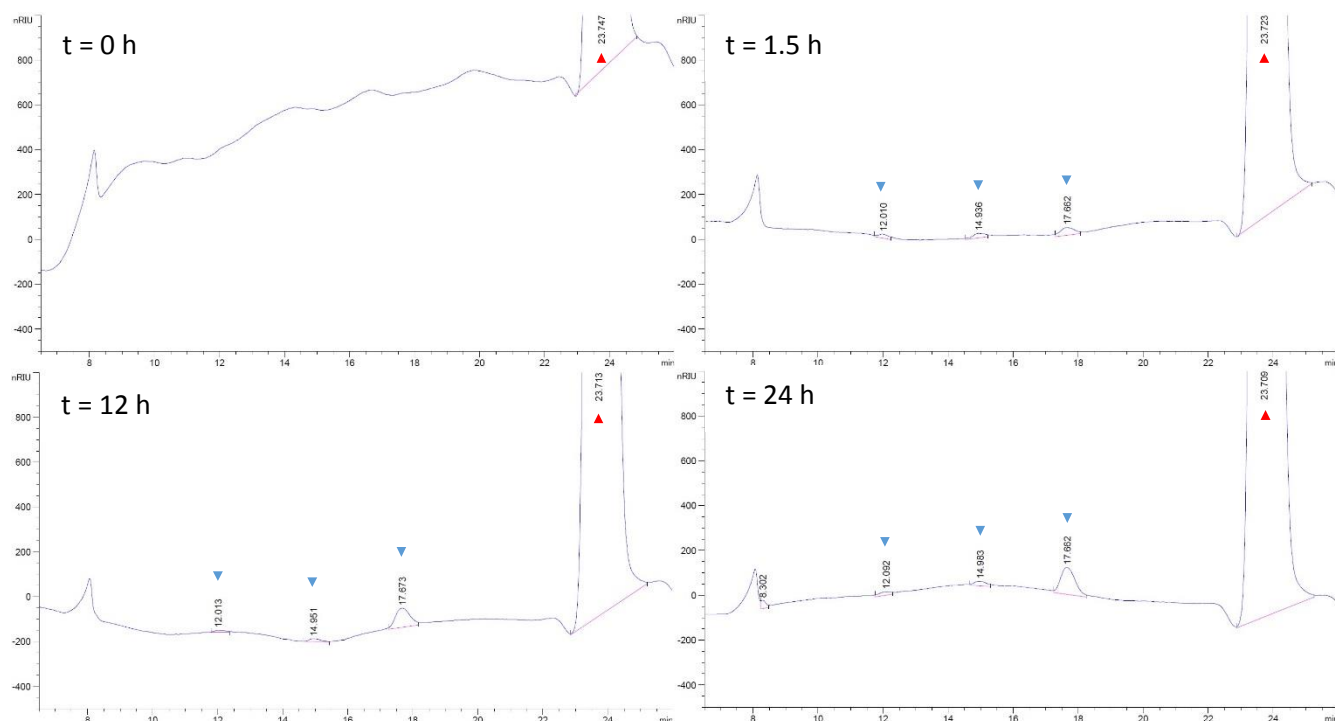


Figure 4.5: HPLC chromatograms of samples taken at various reaction times. Reaction conditions: T = 353 K, P = 100 bar.

▼ = peak associated with standard formalin solution (only peak at 17.6 min was calibrated for HCHO); ▲ = peak associated with methanol

However, in order to confirm that the potential intermediates based on the discussed reaction mechanisms were not present in the samples, a standard solution containing 400 ppm of formalin solution as well as 100 ppm of HCOOH and CH_3COOH was checked on HPLC. The peaks representing CH_3COOH and HCOOH were observed at 7.36 min and 11.46 min, respectively, which were not detected in the samples' chromatograms. The chromatogram of the standard solution is shown in appendix A.5.

4.4 Determination of the Source of Hydrogen Atoms

4.4.1 Labelling H Atoms by Using D₂

First hypothesis is that hydrogenation of CO happens via reaction mechanism 4.1 in which molecular hydrogen gas is dissolved in water and then adsorbed dissociatively on the catalysts surface, followed by surface reaction of adsorbed H and CO. H₂ gas was replaced with D₂ in the reaction whereas H₂O and 5 vol% CH₃OH were used as solvents in the reaction mixture. Temperature was set to 353 K during the process and the reactor was pressurized to 100 bar (CO:H₂ 50:50). Three samples were collected during the process at 24 h, 30 h, and 48 h. The headspace of the blank solution and the reaction product was injected in the injection port at 95 s, 313 s, 588 s, and 887 s. Ten different mass to charge ratio were monitored simultaneously on the RGA software. The mass to charge ratios (m/z) of 20 and 34 were selected to monitor D₂O and CD₃OD profiles. $m/z = 29, 30$ and 31 were selected to monitor HCHO, DCDO, and CH₃OH profiles, respectively.

The mass to charge ratios of 29, 30, and 31 are shown in Figure 4.6. As expected, no peak was observed for HCHO and DCDO (or DCHO) when the blank solution headspace was injected. This confirms that the blank solution did not contain any form of formaldehyde (HCHO, DCHO, or DCDO). Sample injections showed peaks at $m/z= 30$ whereas no peak was observed at $m/z= 29$. This confirms the first hypothesis that the reaction takes place according to mechanism 4.1. Absence of peak at $m/z= 29$ rules out possibility of formation of HCHO and DCHO. Therefore, the hydrogenation of CO proceeded via transfer of adsorbed D atoms only.

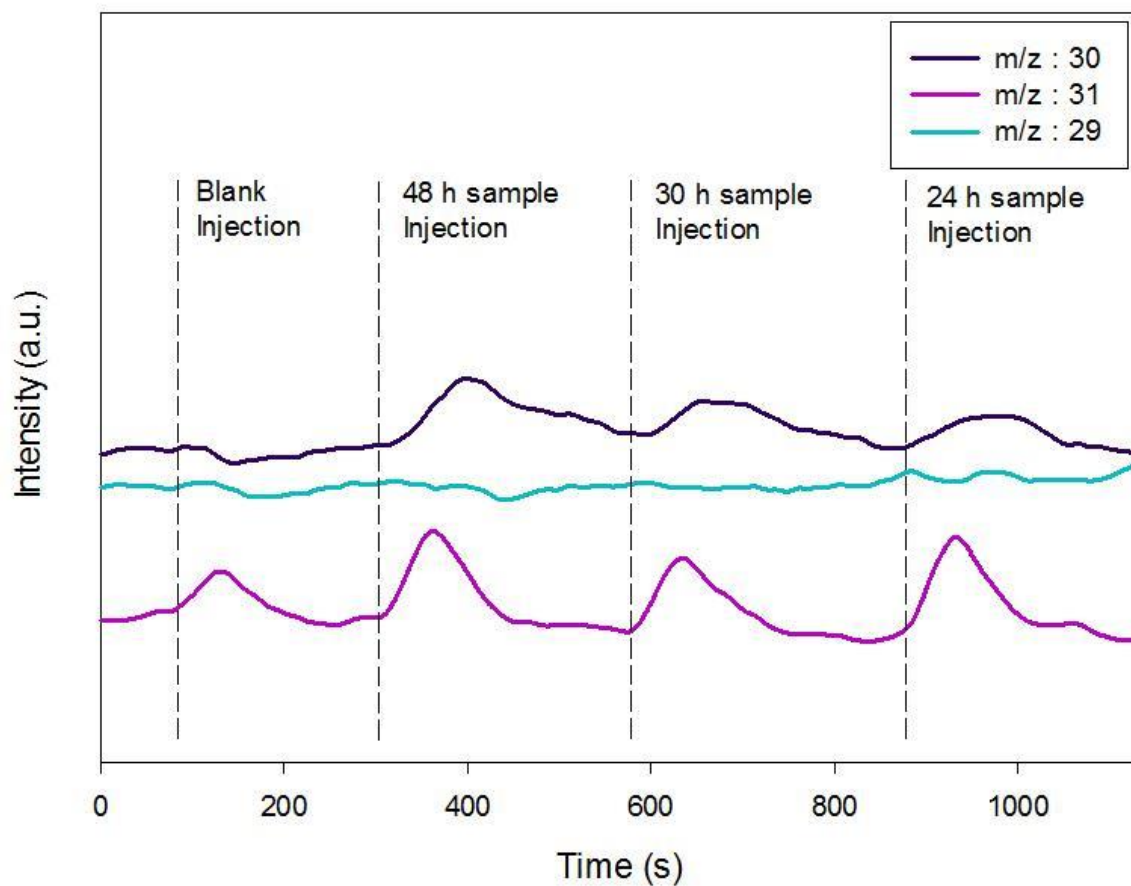


Figure 4.6: Mass to charge ratio profiles for HCHO (29), DCDO (30), and CH₃OH (31) using 5 vol% CH₃OH in H₂O as the reaction mixture

Profiles for $m/z=20$ and 34 , corresponding to D_2O and CD_3OD , were also observed to test for any side products of the reaction (Figure 4.7). No peaks were observed at either m/z ratios which shows that neither D_2O nor CD_3OD were produced in this reaction. This confirms that in the presence of methanol in the reaction mixture HCHO would not hydrogenate further to form methanol since the equilibrium is not favourable.

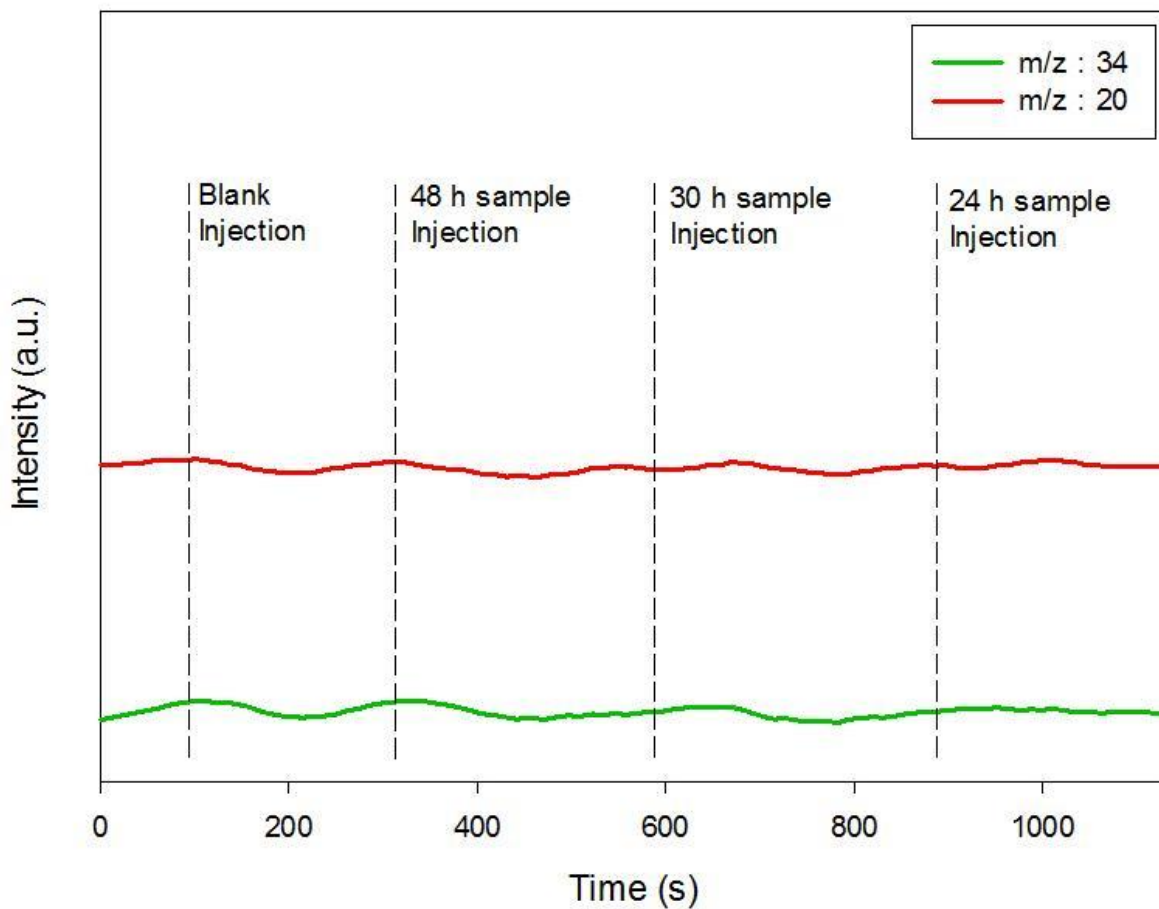


Figure 4.7: Mass to charge ratio profiles for D_2O (20) and CD_3OD (34) using 5 vol% CH_3OH in H_2O as the reaction mixture

4.4.2 Labelling H Atoms by Using D_2O and CD_3OD

To confirm the results of the H_2 replacement experiment, 5 vol% CD_3OD in D_2O was used as the solvent in the solvent replacement experiment. H_2 gas was used in the reactor in this test. In this experiment, the headspace of the blank solution and the samples was injected in the injection port at 93 s, 332 s, 650 s, and 936 s, respectively. The m/z ratios monitored during the injection were 20 for D_2O 34 for CD_3OD , 29 for $HCHO$ 30 for $DCDO$ (or $DCHO$) and 31 for CH_3OH . Figure 4.8 shows peaks at 20 and 34 which shows the presence of D_2O and CD_3OD in each sample.

Chapter 4

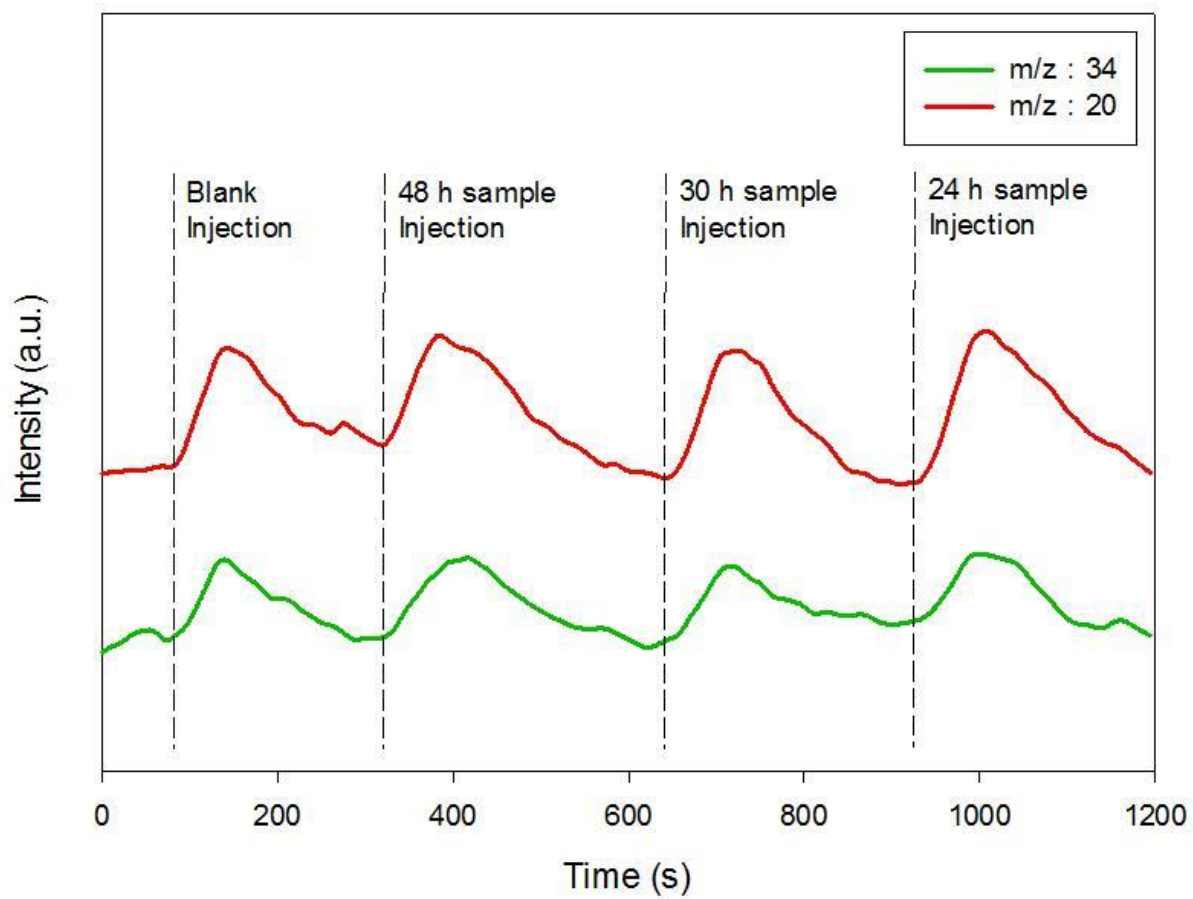


Figure 4.8: Mass to charge ratio profiles for D_2O (20) and CD_3OD (34) using 5 vol% CD_3OD in D_2O as the reaction mixture

Figure 4.9 shows the m/z profiles of 29, 30, and 31.

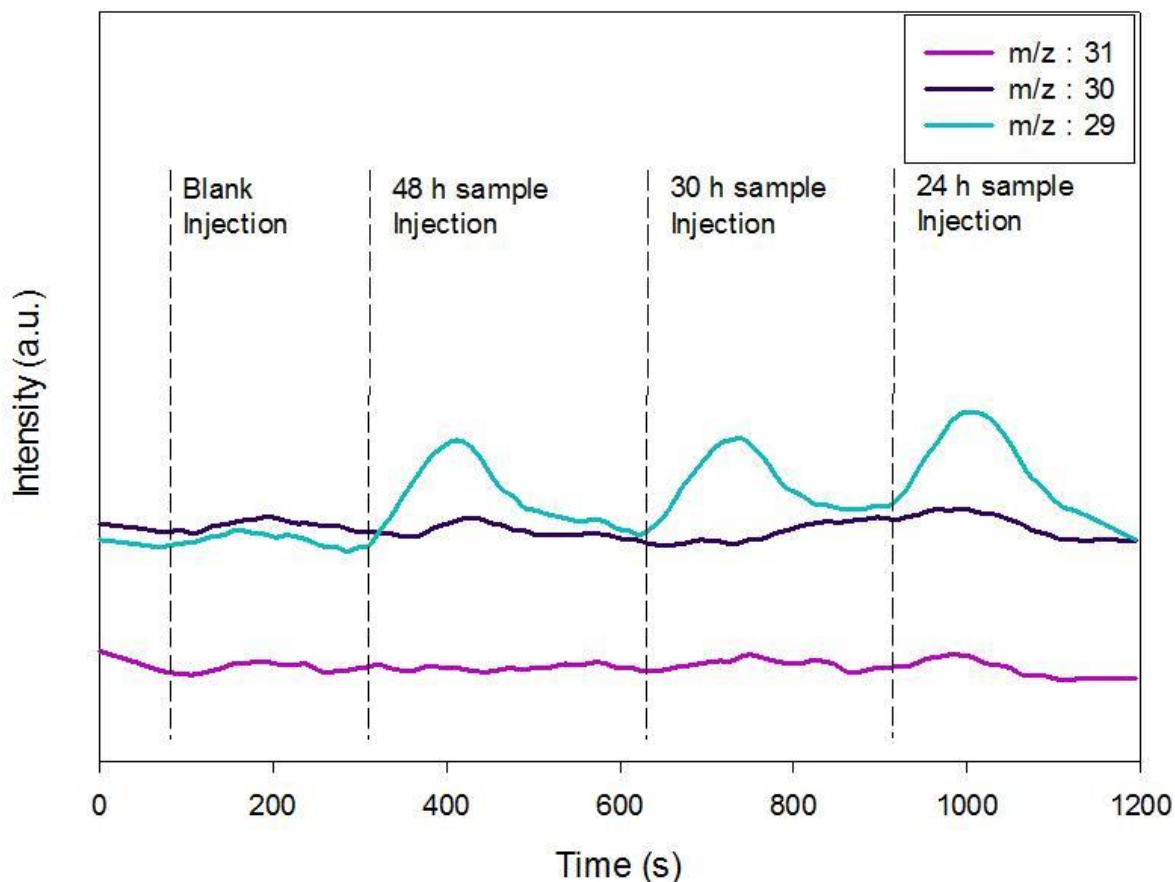


Figure 4.9: Mass to charge ratio profiles for HCHO (29), DCDO (30), and CH₃OH (31) using 5 vol% CD₃OD in D₂O as the reaction mixture

No peak is observed when the blank sample was injected which confirms the absence of HCHO and CH₃OH. HCHO peak at $m/z = 29$ is observed for the samples taken after 48 h, 30 h and 24 h reaction time. This is in agreement with the results achieved in the H₂ replacement experiment. DCDO (or DCHO) peak at $m/z = 30$ was not observed in these samples which indicate that hydrogenation of CO did not take place via deuterium transfer from D₂O or CD₃OD. Figure 4.9 also shows that CH₃OH peak at $m/z = 31$ is not observed which indicate that HCHO did not go through further hydrogenation to form CH₃OH. It is worth noting that CH₂(OH)₂ (or its deuterated form) cannot be detected by this method since CH₂(OH)₂ does not exist in the gas phase. When the liquid sample is heated, CH₂(OH)₂ dehydrates to form HCHO in the gas phase.

Chapter 4

Based on the above mentioned results, it is concluded that no intermediate product forms during the process before the formation of $\text{CH}_2(\text{OH})_2$ and the source of H atoms participating in the formation of HCHO is the gaseous H_2 in the reactor. Considering all possible reaction mechanisms for this reaction, the only possible reaction mechanism which satisfies these criteria is mechanism 4.1.

Therefore, it is proposed that CO and H_2 gas molecules are partially dissolved in the reaction mixture. The dissolved gases are adsorbed on the surface of the catalyst. While CO is adsorbed in its molecular form, H_2 adsorbs dissociatively forming two H atoms. In the next step, H atoms attach to the C atom forming HCHO which desorbs from the surface of the catalyst and hydrates to form $\text{CH}_2(\text{OH})_2$.

4.5 Reaction Mechanism in the Absence of CH_3OH

Although the results show that HCHO does not go through further hydrogenation to form CH_3OH , this fact can be affected in the absence of CH_3OH in the reaction mixture. Therefore, another test run was conducted using pure water as the solvent. The procedure of this test was the same as before. Figure 4.10 shows the comparison of the HCHO yield in the presence and absence of CH_3OH as a solvent.

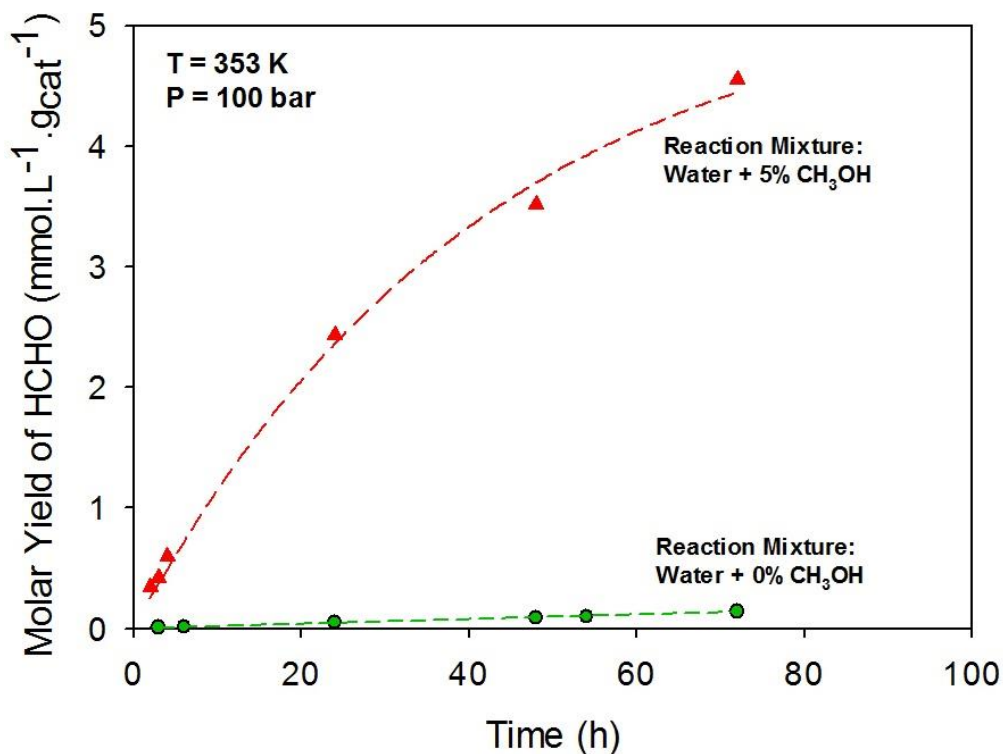


Figure 4.10: The effect of the presence of CH_3OH in the reaction mixture on the molar yield of HCHO

The HCHO yield in the absence of CH₃OH is significantly lower than the yield in the presence of 5 vol% CH₃OH. It was hypothesised that HCHO undergoes further hydrogenation into CH₃OH in the absence of CH₃OH as a solvent. Liquid samples collected at 6 h, 48 h, and 72 h of the run were injected into HPLC to see if CH₃OH is produced through this experiment. Figure 4.11 confirms the production of CH₃OH through this process in the absence of CH₃OH as a solvent. When 5 vol% CH₃OH is used as a solvent, the initial concentration of CH₃OH shifts the equilibrium in the favour of HCHO production. However, in the absence of CH₃OH, HCHO is hydrogenated further into CH₃OH.

The source of HCHO hydrogenation was confirmed by D₂ labelling in the gas phase. The samples collected at 5 h, 48 h and 72 h reaction time were tested in the mass spectrometer (Figure 4.12). Injection of the blank sample did not show any peak, whereas, peaks at $m/z = 34$ and 30 , corresponding to CD₃OD and DCDO is observed for the all the samples. This confirms the hypothesis that in the absence of CH₃OH as a solvent formaldehyde is hydrogenated further in to methanol.

Chapter 4

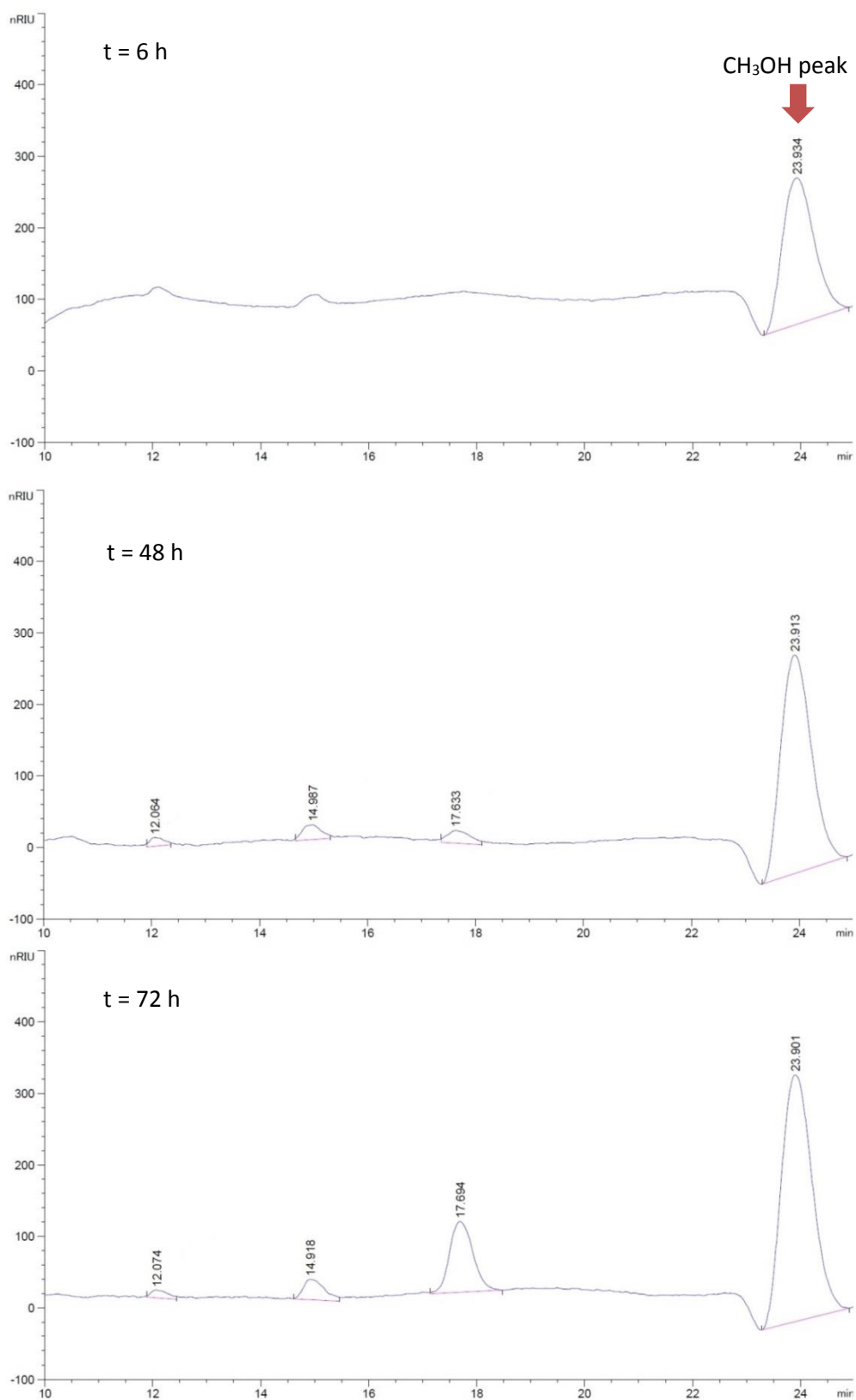


Figure 4.11: The chromatograms of the samples of the run with pure water (no methanol), $T=353$ K, $P=100$ bar

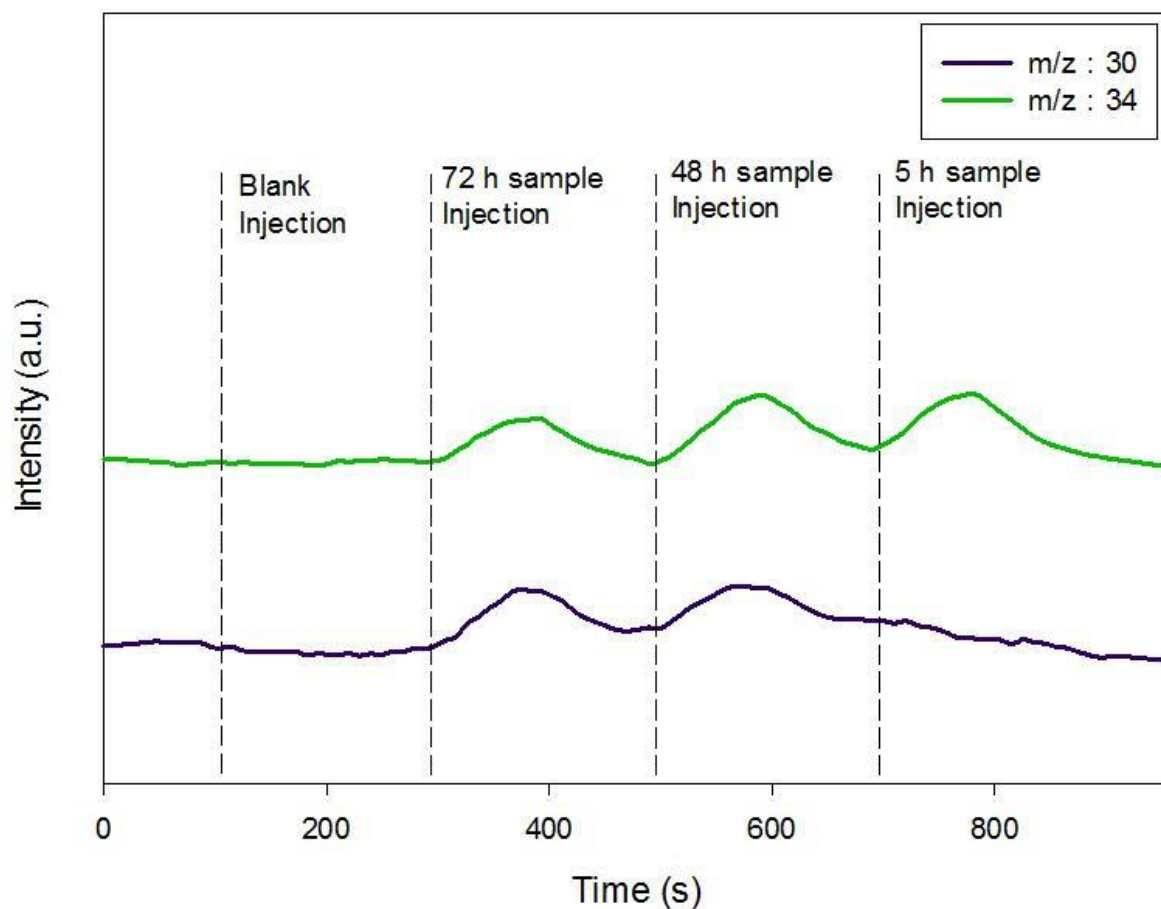
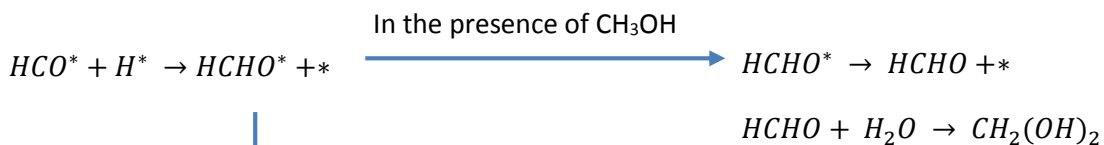
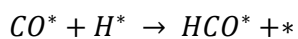
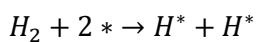
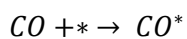


Figure 4.12: Mass to charge ratio profiles for DCDO (30) and CD₃OD (34) using pure H₂O as the solvent

Therefore, the proposed reaction mechanism in this process depends on the presence of CH₃OH as a solvent in the initial reaction mixture. The general reaction mechanism for this process is presented here:



In the absence of CH₃OH



4.6 Conclusion

In this chapter, the reaction mechanism of the CO hydrogenation reaction to HCHO was studied. Considering the harsh conditions of the process, an *in-situ* study of the catalyst surface was not feasible. Therefore, by investigating the samples taken during the experiment at regular intervals as well as isotope labelling of H₂ gas, a reaction mechanism was proposed for this reaction. Analysis of the samples showed that no intermediate product was detected before the formation of HCHO in the reaction environment. To be able to identify the source of H atoms participating in the reaction, two separate test runs were conducted (H₂ replacement and solvent replacement). H₂ was replaced by D₂ in the H₂ replacement run while H₂O and CH₃OH were used as the reaction mixture. To confirm the results of this experiment, H₂O and CH₃OH were replaced by D₂O and CD₃OD as the reaction mixture while H₂ was used in the solvent replacement run. By investigation of the samples on mass spectrometer, it was shown that the source of the H atoms which took part in the formation of HCHO was the gaseous H₂ molecules. Based on the mechanistic investigation of the CO hydrogenation reaction, it was clear that this reaction follows mechanism 4.1. It was proposed that CO and H₂ gases are dissolved in the solvent and adsorb on the surface of the catalyst. As opposed to CO, H₂ adsorbs dissociatively on the catalyst surface to form H atoms. H atoms are attached to CO to form HCHO molecule. In the absence of CH₃OH in the reaction mixture, it was shown that the formed HCHO molecules are further hydrogenated to form CH₃OH which then desorbs from the catalyst surface. However, in the presence of CH₃OH in the reaction mixture, it can be seen that the selectivity towards the formation of HCHO is 100% since no CH₃OH is formed. Desorbed HCHO rapidly reacts with water to form CH₂(OH)₂. Considering the proposed reaction mechanism, solution of gases into the solvent is an important step in this process. Low solubility of CO and H₂ in water is one of limitations of the current method. However, solubility of these reactants may be improved by using other solvents. This possibility is studied in the next chapter.

4.7 References

- Arias-Pérez, R., Lorenzo-Ferreira, R. A., & Alvarez-Devesa, A. (1992). Determination of formaldehyde in particle boards using headspace gas chromatography. *Wood Science and Technology*, *26*(3), 219-226.
- Bahmanpour, A. M., Hoadley, A., & Tanksale, A. (2014). Critical review and exergy analysis of formaldehyde production processes. *Reviews in Chemical Engineering*, *30*(6), 583-604.
- Behrens, M., Studt, F., Kasatkin, I., Köhl, S., Hävecker, M., Abild-Pedersen, F., et al. (2012). The active site of methanol synthesis over Cu/ZnO/Al₂O₃ industrial catalysts. *Science*, *336*(6083), 893-897.
- Copeland, J. R., Foo, G. S., Harrison, L. A., & Sievers, C. (2013). In situ ATR-IR study on aqueous phase reforming reactions of glycerol over a Pt/ γ -Al₂O₃ catalyst. *Catalysis Today*, *205*, 49-59.
- Dojahn, J. G., Wentworth, W. E., & Stearns, S. D. (2001). Characterization of formaldehyde by gas chromatography using multiple pulsed-discharge photoionization detectors and a flame ionization detector. *Journal of Chromatographic Science*, *39*(2), 54-58.
- Ebbesen, S. D., Mojet, B. L., & Lefferts, L. (2007). In situ ATR-IR study of CO adsorption and oxidation over Pt/Al₂O₃ in gas and aqueous phase: Promotion effects by water and pH. *Journal of Catalysis*, *246*(1), 66-73.
- Neurock, M. (1999). First-principles analysis of the hydrogenation of carbon monoxide over palladium. *Topics in Catalysis*, *9*(3-4), 135-152.
- Remediakis, I. N., Abild-Pedersen, F., & Nørskov, J. K. (2004). DFT study of formaldehyde and methanol synthesis from CO and H₂ on Ni(111). *Journal of Physical Chemistry B*, *108*(38), 14535-14540.
- Rosen, M. A., & Scott, D. S. (1988). Energy and exergy analyses of a production process for methanol from natural gas. *International Journal of Hydrogen Energy*, *13*(10), 617-623.
- Soman, A., Qiu, Y., & Chan, L. Q. (2008). HPLC-UV method development and validation for the determination of low level formaldehyde in a drug substance. *Journal of Chromatographic Science*, *46*(6), 461-465.

This page is intentionally left blank

Chapter 5

Effect of Solvents on the Formaldehyde Production in the Slurry Reactor

Abstract

Considering the relatively low solubility of the reactant gases in water, the effect of organic solvents on the yield of formaldehyde is studied in this chapter. Higher solubility of the reactants in organic solvents may increase the yield, however, it is equally important to study the effect of solvent interaction with formaldehyde produced over catalyst surface. Formaldehyde rapidly reacts with water and methanol to produce methylene glycol and hemiformal, respectively and in the process shifts the equilibrium in favour of formaldehyde production. Surprisingly, using water-methanol mixtures reduced the formaldehyde yield. It is theorized that since water molecules fill the space in methanol rings, the stability of methylene glycol and hemiformal, which are stabilized by the hydrogen bonding of the surrounding molecules, is reduced. The highest formaldehyde yield achieved through carbon monoxide hydrogenation was $15.58 \text{ mmol.L}^{-1}.\text{g}_{\text{cat}}^{-1}$ by using methanol as a solvent at 363 K. This yield is four times higher when compared to water as the solvent. Carbon dioxide hydrogenation to formaldehyde is also examined in this study. Although this process is at its preliminary stage at the moment, it shows promising results for future studies. The highest achieved yield through carbon dioxide hydrogenation is $0.62 \text{ mmol.L}^{-1}.\text{g}_{\text{cat}}^{-1}$.

This page is intentionally left blank

5.1 Introduction

A novel method of formaldehyde (HCHO) production through CO hydrogenation was introduced in Chapter 3. In order to have an insight into this process, the reaction mechanism of CO hydrogenation to HCHO in the aqueous phase was studied in Chapter 4. Based on the results obtained in Chapter 4, it was realized that CO and H₂ gases are dissolved in the solvent and then adsorb on the surface of the catalyst. In the absence of CH₃OH in the reaction mixture, it was observed that the formed HCHO molecules are hydrogenated further to form CH₃OH which then desorbs from the catalyst surface. However, in the presence of CH₃OH in the reaction mixture, was observed that the selectivity towards the formation of HCHO is 100%. Considering the relatively low solubility of CO and H₂ in water at 353 K (0.023 mol.L⁻¹ and 0.029 mol.L⁻¹, respectively, calculated based on Henry's law), it is proposed that the yield of HCHO might improve by using other solvents in which the reactant gases are more soluble. Therefore, the effect of solvents on the reaction is studied in this chapter.

The effect of solvents on hydrogenation reactions have been studied in detail (Akpa et al., 2012; Augustine & Techasauvapak, 1994; Bertero et al., 2011; Jianming et al., 2003; Moret et al., 2014; Mukherjee & Vannice, 2006; Rautanen et al., 2000). The solvent effects have been shown to be significant in a similar study of CO₂ hydrogenation into formic acid (HCOOH) in aqueous phase (Moret et al., 2014). It was shown that the HCOOH yield increased by approximately an order of magnitude by using dimethyl sulfoxide (DMSO)-water solution compared to pure water due to the higher activity of the catalyst in DMSO. Liquid phase hydrogenation reaction of toluene (C₇H₈) on Ni/Al₂O₃ showed higher rate using isooctane ((CH₃)₃CCH₂CH(CH₃)₂) and n-heptane (C₇H₁₆) compared with cyclohexane (C₆H₁₂) due to 40% lower hydrogen solubility in C₆H₁₂ compared with other solvents (Rautanen et al., 2000). However, solvent effects on hydrogenation reactions are not always dependant on solubility only. Other parameters such as solvent polarity, catalyst-solvent interactions, and solvent molecular structure may affect the reaction. Although non-polar reactants (such as H₂ in hydrogenation reactions) are more soluble in non-polar solvents, it is known that polar solvents may enhance the adsorption of non-polar reactants on the catalyst surface (Augustine & Techasauvapak, 1994; Singh & Vannice, 2001). The interaction between catalyst support and the solvent can affect the reaction. An interesting example of this case is the effect of hydrophobic and hydrophilic catalyst supports on hydrogenation reaction in two phase water mixtures. Hydrogenation of cyclohexene (C₆H₁₀) and cyclohexanone (C₆H₁₀O) in water/cyclohexane mixture showed that using hydrophobic catalyst

support (such as activated carbon) favours the hydrogenation of C_6H_{10} whereas by using hydrophilic catalyst support (such as SiO_2) $C_6H_{10}O$ is favourably hydrogenated (Koopman et al., 1981). Effect of co-solvents on the molecular structure of the solvation medium is found to have an impact on the selectivity towards the products. Molecular dynamic simulation has shown that glucose selective conversion into 5-hydroxymethyl furfural (HMF) is enhanced by using co-solvents (dimethyl sulfoxide (DMSO), tetrahydrofuran (THF) and N,N-dimethyl formamide (DMF)) due to the arrangement of co-solvent molecules around the H atom of glucose hydroxyl groups (Vasudevan & Mushrif, 2015). It is therefore concluded from literature review that solvents may have complex effects on the conversion and selectivity of the hydrogenation reactions.

Many types of solvents including polar protic (water, methanol and ethanol), polar aprotic (DMSO), and non-polar (C_7H_8) solvents were used in the present study.

Synthesis gas may contain impurities like CO_2 , therefore, the effect of solvents on the hydrogenation of CO_2 in the slurry reactor was also investigated. CO_2 hydrogenation into HCHO has been reported before in the literature (Lunev et al., 2001; Nakata et al., 2014). However, catalytic formation of HCHO directly from CO_2 hydrogenation in the slurry reactor is reported in this study for the first time. CO_2 can react with H_2 to form HCHO in the following way (Eq. 5.1):



Simultaneous hydrogenation of CO and CO_2 resulted from the biomass gasification process could lead to a new process for the production of HCHO.

5.2 Experiments and Methods

Ru-Ni/ Al_2O_3 was used as the catalyst in all the experiments since it provided better yield in the experiments reported in Chapter 3. The catalyst production procedure as well as the characterization results is reported in Chapter 3. In each experiment, 40 ml of the solution was added to a Parr 100 mL non-stirred batch reactor (Parr-4838). 5% v/v CH_3OH was added to each solution to stabilise the produced HCHO molecules and to prevent further hydrogenation of HCHO to CH_3OH . The only exception was when pure CH_3OH was used as the solvent. 1 g of the catalyst was reduced *ex-situ* and added to the reaction mixture. The reactor was pressurized with equimolar CO- H_2 mixture at a total pressure of 100 bar. The pressurized reactor was then heated to the desired temperature at $10^\circ C/min$.

During the reaction, liquid samples were collected using a dip tube and the HCHO concentration was measured using a FluoroQuik fluorometer version 4.3.A using 360nm/490nm as the excitation/emission wavelengths. In this method, a working reagent was prepared by addition of 22 μl of acetoacetanilide ($\text{C}_{10}\text{H}_{11}\text{NO}_2$) and DMSO solution and 33 μl of ammonium acetate ($\text{C}_2\text{H}_3\text{O}_2\text{NH}_4$) solution (Amisience Corporation). 50 μl of the working reagent was mixed with 50 μl of each sample and the mixtures were incubated in the dark for 30 min before measuring the fluorescence intensity. This method of HCHO detection and quantification is used based on previous studies in the literature (Li et al., 2007). Equation 5.1 shows the stoichiometric reaction of CO_2 hydrogenation into HCHO. Since the stoichiometric ratio of CO_2 to H_2 is 1:2, the partial pressure of CO_2 was set to 33 bar and the partial pressure of H_2 was set to 66 bar. The reaction was studied at 353 K. 5% v/v CH_3OH in water and $\text{C}_2\text{H}_5\text{OH}$, and pure CH_3OH were used as the solvents in this case.

5.3 Effect of Solvents on Carbon Monoxide Hydrogenation Process

The effect of solvents on the yield of HCHO production is shown in Figure 5.1. The highest HCHO yield is achieved by using pure CH_3OH followed by 5%v/v CH_3OH /water solution. The rapid reaction of HCHO with water and CH_3OH to form methylene glycol ($\text{CH}_2(\text{OH})_2$) and hemiformal (also known as methoxymethanol) ($\text{C}_2\text{H}_6\text{O}_2$), respectively, shifts the CO hydrogenation reaction equilibrium towards HCHO side which results in higher HCHO yield compared with using other solvents (Bahmanpour et al., 2015).

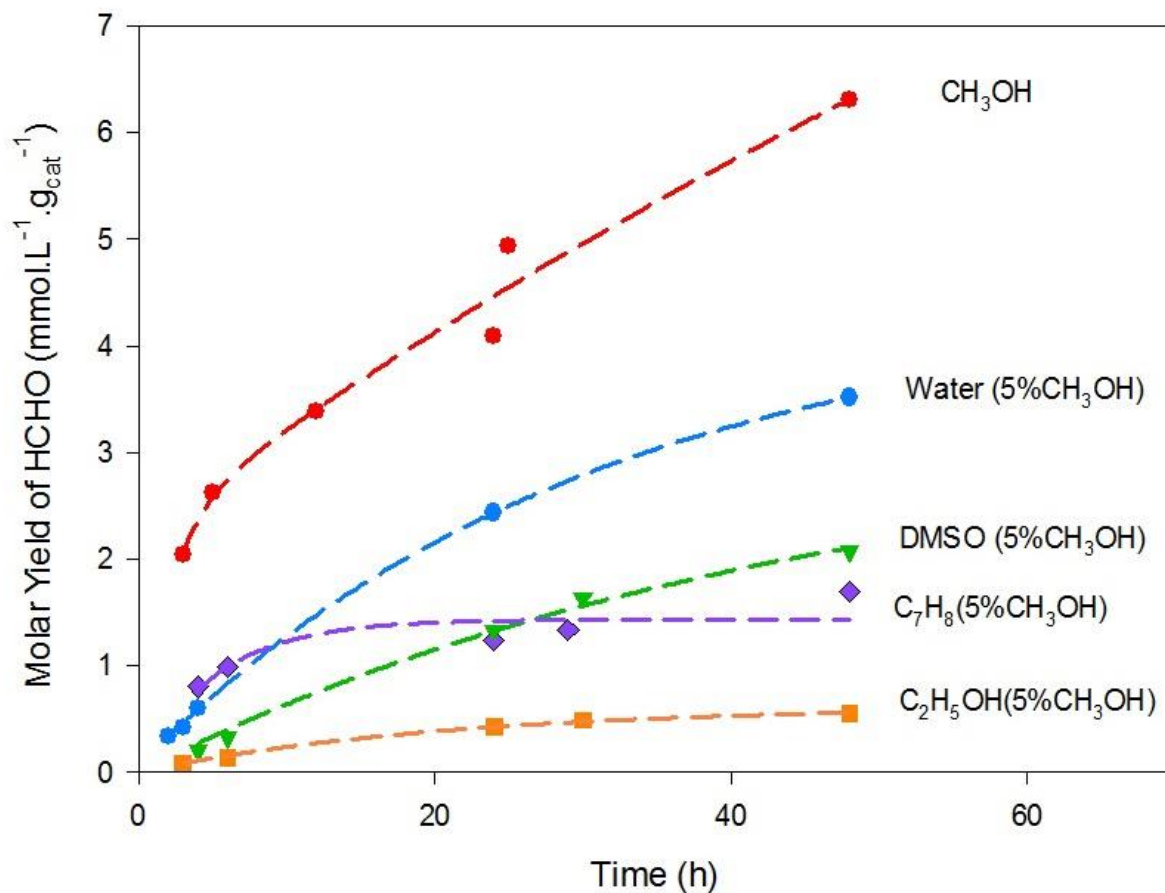


Figure 5.1: The effect of using different solvents on HCHO production yield, T=353 K, P=100 bar, Catalyst: Ru-Ni/Al₂O₃

Higher yield of HCHO in pure CH₃OH solvent may be due to the higher solubility of CO and H₂ compared to water. However, the CO and H₂ solubility is also very high in C₂H₅OH, but the yield of HCHO in this solvent was the lowest (Dake & Chaudharl, 1985; Radhakrishnan et al., 1983). Therefore, it can be concluded that the HCHO yield is a function of reactant solubility as well as the HCHO reactivity and stability in the solvent.

Figure 5.2 shows the effect of composition of water- CH₃OH mixture on the yield of HCHO. It is evident that pure CH₃OH as a solvent results in the highest HCHO yield and the addition of water to CH₃OH in any composition decreases the HCHO yield. Moreover, from Figure 5.3 an interesting trend is observed which shows that the yield of HCHO at t = 48 h is higher at mole fractions of CH₃OH approaching 0 or 1, but the yield is lower for $0 < x < 1.0$. The lowest value of x in Figure 5.3 was set to 4.5×10^{-4} (equal to 0.1 v/v% CH₃OH) which was added to favour the equilibrium towards HCHO.

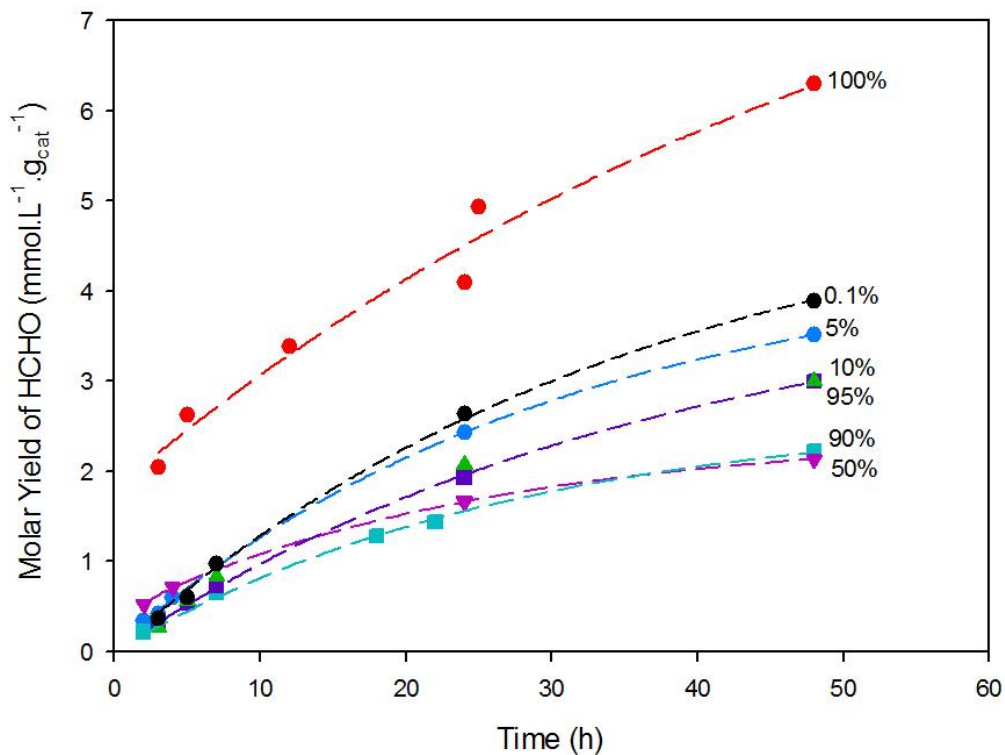


Figure 5.2: Effect of CH₃OH concentration (% v/v) on HCHO yield at T = 353 K, P = 100 bar, Catalyst: Ru-Ni/Al₂O₃

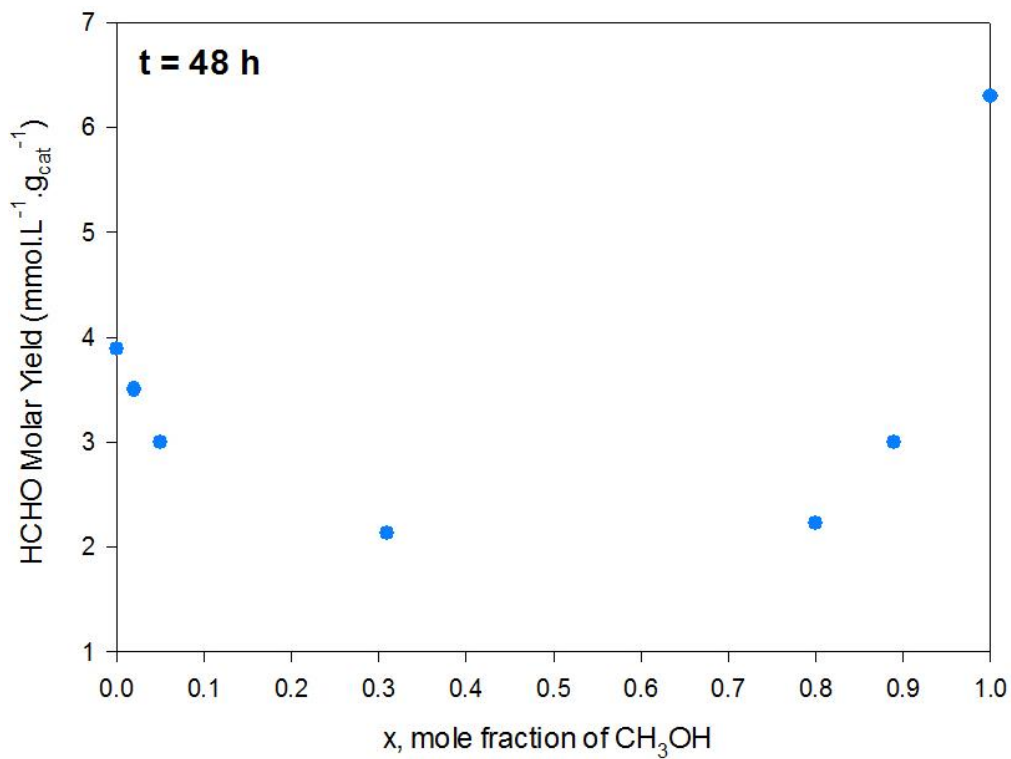


Figure 5.3: Effect of the CH₃OH mole fraction in the solvent mixture on the HCHO yield at t = 48 h, the lowest value of x tested is 4.5×10⁻⁴

It is known that $\text{CH}_2(\text{OH})_2$ and $\text{C}_2\text{H}_6\text{O}_2$ which are formed through HCHO reacting with water and CH_3OH , respectively are unstable molecules. They are stabilized by the hydrogen bonding with the surrounding water or methanol molecules (Boyer et al., 2013). The trend that is observed in Figure 5.3 may be explained by understanding this stabilisation effect of water and methanol via hydrogen bonding. In this thesis it is theorised that the $\text{CH}_2(\text{OH})_2$ molecules are stabilised by hydrogen bonding with water molecules which form cage structure (Izgorodina et al., 2010); and the $\text{C}_2\text{H}_6\text{O}_2$ molecules are stabilised by hydrogen bonding with methanol molecules which form cyclic oligomer structure (Guo et al., 2003). Figure 5.4 shows the theorised process of formation, desorption, and stabilisation of the HCHO molecules in CH_3OH cyclic oligomers when pure CH_3OH was used as a solvent. It is known from literature that water molecules form three dimensional network that dynamically change to form cages and chains (Izgorodina et al., 2010) and CH_3OH molecules form cyclic oligomers of 6 and/or 8 molecules which provide strong hydrogen bonding ($191 \text{ kJ}\cdot\text{mol}^{-1}$) (Guo et al., 2003; Ludwig, 2005). It is also known that the interspace of the CH_3OH cyclic oligomers can be filled with water molecules in water- CH_3OH mixtures (Guo et al., 2003). According to Gao et al., 2003, although CH_3OH is fully soluble in water in all proportions, the mixture is not homogeneously mixed at the molecular level. A chain of 8 CH_3OH molecules bonds with 1-2 water molecules to form a ring and a chain 6 CH_3OH molecules bonds with 2-4 water molecules to form a ring. Their findings also suggest that “free swimming” water molecules (without hydrogen bonding) do not exist in any appreciable amount. Therefore, from the trend observed in Figure 5.3 it can be theorised that the tendency of the CH_3OH cyclic oligomers to accommodate the $\text{C}_2\text{H}_6\text{O}_2$ molecules may decrease in the presence of water molecules, since water molecules may preferentially fill the interspace of the CH_3OH cyclic oligomers, resulting in reduced stability of $\text{C}_2\text{H}_6\text{O}_2$ in water- CH_3OH solutions. The highest mole fraction of CH_3OH at which water would fill the interspace of the CH_3OH cyclic oligomers is 0.89 (configuration of 8 CH_3OH molecules with 1 water molecule). Above this mole fraction ‘water free’ cyclic oligomers of CH_3OH may be found. Figure 5.3 shows that the yield of HCHO increased slightly when the mole fraction of CH_3OH increased from 0.8 to 0.9, however, the yield increased significantly when the mole fraction of CH_3OH was increased to 1.0. This theory may therefore be able to explain the effect of water on the HCHO yield in concentrated CH_3OH solutions. Figure 5.3 closely resembles the excess molar volume of water- CH_3OH mixture which shows non-ideal mixing of water and CH_3OH at the molecular level (Xiao et al., 1997). However, to provide strong evidence to support this theory, further experimental and molecular modelling work similar to the X-ray absorption and X-ray emission

spectroscopy, and density functional theory work of Gao et al. 2003 is necessary. This is beyond the scope of the current thesis.

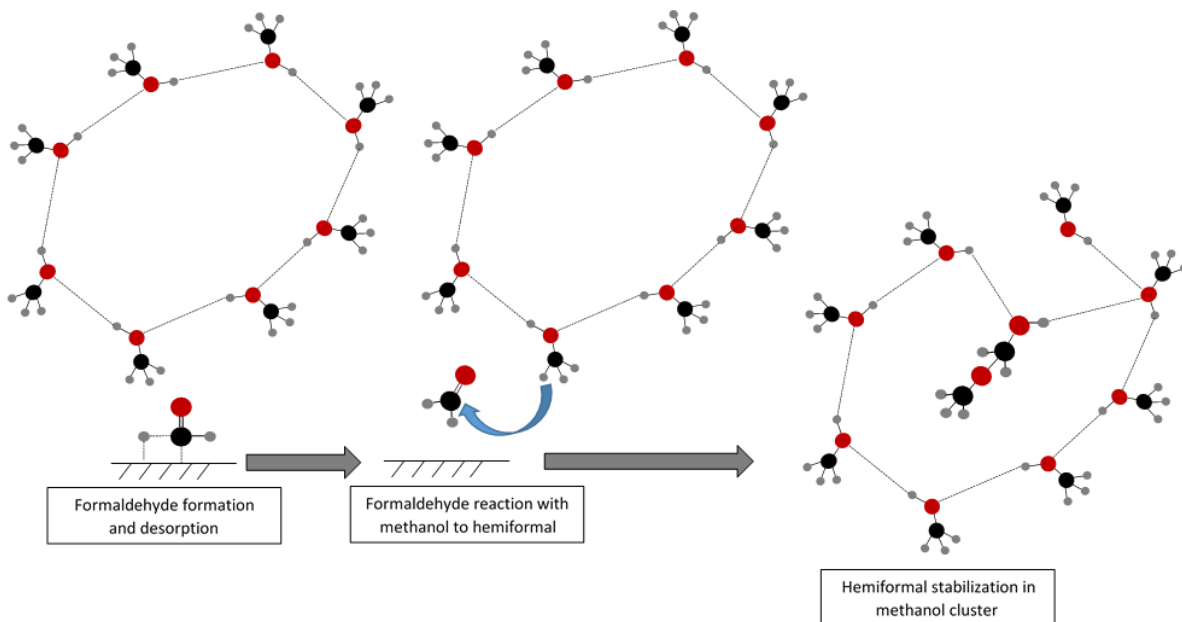


Figure 5.4: A simplified schematic of HCHO formation, desorption and stabilization in CH_3OH . Adapted from(Guo et al., 2003)

The molecular structure of $\text{C}_2\text{H}_5\text{OH}$ molecules may not provide the required molecular space and hydrogen bonding for the produced HCHO molecules since they form winding chain like structure instead of cyclic oligomers or cages (Benmore & Loh, 2000) which may explain the poor yield of HCHO in this solvent.

5.4 Effect of temperature on the HCHO yield in methanol solvent

Figure 5.5 shows the result of HCHO yield at 353 K, 363 K, 373 K, and 403 K using pure CH_3OH . From the initial slope of the curves it can be seen that the rate of reaction increased with temperature, which is in agreement with the previous results reported in Chapter 3. Figure 5.6 shows the Arrhenius plot based on the rate of reaction calculated after $t = 5$ h, assuming first order batch reactor kinetics. The rate of formation is calculated based on the yield of HCHO per unit time. The apparent activation energy, E_a , is calculated to be 8.17 kJ/mol based on this graph. The highest yield is measured to be $15.58 \text{ mmol}\cdot\text{L}^{-1}\cdot\text{g}_{\text{cat}}^{-1}$ which is achieved at 363 K and $t = 100$ h. However, as it can be seen in Figure 5.5, the yield approaches a maximum value at each temperature at long residence times. Moreover, the

maximum yield reduces as the temperature increases, even though the initial rate is higher at higher temperatures.

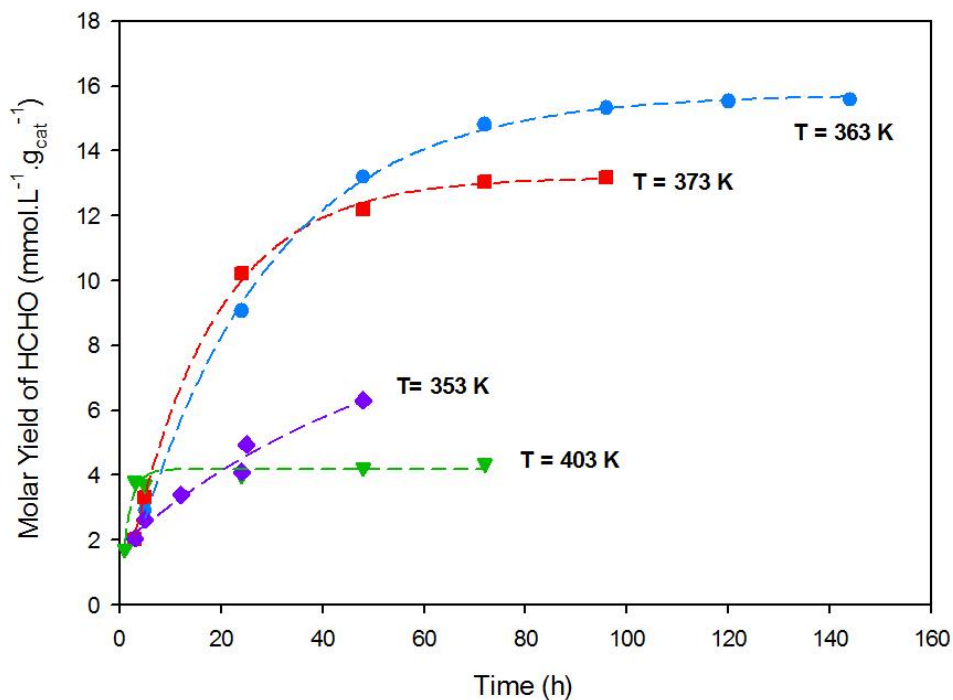


Figure 5.5: Effect of temperature on the molar yield of HCHO, solvent: CH_3OH , $P = 100$ bar

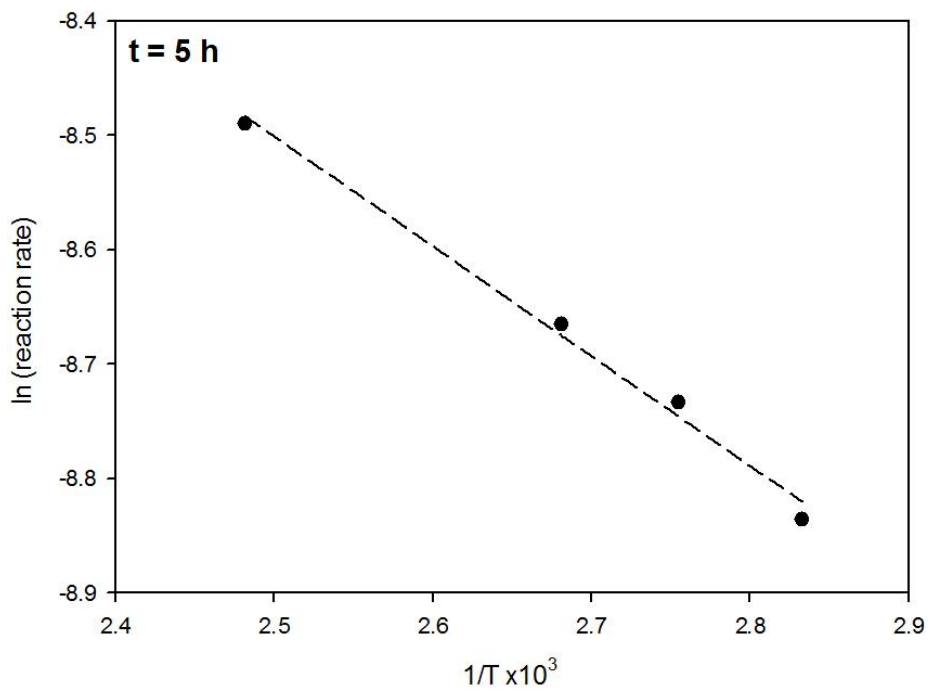


Figure 5.6: Arrhenius plot based on the rate of reaction calculated at $t = 5$ h, solvent: CH_3OH , $P = 100$ bar, Catalyst: Ru-Ni/ Al_2O_3

5.5 Effect of Solvents on Carbon Dioxide Hydrogenation Process

Hydrogenation of CO_2 to produce HCHO was studied by using the identical reaction conditions used in CO hydrogenation in Chapter 3. The results are shown in Figure 5.7. Although the HCHO yield is significantly lower compared to CO hydrogenation, it was important to note that the catalytic hydrogenation of CO_2 to produce HCHO is feasible in the slurry reactor. Similar to CO hydrogenation, the highest HCHO yield is achieved by using CH_3OH as the solvent.

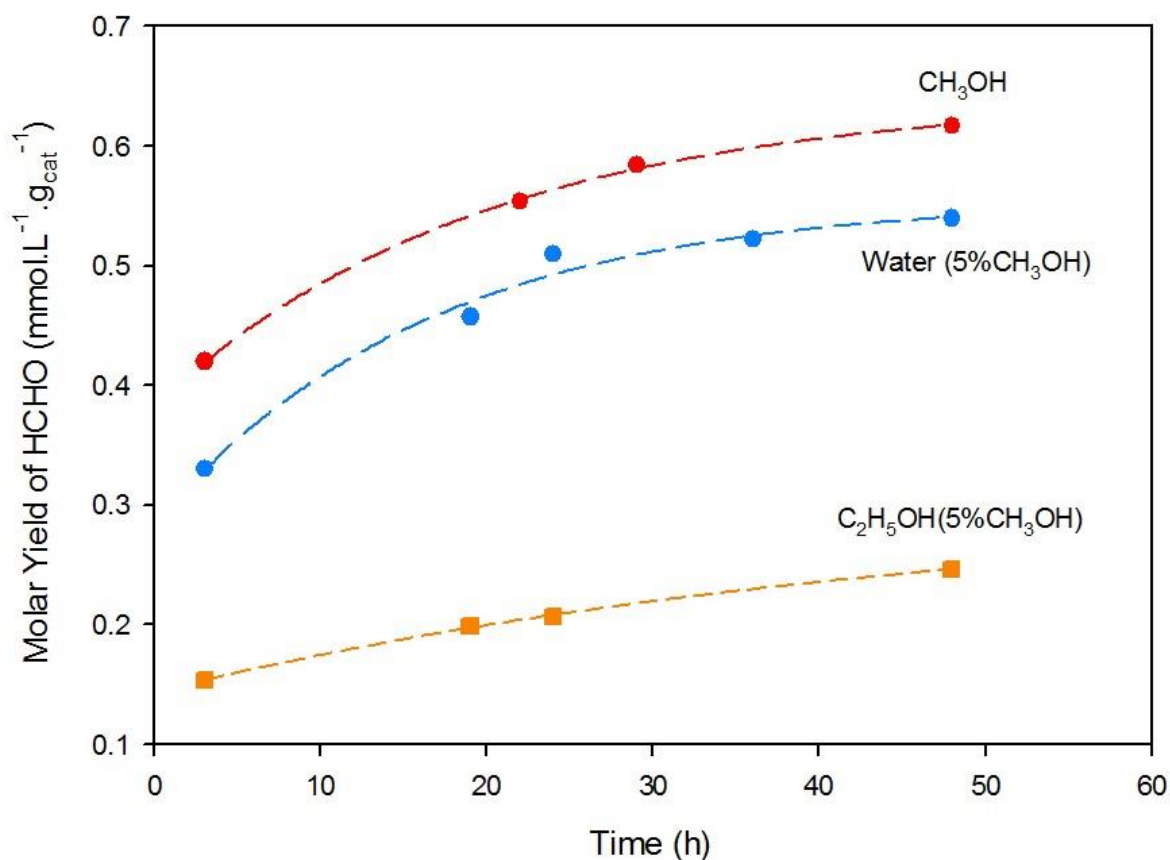


Figure 5.7: CO_2 hydrogenation in the slurry reactor, $T=353\text{ K}$, $P=100\text{ bar}$, Catalyst: $\text{Ru-Ni/Al}_2\text{O}_3$

The CO_2 hydrogenation results presented here are the preliminary results of this study. More detailed studies can be done on optimization, catalyst development, and the mechanism of this process in the future.

5.6 Conclusion

The effects of solvents on the hydrogenation of CO and CO₂ to produce HCHO in the slurry reactor were studied in this chapter. Many types of solvents including polar protic (water, methanol and ethanol), polar aprotic (DMSO), and non-polar (C₇H₈) solvents were used in the present study. It was shown that the highest HCHO yield was achieved by using pure CH₃OH as the solvent followed by 0.1%v/v CH₃OH-water mixture. HCHO reacts with CH₃OH and water to produce C₂H₆O₂ and CH₂(OH)₂, respectively, thereby shifting the equilibrium of hydrogenation towards HCHO production. The CH₃OH and water solvents stabilise the C₂H₆O₂ and CH₂(OH)₂ molecules, respectively, via hydrogen bonding. Lower yield of HCHO was achieved by using water-CH₃OH mixtures compared to pure CH₃OH since water molecules may occupy the CH₃OH cyclic oligomer rings, reducing the stability of HCHO molecules in the solvent. The effect of temperature on HCHO yield using CH₃OH as the solvent was studied and the highest HCHO yield was found to be 15.58 mmol.L⁻¹.g_{cat}⁻¹ at 363 K and 100 bar. It was observed that the reaction rate increased as the temperature increased. However, lower HCHO yield was achieved at higher temperatures and long residence times, since the solubility of the gases as well as the thermodynamic equilibrium of the reaction was less favourable at higher temperatures. CO₂ hydrogenation was investigated to show the feasibility of HCHO production in the catalytic reduction of CO₂ in the slurry reactor. The same trend for HCHO production can be seen in the CO₂ hydrogenation experiments. The highest HCHO yield through CO₂ hydrogenation at 353 K and 100 bar was achieved to be 0.62 mmol.L⁻¹.g_{cat}⁻¹.

5.7 References

- Akpa, B. S., D'Agostino, C., Gladden, L. F., Hindle, K., Manyar, H., McGregor, J., et al. (2012). Solvent effects in the hydrogenation of 2-butanone. *Journal of Catalysis*, 289, 30-41.
- Augustine, R. L., & Techasavapak, P. (1994). Heterogeneous catalysis in organic synthesis. Part 9. Specific site solvent effects in catalytic hydrogenations. *Journal of Molecular Catalysis*, 87(1), 95-105.
- Bahmanpour, A. M., Hoadley, A., & Tanksale, A. (2015). Formaldehyde production via hydrogenation of carbon monoxide in the aqueous phase. *Green Chemistry*, 17(6), 3500-3507.
- Benmore, C. J., & Loh, Y. L. (2000). The structure of liquid ethanol: A neutron diffraction and molecular dynamics study. *Journal of Chemical Physics*, 112(13), 5877-5883.

- Bertero, N. M., Trasarti, A. F., Apesteguía, C. R., & Marchi, A. J. (2011). Solvent effect in the liquid-phase hydrogenation of acetophenone over Ni/SiO₂: A comprehensive study of the phenomenon. *Applied Catalysis A: General*, 394(1-2), 228-238.
- Boyer, I. J., Heldreth, B., Bergfeld, W. F., Belsito, D. V., Hill, R. A., Klaassen, C. D., et al. (2013). Amended safety assessment of formaldehyde and methylene glycol as used in cosmetics. *International journal of toxicology*, 32(6 Suppl), 5S-32S.
- Dake, S. B., & Chaudhari, R. V. (1985). SOLUBILITY OF CO IN AQUEOUS MIXTURES OF METHANOL, ACETIC ACID, ETHANOL, AND PROPIONIC ACID. *Journal of Chemical and Engineering Data*, 30(4), 400-403.
- Guo, J. H., Luo, Y., Augustsson, A., Kashtanov, S., Rubensson, J. E., Shuh, D. K., et al. (2003). Molecular Structure of Alcohol-Water Mixtures. *Physical Review Letters*, 91(15), 1574011-1574014.
- Izgorodina, E. I., Chesman, A. S. R., Turner, D. R., Deacon, G. B., & Batten, S. R. (2010). Theoretical and experimental insights into the mechanism of the nucleophilic addition of water and methanol to dicyanonitrosomethanide. *Journal of Physical Chemistry B*, 114(49), 16517-16527.
- Jianming, Y., Jian, L., & Zhongwei, A. (2003). The solvent effect in catalytic hydrogenation of 4-n-pentylphenol. *Chemistry Bulletin / Huaxue Tongbao*, 66(7), 484-487.
- Koopman, P. G. J., Buurmans, H. M. A., Kieboom, A. P. G., & van Bekkum, H. (1981). Solvent-Reactant-Support interactions in liquid phase hydrogenation. *Recueil des Travaux Chimiques des Pays-Bas*, 100(4), 156-161.
- Li, Q., Sritharathikhun, P., & Motomizu, S. (2007). Development of Novel Reagent for Hantzsch Reaction for the Determination of Formaldehyde by Spectrophotometry and Fluorometry. *Analytical Sciences*, 23(4), 413-417.
- Ludwig, R. (2005). The Structure of Liquid Methanol. *ChemPhysChem*, 6(7), 1369-1375.
- Lunev, N. K., Shmyrko, Y. I., Pavlenko, N. V., & Norton, B. (2001). Selective formation of formaldehyde from carbon dioxide and hydrogen over PtCu/SiO₂. *Applied Organometallic Chemistry*, 15(2), 148-150.
- Moret, S., Dyson, P. J., & Laurency, G. (2014). Direct synthesis of formic acid from carbon dioxide by hydrogenation in acidic media. [Article]. *Nat Commun*, 5.
- Mukherjee, S., & Vannice, M. A. (2006). Solvent effects in liquid-phase reactions. I. Activity and selectivity during citral hydrogenation on Pt/SiO₂ and evaluation of mass transfer effects. *Journal of Catalysis*, 243(1), 108-130.
- Nakata, K., Ozaki, T., Terashima, C., Fujishima, A., & Einaga, Y. (2014). High-yield electrochemical production of formaldehyde from CO₂ and seawater. *Angewandte Chemie - International Edition*, 53(3), 871-874.
- Radhakrishnan, K., Ramachandran, P. A., Brahme, P. H., & Chaudhari, R. V. (1983). SOLUBILITY OF HYDROGEN IN METHANOL, NITROBENZENE, AND THEIR MIXTURES - EXPERIMENTAL DATA AND CORRELATION. *Journal of Chemical and Engineering Data*, 28(1), 1-4.
- Rautanen, P. A., Aittamaa, J. R., & Krause, A. O. I. (2000). Solvent effect in liquid-phase hydrogenation of toluene. *Industrial and Engineering Chemistry Research*, 39(11), 4032-4039.
- Singh, U. K., & Vannice, M. A. (2001). Kinetics of liquid-phase hydrogenation reactions over supported metal catalysts - A review. *Applied Catalysis A: General*, 213(1), 1-24.
- Vasudevan, V., & Mushrif, S. H. (2015). Insights into the solvation of glucose in water, dimethyl sulfoxide (DMSO), tetrahydrofuran (THF) and N,N-dimethylformamide (DMF) and its possible implications on the conversion of glucose to platform chemicals. *RSC Advances*, 5(27), 20756-20763.
- Xiao, C., Bianchi, H., & Tremaine, P. R. (1997). Excess molar volumes and densities of (methanol+water) at temperatures between 323 K and 573 K and pressures of 7.0 MPa and 13.5 MPa. *The Journal of Chemical Thermodynamics*, 29(3), 261-286.

This page is intentionally left blank

Chapter 6

Conclusions

This page is intentionally left blank

6.1 Introduction

In this thesis, a novel method of formaldehyde production was developed. Through this study, the effects of important parameters such as temperature, pressure, and stirring speed were examined. The reaction mechanism was investigated and the effect of solvents on the HCHO yield was studied. In this chapter, the main findings of this research are summarized.

6.2 Gas Phase Reaction and Slurry Phase Reaction

From the thermodynamic investigation of the CO hydrogenation reaction into HCHO, it is found that the reaction is non-spontaneous in the gas phase since the Gibbs free energy of the reaction is positive at room temperature and it increases with temperature. This was proven experimentally since the HCHO yield was insignificant with the maximum value of $8.2 \times 10^{-3} \text{ mmol.L}^{-1} \cdot \text{g}_{\text{cat}}^{-1}$. Moreover, thermodynamic investigation of the slurry reaction showed significantly higher equilibrium constant of the reaction in the aqueous phase. Experimental results showed that the yield of HCHO in the aqueous phase reached $4.55 \text{ mmol.L}^{-1} \cdot \text{g}_{\text{cat}}^{-1}$ after $t = 72 \text{ h}$.

6.3 Effect of Temperature

The Gibbs free energy of CO hydrogenation reaction to form HCHO increases with temperature in both gas and aqueous phase reaction. It was found that in the slurry reactor increasing the temperature increased the reaction rate but the formaldehyde yield reached its maximum value at 363 K, above which the yield reduced. This is in agreement with the thermodynamic calculation. This was observed in all experiments conducted using the slurry reactor. Lower solubility of the reactant gases and formaldehyde in the liquid phase was also responsible to reducing the yield of formaldehyde at high temperatures. The effect of temperature on the stability of the catalyst support was studied in the aqueous phase reaction. Based on the XRD patterns and solid state NMR results, it was shown that the catalyst support went through phase change to form AlOOH after 120 h at 403 K. This phase change was not observed at 353 K which shows the dependence of this phenomenon on temperature.

Chapter 6

6.4 Effect of Pressure

Based on the experimental data in the literature, it was noted that the Gibbs free energy of the reaction decreases as the pressure of the process increases. The results of this thesis confirmed the effect of pressure in both gas and liquid phase reactions. In the liquid phase higher pressures lead to higher gases solubility which is also an advantage. However, the operating pressure of in this thesis was limited to the maximum gas cylinders pressure available.

6.5 Effect of Stirring Speed

Another important parameter to consider was the stirring speed in the slurry phase reactor to study when the reaction changes from mass transfer controlled to kinetically controlled regime. It was observed that increasing the stirring speed from 0 to 800 rpm increased the HCHO yield since stirring decreased the mass transfer limitation by increasing the convective mass transfer coefficient and exposing the catalyst surface to the dissolved gases. However, increasing the stirring speed from 800 rpm to 1200 rpm did not affect the yield because the rate of mass transfer was sufficiently high at 800 rpm and further increasing the stirring rate did not affect the global rate of reaction because the reaction was kinetically controlled.

6.6 Reaction Mechanism

In order to investigate the process and improve the HCHO yield, the reaction mechanism was studied. By investigating the liquid samples for the presence of intermediate and by deuterium labelling technique, it was shown that the gases dissolve in the solvent and are adsorbed on the catalyst surface. While CO adsorbs as a molecule, H₂ dissociates on the catalyst surface. Adsorbed CO molecule is then hydrogenated to form adsorbed HCHO. In water and methanol solvent mixture desorption of HCHO results in rapid hydration leading to methylene glycol formation. In the absence of CH₃OH, HCHO molecules are hydrogenated further to produce CH₃OH. Based on this reaction mechanism, it was concluded that using solvents with higher H₂ and CO solubility may increase the HCHO yield.

6.7 Effect of Solvents

The effect of solvents on the yield of HCHO was studied in this project. Many types of solvents including polar protic (water, methanol, and ethanol), polar aprotic (DMSO), and non-polar (C_7H_8) solvents were used in the present study. It was shown that the highest HCHO yield is achieved by using pure CH_3OH followed by 0.1% v/v CH_3OH /water solution. The rapid reaction of HCHO with water and CH_3OH to form $CH_2(OH)_2$ and $C_2H_6O_2$, respectively, shifts the CO hydrogenation reaction equilibrium towards HCHO side which results in higher HCHO yield compared with using other solvents.

In this study, it was found that the solvent effects on CO hydrogenation to HCHO are not solely dependent on solubility. It was shown that using the solvents with higher ability to stabilise the produced HCHO molecules and its derivatives led to higher HCHO yield. It was observed that the HCHO yield in pure CH_3OH and 0.1% v/v CH_3OH /water solution was higher compared to concentrated CH_3OH -water solution. It was theorised that the tendency of the CH_3OH cyclic oligomers to stabilise the $C_2H_6O_2$ molecules may decrease in the presence of water molecules, since water molecules may preferentially fill the interspace of the CH_3OH cyclic oligomers, resulting in reduced stability of $C_2H_6O_2$ in water- CH_3OH solutions. The highest HCHO yield was measured to be $15.58 \text{ mmol.L}^{-1}.\text{g}_{\text{cat}}^{-1}$ which was achieved at 363 K using pure CH_3OH .

6.8 CO_2 Hydrogenation

The catalytic reduction of CO_2 to HCHO was studied in the same reactor used for CO hydrogenation. In this study, it was shown that the catalytic CO_2 reduction to HCHO was feasible. 5%v/v CH_3OH solutions of water and C_2H_5OH and pure CH_3OH were used for this process. Similar to CO hydrogenation, the highest HCHO yield was achieved by using CH_3OH as the solvent. The highest HCHO yield through CO_2 hydrogenation at 353 K and 100 bar was achieved to be $0.62 \text{ mmol.L}^{-1}.\text{g}_{\text{cat}}^{-1}$. The CO_2 hydrogenation reaction to HCHO should be studied further in future studies.

This page is intentionally left blank

Chapter 7

Recommendations and Future Studies

This page is intentionally left blank

7.1 Introduction

In this research, a novel method of HCHO production was introduced. Direct CO hydrogenation to HCHO was proven to be feasible in this study. However, there is a need for further investigation of this process prior to commercialisation. Considering the novelty of this process, there are several improvements and optimisation necessary. The key aspects to consider for future studies on direct conversion of synthesis gas to HCHO are summarised here.

7.2 Carbon Dioxide Hydrogenation

In this study, it was shown that catalytic CO₂ hydrogenation to HCHO is feasible. It is well known that activating CO₂ at low temperatures is more difficult compared to CO. This process needs to be optimized to achieve higher yield of HCHO. Considering the global issues of greenhouse gas emissions and global warming, utilizing CO₂ to produce value-added chemicals can be an interesting approach for future studies. It is recommended to use other catalysts to enhance CO₂ activation and hydrogenation. Using different solvents to absorb CO₂ on catalyst surface is important in this process. All aspects investigated for CO hydrogenation in this research, can separately be applied for CO₂ hydrogenation to optimize the HCHO yield in this process. It is also interesting to examine simultaneous hydrogenation of CO and CO₂ as they both are present in synthesis gas.

7.3 Catalyst Study

Only two catalysts, i.e. alumina supported Pd-Ni and Ru-Ni, were studied in this thesis. However, catalyst development is an essential part of a process in catalytic reactions. Other noble metals known for their high capability in hydrogenation reactions such as Pt, Rh, and Re can be examined in this process. Using higher content of noble metals also may improve the yield of HCHO. Moreover, it is important to examine other catalyst supports such as CeO₂, ZnO₂, and CeO₂-ZnO₂. The catalysts used in this research were prepared using wet impregnation method. Using other methods of catalyst preparation which may enhance the surface area and/or metal dispersion may improve the process.

Chapter 7

It is important to investigate the mass of the catalyst while using pure CH₃OH to confirm that the experiments are conducted in a kinetically controlled regime.

Addition of noble metals as the promoters may enhance the reducibility and stability of the catalyst. However, it is very important to study the mechanism of promoter effect on the catalyst functionality in detail. It is therefore suggested that the molecular structure of the catalyst as well as the atom bindings should be investigated using experimental methods such as X-ray Absorption Spectroscopy (XAS) analysis.

7.4 Process Optimization

The feasibility of CO hydrogenation to HCHO was shown in this research. However, the HCHO molar yield was significantly lower compared to the industrial method of HCHO production. There is a potential to optimize the conditions of this process to overcome the relatively low productivity of this method. Considering the novelty of this method, not enough information was available in the literature to improve the conditions of the process. It is therefore suggested to investigate the conditions of the process using computational modelling and simulation to find the optimum conditions for the process. This approach can provide an insight into the mechanism of the process.

7.5 *In-situ* Study of the Reaction Mechanism

In this study, the reaction mechanism was investigated using *ex-situ* investigation of the potential intermediate products in the samples collected during the reaction in addition to isotope labelling. However, it is essential to investigate the catalyst surface to study the formed species and confirm the mechanism. *In-situ* ATR-FTIR methods using high pressure cell is recommended for further investigation of the reaction mechanism. The investigation of the catalyst surface combined with the computational modelling provides a better understanding of the reaction conditions. This may reveal the main obstacles of the process which is the first step to further improvement of HCHO production.

7.6 Investigation of the Solvent-Formaldehyde Interaction Theory

The stabilisation of formaldehyde molecules in the water-methanol mixtures was justified based on the previous findings on the water-methanol interactions in the literature. The presented theory in this thesis needs further investigation through molecular dynamic modelling and experiments. It is critical to confirm the developed theory based on theoretical and experimental studies for further improvement of the formaldehyde yield and gaining an insight into the molecular interactions between the solvent molecules and the desorbed formaldehyde molecules

This page is intentionally left blank

Appendix:

This page is intentionally left blank

A.1 Critical Review and Exergy Analysis of Formaldehyde Production Processes:

DE GRUYTER

Rev Chem Eng 2014; aop

Ali Mohammad Bahmanpour, Andrew Hoadley and Akshat Tanksale*

Critical review and exergy analysis of formaldehyde production processes

Abstract: Formaldehyde is one of the most important intermediate chemicals and has been produced industrially since 1889. Formaldehyde is a key feedstock in several industries like resins, polymers, adhesives, and paints, making it one of the most valuable chemicals in the world. However, not many studies have been dedicated to reviewing the production of this economically important product. In this review paper, we study the leading commercial processes for formaldehyde production and compare them with recent advancements in catalysis and novel processes. This paper compares, in extensive detail, the reaction mechanisms and kinetics of water ballast process (or BASF process), methanol ballast process, and Formox process. The thermodynamics of the reactions involved in the formaldehyde production process was investigated using HSC Chemistry™ software (Outotec Oyj, Espoo, Finland). Exergy analysis was carried out for the natural gas to methanol process and the methanol ballast process for formaldehyde production. The former process was simulated using Aspen HYSYS™ and the latter using Aspen Plus™ software (Aspen technology, Burlington, MA, USA). The yield and product specifications from the simulation results closely matched with published experimental data. The exergy efficiencies of the natural gas to synthesis gas *via* steam reforming, methanol synthesis, and formaldehyde synthesis processes were calculated as 60.8%, 61.6%, and 66%, respectively. The overall exergy efficiency of natural gas conversion into formaldehyde was found to be only 43.2%. The main sources of exergy losses were the steam reformer and methanol loss in formaldehyde synthesis process. Despite high conversions and selectivities of these processes, the low exergy efficiency suggests that innovations in formaldehyde production processes could give a more sustainable product. Novel methods of direct conversion of natural gas or synthesis gas into formaldehyde will improve the exergy efficiency, but the conversion rate must also be increased with advancements in catalysis.

*Corresponding author: Akshat Tanksale, Department of Chemical Engineering, Monash University, Clayton, Victoria 3800, Australia, e-mail: akshat.tanksale@monash.edu

Ali Mohammad Bahmanpour and Andrew Hoadley: Department of Chemical Engineering, Monash University, Clayton, Victoria 3800, Australia

Keywords: exergy analysis; formaldehyde; kinetics and mechanism; methanol ballast process.

DOI 10.1515/revce-2014-0022

Received May 28, 2014; accepted August 25, 2014

1 Introduction

Formaldehyde is one of the simplest molecules in organic chemistry, which has a wide range of applications in chemical processes. It is produced in nature by photochemical processes in atmosphere or by incomplete combustion of organic materials (Reuss et al. 2003). Formaldehyde gas is colorless at ambient temperature with an irritating odor that unfavorably affects eyes and skin. The effects of formaldehyde on human health have been studied. Formaldehyde is toxic and probably a carcinogen because there is enough evidence that it can cause nasopharyngeal cancer (Cogliano et al. 2005). Some physical properties of monomeric formaldehyde can be found in Table 1 (Reuss et al. 2003).

Formaldehyde's heat of formation, heat capacity, and entropy are given in Table 2 for a wide range of temperatures and atmospheric pressure (Walker 1967).

The gas mixture with air is flammable at 293.15 K or higher (National Fire Protection Association 1994). Formaldehyde is considered as a reactive compound. At high temperatures (>423.15 K), it tends to undergo heterogeneous decomposition to produce methanol and carbon dioxide. However, if the temperature goes higher (>623.15 K), it may tend to form synthesis gas (hydrogen and carbon monoxide mixture) (Bone and Smith 1905, Calvert and Steacie 1951). It can be easily involved in both oxidation and reduction reactions. For example, in the presence of hydrogen, it can be reduced to form methanol over a nickel catalyst. Nitric acid, potassium permanganate, potassium dichromate, or oxygen can readily oxidize formaldehyde to form formic acid, carbon dioxide, and water (Walker 1967).

At atmospheric pressure, formaldehyde condenses at 253.95 K and freezes at 155.15 K as a white paste. In the liquid phase, its density is 0.8153 g/cm³ at 253.15 K and

A.2 Formaldehyde Production via Hydrogenation of Carbon Monoxide in the Aqueous Phase

Green Chemistry



PAPER

View Article Online
View Journal

Cite this: DOI: 10.1039/c5gc00599j

Formaldehyde production *via* hydrogenation of carbon monoxide in the aqueous phase

Ali Mohammad Bahmanpour, Andrew Hoadley and Akshat Tanksale*

Formaldehyde (HCHO) is an essential building block in many industries for producing value-added chemicals like resins, polymers and adhesives. Industrially, formaldehyde is produced *via* partial oxidation and/or dehydrogenation of methanol. Methanol is produced from natural gas in a series of processes, with synthesis gas as an intermediate. This study presents for the first time, formaldehyde production *via* hydrogenation of carbon monoxide in the aqueous phase, which eliminates the need for methanol synthesis, which may potentially save capital costs and reduce energy consumption. Gas phase hydrogenation of CO into formaldehyde is thermodynamically limited and therefore, resulted in a low CO conversion of only $1.02 \times 10^{-4}\%$. However, the aqueous phase hydrogenation of CO into formaldehyde was found to be thermodynamically favourable and kinetically limited. The highest CO conversion of 19.14% and selectivity of 100% were achieved by using a Ru–Ni/Al₂O₃ catalyst at 353 K and 100 bar. The rapid hydration of formaldehyde in the aqueous phase to form methylene glycol shifts the CO hydrogenation reaction equilibrium towards formaldehyde formation. Increasing the pressure and stirring speed increased the yield of formaldehyde, whereas increasing the temperature above 353 K resulted in a lower yield.

Received 19th March 2015.

Accepted 22nd April 2015

DOI: 10.1039/c5gc00599j

www.rsc.org/greenchem

Introduction

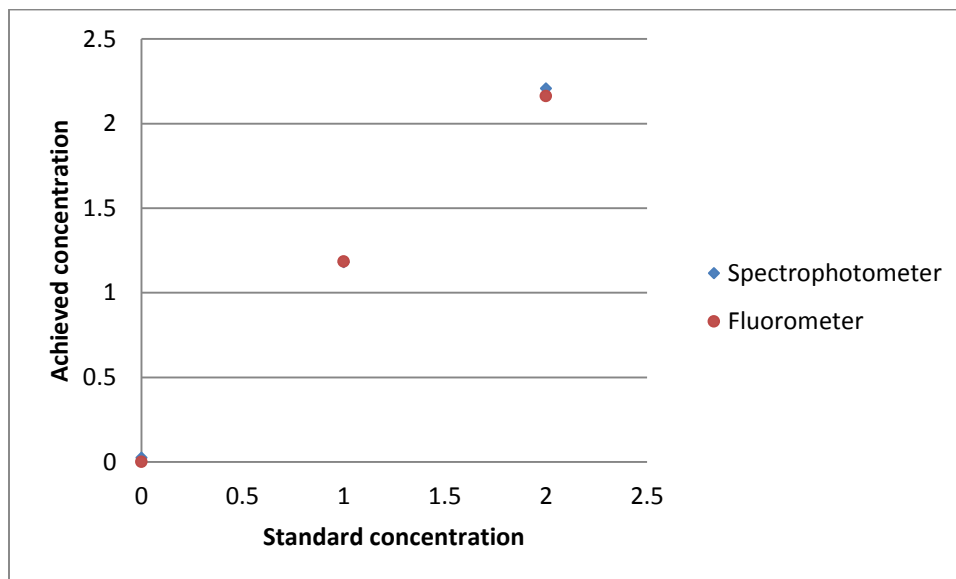
Industrially, formaldehyde (HCHO) is produced in three stages – (a) steam reforming of natural gas to produce syngas (Table 1, eqn (1)), (b) methanol (CH₃OH) synthesis (eqn (2)) and (c) partial oxidation of CH₃OH to produce HCHO (eqn (3)). Alternatively, HCHO is industrially produced *via* dehydrogenation of CH₃OH (eqn (4)).^{1,2} However, these are all high temperature reactions which require combustion, compression and large process units for purification, which are the root cause of energy losses.^{3,4} We have recently shown that this series of processes from natural gas to HCHO production suffers from ~57% losses in exergy (*i.e.* energy quality).⁵ Given the large quantity of HCHO produced in the world, when combined with the high losses in exergy, leads to high energy losses and also high CO₂ emissions, globally. Many researchers have tried to overcome this issue by finding ways to produce HCHO directly from natural gas by partial oxidation of CH₄ (eqn (5)).^{6–8} However, there has been no significant progress to date due to low CH₄ conversion and poor selectivity.⁶ The rate of HCHO decomposition into CO and H₂ is much greater than the rate of partial oxidation of CH₄, particularly at

temperatures in excess of 373 K, which means that in order to produce HCHO selectively, one must limit the conversion of CH₄ in eqn (5) to a very small value. Moreover, if we consider that natural gas is a valuable energy resource, it becomes evident that an alternative feedstock for HCHO production is much needed. An alternative is direct conversion of synthesis gas into HCHO. Syngas can be produced from a range of sources including biomass and it allows the mole fractions of CO to H₂ to be controlled more easily by the use of H₂O and CO₂ which are helpful in climate change abatement.⁹ Gas phase hydrogenation of CO to produce HCHO (eqn (6)) is not feasible because of the positive Gibbs free energy change of the reaction.¹⁰ Only a trace amount of HCHO in the product has been reported with the highest CO conversion of 0.2%.¹¹ Therefore, direct conversion of synthesis gas into HCHO has not been studied extensively. In this report, hydrogenation of CO into HCHO in a slurry reactor is presented as a viable alternative. By comparing with gas phase conversion in a fixed bed reactor, it is demonstrated that the thermodynamic limitation can be overcome in the slurry reactor. A low temperature active catalyst is desirable for the slurry phase reaction as the reaction was found to be favourable below 373 K. In general, Ni Pd and Ru are considered as active hydrogenation catalysts in the literature for many reactions.^{12–21} Based on the density functional theory (DFT) studies performed in the literature, Pd and Ni have been shown to produce HCHO as an intermediate of CO hydrogenation to produce CH₃OH.^{22,23} Previous studies

Catalysis for Green Chemicals Group, Department of Chemical Engineering,
Monash University, Clayton, VIC 3800, Australia.
E-mail: akshat.tanksale@monash.edu; Fax: +61 3 99053686; Tel: +61 3 99024388

A.3 Consistency of the Formaldehyde Detection Methods

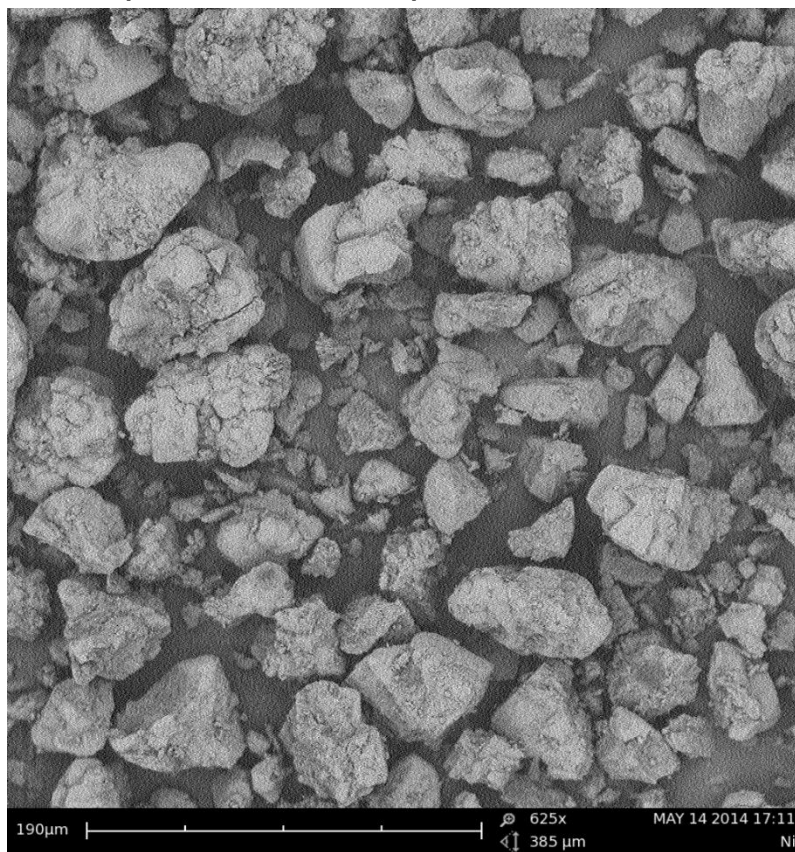
The formaldehyde detection methods used in this thesis (i.e. Spectrophotometric method and fluorometric method) are compared here to evaluate the consistency and accuracy of these detection methods.



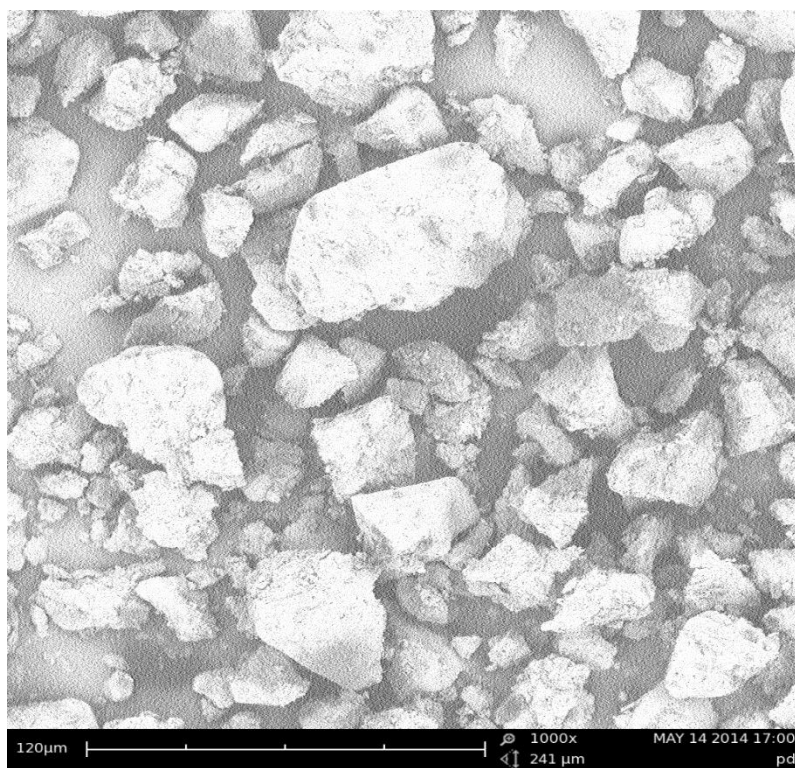
Appendix

A.4 SEM Images of Fresh Ru-Ni/Al₂O₃ and Pd-Ni/Al₂O₃

Ru-Ni/Al₂O₃:



Pd-Ni/Al₂O₃:



A.5 Standard solution containing 400 ppm formalin, 100 ppm HCOOH and CH₃OCOH on HPLC

